



**ISAS - INTERNATIONAL SCHOOL
FOR ADVANCED STUDIES**

**Density and Velocity Fields
in the Universe:
an Introduction**

Magister Philosophiæ

CANDIDATE

SUPERVISOR

Paolo Catelan

Prof. Dennis W. Sciama

Academic year 1991-1992

Astrophysics Sector

**SISSA - SCUOLA
INTERNAZIONALE
SUPERIORE
DI STUDI AVANZATI**

TRIESTE
Strada Costiera 11

TRIESTE

*A Francesco e Sabino,
che non sarebbero d'accordo.*

Le Stelle

Si suona il flauto per dichiarare l'amore o per annunciare il ritorno dei cacciatori. Gli indios waiwai convocano col flauto i loro invitati. Per i tukano il flauto piange; e per i kalina il flauto parla, mentre il corno grida.

Sulle rive del Río Negro, il flauto assicura agli uomini il potere. I flauti sacri sono tenuti nascosti e ogni donna che si avvicina merita la morte.

In tempi molto remoti, quando le donne possedevano i flauti sacri, gli uomini raccoglievano la legna e l'acqua e preparavano il pane di manioca.

Narrano gli uomini che il Sole si indignò alla vista di un mondo nel quale erano le donne a regnare. Il Sole scese nella selva e fecondò una vergine, spruzzandole succo di foglie.

Così nacque Jurupari.

Jurupari rubò i flauti sacri e li consegnò agli uomini. Insegnò loro a nascondersi e a difenderli e a celebrare feste rituali senza donne. Raccontò loro, inoltre, i segreti che dovevano trasmettere ai figli maschi sussurrandoli all'orecchio.

Quando sua madre scoprì il nascondiglio dei flauti sacri, Jurupari la condannò a morte; e con i brandelli del suo corpo fece le stelle del cielo.

Eduardo Galeano

Memoria del Fuoco

Acknowledgments

I have to thank my actual supervisor Prof. Dennis W. Sciama, and Prof. Aldo Treves and Dr. Antonio Lanza for much help, guidance and financial support throughout these first two years at SISSA-ISAS.

I am very grateful to Prof. Francesco Lucchin and Prof. Sabino Matarrese, because, since many years, they continuously inspire and follow my efforts in trying to understand cosmology.

Many other people however have played some role in this. In particular, I wish to acknowledge Prof. Robert J. Scherrer, at Ohio State University, for his hospitality during my visit there, when part of this work was begun; Bob is trying to explain to me the secrets of “seeded” cosmology.

Dr. Manolis Plionis and Dr. Peter Coles are greatly acknowledged for many discussions and encouragements; they are trying to introduce me to the world of observational data cosmology.

Dr. Paul Haines has carefully read the manuscript during the preparation, improving my English. Dr. Joe Pesce demonstrated to have a large amount of patience, stored somewhere else, when I had to \TeX print this Thesis. Dr. Lauro Moscardini, Dr. Enzo Branchini, Dr. Stefano Borgani and Dr. Riccardo Valdarnini discussed many points presented in it.

Prof. Francesco Lucchin, Prof. Sabino Matarrese and Dr. Lauro Moscardini (in §6.9), Prof. Robert Scherrer (in Chapter VII), Dr. Manolis Plionis and Dr. Peter Coles (in Appendix C) kindly allowed me to reproduce preliminary results of our joint work.

THANKS to Dr. José “Pepe” Guillermo Lorenzana .

Gisselle Carphio Mariño has been really a “compañera” during the last weeks.

CONTENTS

I	Background Cosmology	6
II	Statistical Predictions of Large Scale Structures	15
2.1	Random Fields	15
2.2	Ergodic Hypothesis	16
2.3	Path-Integral Approach	17
2.4	Nature of Density Distribution	18
III	Statistical Measures of Galaxy Distribution	22
3.1	Definitions	23
3.2	Observational Data	26
3.3	Power Spectra	32
IV	Growth of Perturbations	41
4.1	Equations of Motion for Matter	43
4.2	An Application of Linear Theory: The Local Group Motion	53
V	The Mean Mass Density in the Universe	56
5.1	Dark Matter in Spiral Galaxies	56
5.2	Correlation Analysis	58
5.3	Non Baryonic Dark Matter in the Universe	63
VI	Biased Galaxy Formation	71
6.1	Missing Mass Problem: Can the Universe Be Flat?	71
6.2	Voids	72

6.3	Difficulties in Cosmogonic Scenarios	73
6.4	Physical Bias Mechanism	75
6.5	Uniform Component	76
6.6	High Peak Biasing	77
6.7	Bias in a ‘Top-Down’ Scenario (Neutrinos)	79
6.8	The Kaiser Biased Model	80
6.9	Weighted Bias and Galaxy Clustering	84
VII	Non Linear Gravitational Evolution: Perturbative Theory	91
7.1	Second and Third Order Perturbations	94
7.2	An Application of the Non Linear Theory: Skewness as a Cosmo- logical Probe	102
A	Gaussian Random Fields	109
B	Cumulant Expansion	111
C	Evidence for Low Ω_0 Universe	115
C.1	Introduction	117
C.2	Dipole Calculations	121
C.2.1	Formalism	121
C.2.2	An Illustrative Model	122
C.2.3	Comments	125
C.3	Application to the QDOT Survey	126
C.4	Evidence for Contributions from Large Scales: Comparison with the Cluster Dipole	130
C.5	Conclusions	134
	References	143

INTRODUCTION

In this Thesis I review some topics of modern cosmology I am interested in.

The layout of this work is as follows. In Chapter I, I summarize the fundamental assumptions of physical cosmology, then fixing basic concepts and notation. The link between matter fluctuations and metric fluctuations in Newtonian approximation and the role of the comoving coordinates in describing the dynamics of particles in an expanding Universe are discussed. The Newtonian theory is accurate for cosmological perturbations with sizes that are very much smaller than the Hubble radius.

Most theories of galaxy formation assume that galaxies and other large-scale structures grew by gravitational instability from initially small stochastic perturbations δ to the energy density of the Universe.

An important point is that no cosmological theory attempts to predict the initial conditions $\delta(\mathbf{x}, t)$ exactly. A “complete” theory might predict e.g. the mean abundance of clusters and of galaxies and the mean distance of galaxies, but not the specific locations of galaxies and clusters in our Universe. In other words, theories predict only the *statistical* properties of $\delta(\mathbf{x}, t)$, in particular the *spatial* statistical properties.

The statistical predictions about large scale structures in the Universe are commented in Chapter II, where the concept of “random field” is introduced. The Gaussian and non-Gaussian nature of primordial density distribution are compared. Technical aspects of Gaussian random fields can be found in Ap-

pendix A.

Quantifying the large scale structures of the Universe is a difficult task and a variety of techniques have been developed to approach it. In Chapter III, I describe in some detail the most commonly used statistical measurements of galaxy clustering, the correlation functions and their Fourier transform, the power spectra; if someone is interested in, the cumulant expansion theorem is presented in Appendix B.

The most largely accepted scenario to approach the structure formation is the so called gravitational instability scenario, which treats essentially noise amplification, ie. linear (small) perturbations at some early time grow to non linearity under their own self gravitation. I describe in Chapter IV the fundamental equations governing the growth of matter perturbations. Linear solutions are discussed in detail.

Measuring the mass content of the Universe is one of the most important tasks in observational cosmology, but it is not easy at all. In Chapter V, I review dynamical techniques for estimating the density parameter Ω_0 . The missing mass problem and non baryonic universes are then analyzed.

Until fairly recently cosmologists tacitly assumed that the luminous matter traces the matter distribution ie. the mass-to-light ratios M/L of different cosmic structures were the same. However, there is a great deal of observational and theoretical evidence that this is not the case (Chapter V).

Such a evidence leads in a natural way to the concept of “biased” galaxy formation ie. galaxy formation (or, more in general, cosmic structure formation)

occurring in such a way that galaxies do not fairly trace the underlying mass distribution. In most biased scenarios, one is able to relate luminous matter and “dark matter” by involving a very specific form of bias, although such a prescription is not unique. In Chapter VI, I talk about the motivations for biasing the galaxy distribution, possible physical mechanisms and the types of bias expected in various cosmological scenarios.

Since the Kaiser’s suggestion (1984) that the prominent structures in the Universe formed in correspondence of the high peaks of the primordial fluctuation field, the biased approach characterized the way with which cosmologists analyze the structure formation in the Universe, although the relation between light and matter has become sometimes obscure. Mathematically, to describe “what is” a peak of the background density field is not just easy. In §6.9 a new “weighted” biasing scheme for galaxy clustering is considered. Contrary to previous treatments, the biased density field coincides with the background mass-density whenever the latter exceeds a given threshold. All the observables in this approach can be continuously defined down to the unbiased case. The two-point function of biased objects, which is computed for underlying Gaussian density fluctuations, turns out to be quite different from that obtained in previous treatments even at large distances and for high threshold.

The cosmological implications of this new biasing scheme have yet to be analyzed. The results seem promising. To weight a proto-structure with its own mass above a given threshold permits one to recover the unbiased observables simply by taking the limit $\nu \rightarrow -\infty$. New observables, like the mass fluctuation *in* the excursion regions, can be defined. In general, the weighted peak-peak correlation functions are *enhanced* with respect to the classical Kaiser peak-peak correlations, overall at small and intermediate scales ($\omega \sim 1$), while the standard expressions of the biased two-point correlation functions are recovered at very

large separations ($\omega \rightarrow 0$), essentially because the intermediate scale information is lost there. It has to be explored if in this description more power on large scale is possibly originated in the standard CDM model.

The linear growth laws discussed in Chapter IV hold until $\delta \approx 1$. When the perturbation amplitudes approach unity, non linear gravitational effects become important.

The evolution of linear perturbations of FRW models has been discussed by a large number of authors and little of this material is controversial. In contrast, the evolution of non-linear cosmological perturbations is still poorly understood despite the existence of a large literature on the topic. After reviewing the recent literature on the subject, though this is changing too rapidly to make such an enterprise worthwhile, I analyze in Chapter VII second and third perturbative order equations of motion for density and velocity fields. New cosmological observables are considered, like skewness and kurtosis of density and velocity fields.

Gaussian fields have zero skewness by definition, but the presence of a non-zero skewness in the e.g. IRAS data, does not necessarily imply non-Gaussian initial conditions: even if the initial probability distribution of the mass density contrast δ is Gaussian then symmetric, an asymmetry will inevitably develop later, as a second order effect, under the influence of gravity. Indeed, δ can grow indefinitely in regions where it was initially positive, whereas in the voids it can never decrease below -1 .

I review how gravity can induce skewness in an initially Gaussian distribution, computing and solving the second order solutions of the equations of motion for matter. Next, the skewness in density field, assumed Gaussian at early time (e.g. at recombination), is calculated, also suggesting how to work

out the skewness in the more general case in which δ is non-Gaussian at the beginning. I conclude discussing how the observations can be used to distinguish “conventional” models from an intrinsically non-Gaussian alternative.

Finally, in Appendix C, the QDOT survey is analysed in order to investigate the convergence properties of the estimated dipole and the consequent reliability of the derived value of $\Omega_0^{0.6}/b$. It is found that there is no compelling evidence that the QDOT dipole has converged within the limits of reliable determination and completeness. Therefore the value of Ω_0 derived by Rowan-Robinson *et al.* (1990) should be considered only as an upper limit. Furthermore, it is found strong evidence that the shell between 140 and 160 h^{-1} Mpc does contribute significantly to the total dipole anisotropy and therefore to the motion of the Local Group with respect to the Cosmic Microwave Background. This shell contains the Shapley concentration, but it is argued that this concentration itself cannot explain all the gravitational acceleration produced by it; there must exist a coherent anisotropy which includes this structure, but extends greatly beyond it. With the QDOT data alone, it is impossible to determine precisely the magnitude of any such anisotropy but any contribution to the Local Group motion from large scales would favour a value of $\Omega_0^{0.6}/b_{IRAS} \leq 0.6$, smaller than previous estimates based on IRAS galaxies; such a result would be consistent with the dipole measured from samples of rich clusters, which are much more complete at large depths.

CHAPTER I

Background Cosmology

We summarize here the fundamental assumptions of physical cosmology:

- The observable part of our Universe may be approximated as part of a homogeneous and isotropic Friedmann-Robertson-Walker (FRW) universe. The assumptions of large-scale homogeneity and isotropy is often called the *COSMOLOGICAL PRINCIPLE*.
- To describe the evolution and structure of space time we apply General Relativity Theory, mainly in its Newtonian approximation.
- We live in a *perturbed* FRW Universe: the metric fluctuations are small within our horizon, although density fluctuations are not necessarily small.

Three main tested observational facts support the so called Hot “Big Bang” Cosmological model (Gamow 1946):

- **THE UNIVERSE IS EXPANDING.** During the thirties, Hubble discovered that (distant) galaxies are receding from us according to the Hubble’s law

$$v = Hr , \tag{1.1}$$

where v is the recession velocity, H is the Hubble constant, r is the estimated distance of the galaxy. This expansion corresponds to a true geometrical space-time expansion (see Hubble 1934; 1936).

- THE MICROWAVE BACKGROUND. Penzias and Wilson (1965) discovered the so called cosmic micro background radiation (CBR, MWB), measured as an excess antenna temperature in the first experimental studies for the Telstar project. Soon it was realized that this could be relic black-body radiation left by a primeval fire ball (Dicke *et al.* 1965). This has been definitively confirmed by the recent measurement of COBE (Mather *et al.* 1990; Smoot *et al.* 1991).
- LIGHT ELEMENT COSMIC ABUNDANCES. The hot big bang model predicts the nucleosynthesis of the light elements (e.g. Wagoner 1973) with abundances which are remarkably close to the estimates obtained from observations (Yang *et al.* 1984; more recent: Walker *et al.* 1991).

The synthesis of the light elements is determined by (nuclear) events occurring in the epoch from $\sim 1 s$ to $\sim 1000 s$ in the history of the Universe, when temperatures varied from $\sim 10^{10} K$ or higher ($\gtrsim 1 MeV$) to $\sim 10^9 K$ or higher ($\gtrsim 0.1 MeV$): thus the observed abundances offer a probe of the Universe at epoch far earlier than those probed by CBR ($t \sim 10^5 yr$; $T \sim 10^4 K \sim 1 eV$) (see e.g. Weinberg 1972).

The zeroth-order Hubble expansion is described by the cosmic scale factor $a(t)$ that satisfies the Friedmann equation

$$H^2 \equiv \left(\frac{\dot{a}}{a}\right)^2 = \frac{8\pi}{3} G \rho_b(t) - \frac{k}{a^2}. \quad (1.2)$$

$\rho_b(t)$ is the background total mean density in the Universe; k is the curvature constant. The Hubble parameter has present value $H_0 = 100 h km/s/Mpc$, where almost certainly $0.5 \lesssim h \lesssim 1$; several recent determinations favor $h \approx 0.8$ (Jacoby, Ciardullo & Ford 1990; Tonry 1991; anyway see the fine review: Huchra

1992). The present value of a , $a_o \equiv a(t_o)$, is by definition equal to one. The Eq.(1.2) is the most important equation in cosmology; solving for k we get

$$k = (\Omega_o - 1)H_o^2 , \quad (1.3)$$

where $\Omega_o \equiv \Omega(t_o)$, $\Omega(t)$ being the density parameter, defined by

$$\Omega(t) \equiv \frac{8\pi G \rho_b(t)}{3 H(t)^2} \equiv \frac{\rho_b(t)}{\rho_{cr}(t)} , \quad (1.4)$$

and ρ_{cr} is the critical density. $\rho_b(t)$ is the sum of the matter, radiation and vacuum energy contributions. It satisfies the energy equation

$$\frac{d\rho_b}{dt} = -3 \left(\rho_b + \frac{p_b}{c^2} \right) \frac{\dot{a}}{a} , \quad (1.5)$$

where p is the pressure (subscripts refer to the background). The equation of state $p = p(\rho)$ relates p versus ρ (see Weinberg 1972).

If the Universe is dominated by non relativistic matter, for which $p \ll \rho c^2$, like in the late stages of the expansion of the Universe, when the matter is the only dynamically important constituent, its adiabatic expansion dilutes the mass density inversely with volume ie.

$$\rho_b = \rho_o a^{-3} \quad (\text{matter era}) , \quad (1.6)$$

where

$$\rho_o \equiv 1.88 \times 10^{-29} \Omega_o h^2 g cm^{-3} \quad (1.7)$$

is the present mean density; Ω_o lies in the range (see e.g. Peebles 1986)

$$0 < \Omega_o < \text{few} . \quad (1.8)$$

Some preliminary aspects of the evolution of the model might be noted; for instance from (1.2) and (1.6) we get

$$\frac{1 - \Omega(t)}{\Omega(t)} = a(t) \frac{1 - \Omega_o}{\Omega_o} , \quad (1.9)$$

therefore we see that $\Omega = 1$ is an unstable fixed point during the evolution of the Universe: as $a(t)$ increases, Ω increasingly deviates from $\Omega = 1$; if $\Omega \equiv 1$ at the beginning, then $\Omega_0 = 1$ (a very interesting kinematical analysis of the behaviour of the parameter $\Omega(t)$ is given in Madsen & Ellis (1988)). The Einstein-de Sitter model has $\Omega = 1$ and $p = 0$ ($= \Lambda = \text{cosmological constant}$); in such a model we have

$$a \propto t^{2/3} , \quad (1.10)$$

$$6\pi G\rho_b t^2 = 1 , \quad (1.11)$$

that we'll use often. The Einstein-de Sitter model is a favored model among cosmologists, above all the inflationary ones (Guth 1981): in fact inflation predicts $\Omega = 1$ with great precision (however, see Ellis 1988); anyway, both the open ($\Omega_0 < 1$) and closed ($\Omega_0 > 1$) very early universes expand like the Einstein-de Sitter solution, $a \propto t^{2/3}$.

The curvature constant k appears in the expression of the Robertson-Walker metric (RW) line element; it can be obtained directly starting from the homogeneity and isotropy hypothesis (see Weinberg 1972)

$$\begin{aligned} ds^2 &= g_{\mu\nu} dx^\mu dx^\nu \\ &= c^2 dt^2 - a^2 \left[(1 - kx^2/c^2)^{-1} dx^2 + x^2 (d\theta^2 + \sin^2\theta d\varphi^2) \right] . \end{aligned} \quad (1.12)$$

The coordinates x , θ and φ are comoving, fixed to fluid element: we obtain a proper distance r multiplying the comoving distance x by the scale factor $a(t)$.

The effects of curvature are negligible in correspondence of scales much smaller than the Hubble length $cH_0^{-1} = 3000 h^{-1} Mpc$, which is a convenient measure of the distance to the horizon (about the distance that free photons have travelled since the big bang): because of (1.3) and (1.8), the condition $x \ll cH_0^{-1}$ implies $kx^2/c^2 \ll 1$; typically the Universe is well sampled only on

scales much smaller than the Hubble length (an all-sky redshift survey of galaxies detected by IRAS has been used to map the Universe out to $\sim 140 h^{-1} Mpc$ (Saunders *et al.* 1991)), and if we restrict ourselves to structures much smaller than this, the curvature term may be neglected in the RW metric (1.12) (but not necessarily in the dynamical Friedmann equation); the RW line element reduces to the simplified form $ds^2 = c^2 dt^2 - a^2 d\mathbf{x} \cdot d\mathbf{x}$, $\mathbf{x} = (x_1, x_2, x_3)$ being Cartesian comoving coordinates.

The proper position will be denoted by

$$\mathbf{r} = a(t) \mathbf{x} . \quad (1.13)$$

Sometimes in cosmology the *conformal time* is introduced

$$\tau \equiv \int_0^t \frac{dt}{a(t)} . \quad (1.14)$$

Transforming t in τ reduces (1.12) to a conformally equivalent metric ie.

$$ds^2 = a(\tau)^2 \left[c^2 d\tau^2 - (1 - kx^2/c^2)^{-1} dx^2 - x^2(d\theta^2 + \sin^2\theta d\varphi^2) \right] , \quad (1.15)$$

which is conformally flat in the limit of small scales ($kx^2/c^2 \ll 1$); adopting this metric, the equations of motion for the matter have a very simple form, as we'll see. We indicate there τ by the usual symbol t , unless differently indicated.

During the matter-dominated epoch (post-recombination universe: below 4000 K the atomic H is almost completely formed) the large-scale structures are developing, so the fluctuations in the background radiation (and any other eventual relativistic components, as neutrinos) are negligible with respect to the non relativistic density fluctuations, the only dynamically significant; these lead to fluctuations in the metric, which can be described just by one scalar field, the Newtonian gravitational potential ϕ ; we know indeed that, solving the Einstein

equations to first order in ϕ/c^2 we get $g_{00} = 1 + 2\phi/c^2$ (see e.g. Weinberg 1972); in the conformal Newtonian gauge we have

$$ds^2 = a(\tau)^2 \left[(1 + 2\phi/c^2) c^2 d\tau^2 - (1 - 2\phi/c^2) d\mathbf{x} \cdot d\mathbf{x} \right]. \quad (1.16)$$

This form of the metric highlights the metric fluctuations induced by a non perfectly homogeneous and isotropic distribution of matter, at least at small scales. Note that the metric fluctuations are small even if the matter density fluctuations are not so small: $\delta M \sim \phi$ (see below).

The coordinate velocity of a matter particle in conformal time is just the peculiar velocity ie. the velocity measured by an observer at the particle position and at fixed \mathbf{x} :

$$\mathbf{v} \equiv \frac{d\mathbf{x}}{d\tau} = a \frac{d\mathbf{x}}{dt} = \frac{d\mathbf{r}}{dt} - H\mathbf{r}. \quad (1.17)$$

Note that, of course, the Hubble velocity is subtracted; also, the proper velocity of a particle relative to the origin can be written, from Eq.(1.17), as

$$\frac{d\mathbf{r}}{dt} = a \dot{\mathbf{x}} + \dot{a} \mathbf{x}, \quad (1.18)$$

where dot indicates time derivatives d/dt .

The gravitational potential perturbation in the metric (1.16) corresponds to the Newtonian gravitational force. The geodesics in this metric correspond to the equations of motion. For a massive test particle m (see Peebles 1980, §7)

$$\mathbf{p} = m a^2 \dot{\mathbf{x}}, \quad (1.19)$$

$$\frac{d\mathbf{p}}{dt} = -m \nabla \phi, \quad (1.20)$$

where the gradient is with respect to \mathbf{x} . According to (1.19) and (1.20),

$$\frac{d\mathbf{v}}{dt} = -\frac{\dot{a}}{a} \mathbf{v} - \frac{\nabla \phi}{a}. \quad (1.21)$$

The extra ‘‘Hubble drag’’ term $-\dot{a} \mathbf{v}/a$ arises because we are using comoving coordinates and it is not due to some cosmic force; the comoving coordinates define a non inertial, because expanding, reference frame: if $\phi \equiv 0$, \mathbf{p} is constant, but $\mathbf{v} \propto a^{-1}$ because of the Hubble expansion.

The zero-zero component of the Einstein equation for an ideal fluid is, to first order in ϕ/c^2 (see Peebles 1980, §7)

$$\nabla^2 \phi = 4\pi G a^2 [\rho(\mathbf{x}, t) - \rho_b(t)], \quad (1.22)$$

where $\rho(\mathbf{x}, t)$ is the mass density at the point (\mathbf{x}, t) . Eq.(1.22) is known as the (comoving) Poisson equation. We stress the fact that the source for ϕ is always the fluctuating part of the non relativistic matter density. Also note that (1.16), obtained from the standard weak field approximation (see e.g. Landau & Lifshitz 1979, Eq. (105.9)), does not assume that $\delta\rho \equiv \rho - \rho_b$ is small. The reason is just because we assumed that $\phi \ll c^2$: if a region of scale λ contains a mass $M \sim \rho_b \lambda^3$, where the density ρ_b is roughly uniform, the condition $\phi \ll c^2$ implies that $G\rho_b \lambda^2 \ll c^2$; in the Friedmann-Lemaitre models Hubble constant is $H \sim (G\rho_b)^{1/2}$ (see Eq.(1.11)); therefore in the Newtonian approximation we are neglecting terms of order $(\lambda H/c)^2$ ie. we assume that perturbation are small with respect the Hubble scale; more in detail, the source of ϕ is the fluctuation $\delta\rho$, then $\phi/c^2 \sim (H\lambda/c)^2 \delta\rho/\rho_b$ and, on scales much smaller than the horizon, ϕ/c^2 may be small even though $\delta\rho/\rho_b$ is very large.

Apart from the baryonic matter, the Universe contains a homogeneous sea of black body radiation, with temperature (e.g. Weinberg 1972; Mather *et al.* 1990; see also Gush, Halpern & Wishnow 1990)

$$T(t) = T_0(1 + z), \quad (1.23)$$

$$T_o = 2.735 \pm 0.06 K , \quad (1.24)$$

where z is the cosmological redshift (because expansion)

$$\lambda_o = \frac{a(t_o)}{a(t)} \lambda = (1 + z) \lambda . \quad (1.25)$$

λ_o is the wavelength observed now (t_o), of radiation emitted at epoch t at wavelength λ by an object comoving with the fluid; the redshift z often is used as a label of an epoch, just because

$$z = a^{-1} - 1 . \quad (1.26)$$

The Hubble law, $\dot{r} = Hr$, gives the redshift of an object at proper distance $r \ll cH_o^{-1}$:

$$z \approx H_o r / c , \quad (1.27)$$

which is a good approximation for $z \ll 1$.

The mean mass density in the radiation is

$$E_b(t) = E_o (1 + z)^4 , \quad (1.28)$$

$$E_o = a_s T_o^4 / c^2 = 4.5 \times 10^{-34} g cm^{-3} . \quad (1.29)$$

At the beginning, the Universe is radiation dominated; instead of (1.10) and (1.11), during the radiative-era we have

$$a \propto t^{1/2} , \quad (1.30)$$

$$\frac{32}{3} \pi G \rho_b t^2 = 1 , \quad (1.31)$$

in an Einstein-de Sitter universe; (1.6) is substituted by

$$\rho_b \propto a^{-4} \quad (\text{radiation era}) . \quad (1.32)$$

The crossover between the matter era and radiation era occurs at the equivalence epoch, a_{eq} , when $\rho_r \equiv \rho_m$; detailed calculations show that $z_{eq} \approx 10^4$.

The other important cosmological epoch is that of recombination, z_{rec} , after the temperature has fallen below $4000 K$, the baryonic matter is essentially unionized and the matter and radiation therefore decouple.

After reviewing some basics in standard cosmology, we start to enter more in detail in that branch of modern cosmology in which we are interested in, the statistical analysis of the large-scale matter distribution in the Universe.

CHAPTER II

Statistical Predictions of Large Scale Structures

Most theories of galaxy formation assume that galaxies and other large-scale structures grew by gravitational instability from initially small stochastic perturbations δ to the energy density of the Universe (Chapter IV).

An important point is that no cosmological theory attempts to predict the initial conditions $\delta(\mathbf{x}, t)$ exactly. A “complete” theory might predict e.g. the mean abundance of clusters and of galaxies and the mean distance of galaxies, but not the specific locations of galaxies and clusters in our Universe. In other words, theories predict only the *statistical* properties of $\delta(\mathbf{x}, t)$, in particular the *spatial* statistical properties and, for this reason, the temporal parameter t is commonly understood, all statistical computations being made at a given cosmic time t .

2.1 Random Fields

In the statistical description of the matter distribution on large, the energy- density fluctuation field in the Universe

$$\delta(\mathbf{x}) \equiv \frac{\rho(\mathbf{x}) - \langle \rho(\mathbf{x}) \rangle}{\langle \rho(\mathbf{x}) \rangle}, \quad (2.1)$$

is treated as a *random field* ie. a set of random variables, one for each point \mathbf{x} in the three dimensional real space, defined by the set of finite-dimensional *joint*

probability distribution function

$$P_N[\delta(\mathbf{x}_1), \delta(\mathbf{x}_2), \dots, \delta(\mathbf{x}_N)] d\delta(\mathbf{x}_1) d\delta(\mathbf{x}_2) \dots d\delta(\mathbf{x}_N) \quad (2.2)$$

(Here, by forcing the notation, $\delta(\mathbf{x})$ also indicates the *value* of the *field* $\delta(\mathbf{x})$ at the point \mathbf{x}). This is the probability that the function $\delta(\mathbf{x})$ has values in the range $[\delta(\mathbf{x}_i), \delta(\mathbf{x}_i) + d\delta(\mathbf{x}_i)]$, with $i = 1, 2, \dots, N$, N an arbitrary integer and $\mathbf{x}_1, \mathbf{x}_2, \dots, \mathbf{x}_N$ are N arbitrary points in the euclidean space (Kac & Logan 1979; Adler 1981; Vanmarcke 1983; Bardeen *et al.* 1986 (BBKS)).

By *random process* we mean that $\delta(\mathbf{x})$ for our Universe is just a *random realization* from a statistical *ensemble* of universes.

The assumption that the Universe is homogeneous and isotropic on average implies that the density field $\rho(\mathbf{x})$, ie. $\delta(\mathbf{x})$, is a homogeneous and isotropic random process (sometimes called *stationary*; see e.g. Fall 1979). So, the averages over the ensemble in (2.1), $\langle \cdot \rangle$, are invariant with respect to spatial translations and rotations. Observations probe only the spatial distribution in one realization of $\delta(\mathbf{x})$. On the other hand, theory specifies the probability distribution over an ensemble.

2.2 Ergodic Hypothesis

Actually implicit in all theoretical discussions is the *Ergodic Hypothesis*: ensemble averages equal spatial averages taken over one realization of the random field. The Ergodic Hypothesis has been demonstrated for a Gaussian random field (see Appendix A) *iff* its power spectrum (see §3.3) is continuous as a function of k (Adler 1981; see also BBKS). Essentially, the Ergodic Hy-

pothesis requires spatial correlations (§3.1) to decay sufficiently rapidly with increasing separation so that there exist many statistically independent volumes in one realization. These conditions are satisfied in a large class of theories of primordial scenarios, including quantum fluctuations produced during inflation (Brandenberger 1985). If the Ergodic Hypothesis is assumed valid, then all the information is available from a single sample of $\delta(\mathbf{x})$ over all space, and we have to hope that by measuring $\delta(\mathbf{x})$ over a sufficiently large volume arbitrarily precise tests of theories can be made.

2.3 Path-Integral Approach

An alternative approach, which has been extensively explored in recent years, is to apply the *path-integral approach* of Feynman & Hibbs (1965). More in general, the random field $\delta(\mathbf{x})$ is fully described by the joint probability distribution *functional* $P[\delta(\mathbf{x})]$ with measure

$$P[\delta(\mathbf{x})] [d\delta(\mathbf{x})], \quad (2.3)$$

which is obtained from (2.2) for $N \rightarrow \infty$, with the points \mathbf{x}_i covering the whole Universe; the limit may be made well-defined (see Bertschinger 1992), the corresponding measure is called a Wiener measure. By the assumption of statistical homogeneity, even though $\delta(\mathbf{x})$ is not constant, the distribution $P[\delta(\mathbf{x})]$ is independent of position \mathbf{x} . One recovers the n-point distribution by

$$\begin{aligned} P_N(\alpha_1, \dots, \alpha_N) d\alpha_1 \cdots d\alpha_N &= \left\langle \prod_{h=1}^N \delta_D(\delta(\mathbf{x}_h) - \alpha_h) \right\rangle \\ &= \int [d\delta] \prod_{h=1}^N \delta_D(\delta(\mathbf{x}_h) - \alpha_h) P[\delta]. \end{aligned} \quad (2.4)$$

This approach is not necessary for any of the applications we are interested in, but it surely permits us to develop in a relatively simple formalism

a statistical study of the field $\delta(\mathbf{x})$, obtaining results that may not be easily worked out using the classical prescription, above all in the case in which the density distribution is a generic *non-Gaussian* type distribution. (see Fry 1984; Politzer & Wise 1986; Lucchin, Matarrese & Bonometto 1986; Goroff *et al.* 1987; Bertschinger 1988; Cline *et al.* 1988; Catelan, Lucchin & Matarrese 1988a; see also 1988b; Coles 1988; Lucchin, Matarrese & Vittorio 1988; Scherrer & Bertschinger 1991).

2.4 Nature of Density Distribution

One of the most challenging and interesting problems to solve is to establish the nature of the distribution (2.3).

In the last decade of studies of cosmological large-scale structures, attention has been focused mainly on the two-point galaxy correlation function (§ 3.1) and on the analysis of the primordial density fluctuations *Gaussian* distributed (we briefly discuss the technical aspects of Gaussian fields in Appendix A).

Indeed the simplest and more usually accepted hypothesis is that the distribution (2.3) is Gaussian.

A reason justifying this is a *principle of simplicity*, according to which all the *complications* should arise during the non-linear evolution of the perturbations after the recombination (see e.g. Primack 1984; Chapter VII). If we had to translate this statement into the language of field theory, we could say that the density fluctuation field was initially free, and all its interactions are due to the subsequent action of gravity. Stated in such a manner, it appears as a

quantitative formulation of our intuitive idea that the gravitational interaction has to play the main dynamical role on large scales. Furthermore, it is known that a Gaussian distribution provides us many practical advantages.

The *Central Limit Theorem*, which tells us that the probability distribution of the sum, or mean, of many random variables, being both (nearly) independent and (nearly) identically distributed, tends to a Gaussian distribution (see e.g. Feller 1971; Adler 1981; Vanmarcke 1983), is largely used to justify such a restrictive hypothesis. Also, the Gaussian functional distribution, being exponential of a quadratic form, involves extremely simple analytical calculations; this is due to the fact that a Gaussian distribution is completely determined by its power spectrum (see below) ie. by its 2-point correlation function (which corresponds to the Green's function of a free scalar field): a possible definition of Gaussian distribution is indeed when all the reduced or connected correlations (see Appendix B) of order higher than second are *zero*¹.

There exist many usually invoked arguments asserting that, during the linear phase of evolution of perturbations, the second order correlations constitute all that is necessary to know. During the major part of the primordial history of the Universe, the clustering process is negligible, as one observes in correspondence of the largest scales, and the connected correlations of higher order are assumed be negligibly small (however see e.g. Baumgart & Fry 1991). Furthermore, the inflationary model (see e.g. Kolb & Turner 1990) predicts the existence of scale-free primordial Gaussian density fluctuations ie. fluctuations that cross the horizon with constant scale-independent mass variance (§3.3; Bardeen, Steinhardt & Turner 1983).

¹There exists only *one* positive definite density probability $p(x)$ with only a mean and a variance, the Gaussian distribution (see Fry 1985).

However, non-Gaussian fluctuations for structure formation have been advocated by numerous cosmologists.

Peebles (1983; 1987) has suggested that the distribution of galaxies is not adequately described by a Gaussian process: actually the distribution of galaxies is surely non-Gaussian on small scales (as confirmed, for instance, by detection of low order connected galaxy correlations; see §3.2; Saunders *et al.* 1991) and, from a certain moment onwards, we must think that the assumption of Gaussian distribution is inadequate; we could deduce that such moment corresponds to the beginning of the non-linear regime, but there exist many indications asserting that it could be very antecedent to that phase (Fry 1984; 1985; Baumgart & Fry 1991).

Non-Gaussian distributed perturbations can be assumed to be the most general starting point for computing a number of cosmological observables, such as spatial correlation functions (Matarrese, Lucchin & Bonometto 1986), expected size and frequency of high density regions (Catelan, Lucchin & Matarrese 1988) and of fine-scale hotspots and coldspots in the microwave background distribution on the sky (Coles & Barrow 1987).

A strong theoretical reason for analyzing non-Gaussian probabilities is that the fractional density enhancement $\delta(\mathbf{x})$ must satisfy the fundamental constraint

$$\delta(\mathbf{x}) \geq -1 \tag{2.5}$$

everywhere, because the semipositivity of the mass density $\rho(\mathbf{x})$. The normal distribution cannot allow for this constraint, because it predicts a finite chance that δ assumes a value smaller than -1 (the consequences of this are particularly relevant in the ‘weighted’ biased scheme presented in § 6.9; Catelan *et al.* 1992). Since cosmological perturbations can only be assumed normally distributed dur-

ing the very linear stage of their evolution, this latter problem is commonly disregarded. In this stage the probability of getting one of these “negative mass” events is negligibly small; one can recall the Chebyshev inequality (e.g. Feller 1971), stating that, given any distribution function $p(\delta)$, the *a priori* probability that $\delta < -1$, in a randomly chosen point, is not larger than the mean square fluctuation σ^2 , where linearity implies $\sigma^2 \ll 1$.

Variations of the inflation model which yields to *non-Gaussian* primordial fluctuations which are basically scale-invariant have been recently widely discussed (Matarrese, Ortolan & Lucchin 1988; Barrow & Coles 1990; Salopek & Bond 1991; Mollerach *et al.* 1991; Salopek 1992). In the context of inflationary models, Allen, Grinstein & Wise (1987) and Kofman & Linde (1987) constructed axion models with non-Gaussian fluctuations. Late-time phase transitions (Hill, Schramm & Fry 1989), cosmic string models (Vilenkin 1981; Turok 1984; Scherrer, Melott & Bertschinger 1989) and global textures (Turok 1989; Turok & Spergel 1990; 1991) are additional models whose statistics may not be described by a Gaussian distribution (Scherrer & Bertschinger 1991; Scherrer 1992). The importance of the high order moments of density distribution for the final destiny of the large scale structures has been recently analyzed in a series of N-body simulations by Messina *et al.* (1990; 1992), Moscardini *et al.* (1991), Matarrese *et al.* (1991) and Weinberg & Cole (1992).

Particular non-Gaussian random fields are usually defined e.g. by performing a nonlinear transformation on an underlying Gaussian random field; a possible statistics obtained in this way is the *lognormal distribution*, the prototype for multiplicative processes, which has been widely analyzed in cosmological framework (Coles & Barrow 1987; Lucchin & Matarrese 1988; Coles 1989; Coles & Jones 1990); negative mass events are not allowed in this statistics.

CHAPTER III

Statistical Measures of Galaxy Distribution

We now review some of the statistics, and observational data about those statistics, usually applied by cosmologists to describe the spatial distribution of galaxies and clusters.

The first systematic analyses of galaxies surveys concentrated on the measurement of low order galaxy correlation functions for two-dimensional sky survey (Totsuji & Kihara 1969; Peebles 1980; Sharp, Bonometto & Lucchin 1984). The same methods have been applied to the CfA survey (Shanks *et al.* 1983; Davis & Peebles 1983), the Abell cluster catalogue (Bahcall and Soneira 1983; Klypin and Kopilov 1983; Postman, Huchra & Geller 1992) and to the recent new catalogues e.g. the APM galaxy survey (Maddox *et al.* 1990; Dalton *et al.* 1992; Efstathiou *et al.* 1992). The cross correlations of galaxies and rich clusters have also been studied (Lilje & Efstathiou 1983)

A simple linear integral equation, Limber's equation (Limber 1953), provides us with the ability to obtain the *angular* correlations starting from the knowledge of the spatial correlations and/or viceversa (for a thorough exposition see Peebles 1980; for the inversion of Limber's equation see also: Fall & Tremaine 1977; Bonometto & Lucchin 1978).

3.1 Definitions

The probability that an object (galaxy, cluster of galaxies) is found in the infinitesimal volume δV chosen at random is defined by

$$\delta P = n \delta V , \quad (3.1)$$

where the mean number density n is independent from the position; this is an average on the ensemble. The probability of finding more than one object in δV is an infinitesimal of higher order if we assume, in the cases of practical interest, that the objects do not cluster in arbitrarily dense regions.

The two-point correlation function $\xi^{(2)}$ is defined in such a way that

$$\delta P = n^2 [1 + \xi^{(2)}(r_{12})] \delta V_1 \delta V_2 \quad (3.2)$$

is the *joint probability* of finding (two) objects in the volumes δV_1 and δV_2 , chosen at random and separated by the distance r_{12} . Consistently with the assumption of homogeneity and isotropy, $\xi^{(2)}$ has been written like a function of spatial separation. For a purely random process, the probabilities of finding objects in δV_1 and δV_2 are independent, so that the joint probability is the product of the single point probabilities

$$\delta P = n^2 \delta V_1 \delta V_2 , \quad (3.3)$$

In this case $\xi^{(2)} \equiv 0$; if the positions of the objects are correlated, $\xi^{(2)} > 0$; if the positions are anticorrelated, $-1 \leq \xi^{(2)} < 0$. $\xi^{(2)}$ is the excess or the defect of probability with respect to a purely random distribution (Poisson distribution).

An equivalent way to introduce the correlations is possible when the distribution of objects can be (approximately) described by a *continuous* density function, $\rho(\mathbf{x})$. A link relating discrete and continuous distributions is given, for example, defining the number density field for a point-like process as a sum over

Dirac delta function:

$$\rho(\mathbf{r}) = \sum_i \delta_D(\mathbf{r} - \mathbf{x}_i) , \quad (3.4)$$

with mean over the statistical ensemble of point processes

$$\langle \rho(\mathbf{r}) \rangle \equiv n . \quad (3.5)$$

The two-point function is then introduced as

$$\xi^{(2)}(r) \equiv \langle [\rho(\mathbf{x}) - \langle \rho \rangle] [\rho(\mathbf{x} + \mathbf{r}) - \langle \rho \rangle] \rangle / \langle \rho \rangle^2 = \langle \delta(\mathbf{x}) \delta(\mathbf{x} + \mathbf{r}) \rangle . \quad (3.6)$$

We stress the fact that $\xi^{(2)}(r)$ has a *different* meaning in this case: in the continuous case, $\xi^{(2)}(r)$ is the *autocovariance function* of the field $\delta(\mathbf{r})$ ie. a measure of the degree of spatial correlation of the density fluctuation $\delta(\mathbf{r})$; in the discrete case, we repeat, correlations are defined in term of probabilities of finding discrete objects at specified points.

If, viceversa, one is interested in generating a discrete distribution from a continuous one, the simplest method is to employ the *Poisson process* : given the continuous realization $\rho(\mathbf{x})$, one randomly places *one* particle in each volume $\delta V \equiv d\mathbf{x}$ with probability $\rho(\mathbf{x})d\mathbf{x}$ and independent probabilities for all volume elements. Correlations are built into the point process by correlations in the density field $\rho(\mathbf{x})$; for instance, the result of discretizing the continuous process $\delta(\mathbf{x})$ writes

$$\langle \delta(\mathbf{x}_1) \delta(\mathbf{x}_2) \rangle_{(d)} = \xi^{(2)}(r_{12}) + n^{-1} \delta_D(\mathbf{x}_1 - \mathbf{x}_2) , \quad (3.7)$$

where the Dirac delta function contribution to the correlation arises from discreteness, and it is not present in the continuous case; the outcome is a double random process, with one level of stochasticity coming from the random field $\rho(\mathbf{x})$ and a second from the Poisson sampling (see Peebles 1980, §33; Fry 1985a; Scherrer & Bertschinger 1991).

According to (3.6), it is possible to write

$$1 + \xi^{(2)}(r) = \langle \rho(\mathbf{x}) \rho(\mathbf{x} + \mathbf{r}) \rangle / \langle \rho \rangle^2, \quad (3.8)$$

and we can see that $\xi^{(2)}$ is the *connected* part of the two-point *complete* correlation function $\langle \rho(\mathbf{x}) \rho(\mathbf{x} + \mathbf{r}) \rangle / \langle \rho \rangle^2$.

In a similar fashion, the three-point function $\xi^{(3)}(r_{12}, r_{23}, r_{13}) \equiv \zeta$ is such that

$$\delta P = n^3 \left[1 + \xi^{(2)}(12) + \xi^{(2)}(23) + \xi^{(2)}(13) + \xi^{(3)}(12, 23, 13) \right] \delta V_1 \delta V_2 \delta V_3, \quad (3.9)$$

is the joint probability of finding (three) objects in the volume elements $\delta V_1, \delta V_2, \delta V_3$, separated by the distances r_{12}, r_{23}, r_{13} . The assumption of the homogeneity and isotropy of the Universe on large scales means that $\xi^{(3)}$ depends on the absolute value of the separations only, and it is a symmetric function of the three separations. If the distribution of the objects is described by a continuous density function, we have that

$$\xi^{(3)}(r, s, |\mathbf{r} - \mathbf{x}|) = \langle \delta(\mathbf{x}) \delta(\mathbf{x} + \mathbf{r}) \delta(\mathbf{x} + \mathbf{s}) \rangle \quad (3.10)$$

ie.

$$1 + \xi^{(2)}(r_{12}) + \xi^{(2)}(r_{23}) + \xi^{(2)}(r_{13}) + \xi^{(3)}(r_{12}, r_{23}, r_{13}) = \langle \rho(\mathbf{x}_1) \rho(\mathbf{x}_2) \rho(\mathbf{x}_3) \rangle / \langle \rho \rangle^3, \quad (3.11)$$

where $r_{ij} \equiv |\mathbf{x}_i - \mathbf{x}_j|$. $\xi^{(3)}$ is the *connected* part of the 3-point *complete* function (3.11), which is zero if the density distribution is Gaussian.

In general, by supposing that the distribution is approximately continuous, the N-point correlation function is defined by

$$\delta P = \left\langle \prod_{h=1}^N \rho(\mathbf{x}_h) \right\rangle \prod_{h=1}^N \delta V_h, \quad (3.12)$$

and the N-point joint probability contains all the *connected* correlations until order N, different from zero only for non-Gaussian distributions (we discuss in Appendix B the role of the reduced or connected moments in describing a general probability distribution).

As we shall see, the only galaxy correlation functions actually estimated are not above the fourth order; those higher than fourth order are undetermined because the scarcity of the available data (see Sharp, Bonometto & Lucchin 1984; Baumgart & Fry 1991).

3.2 Observational Data

One of the main observational tests of the large scale matter distribution is supplied by the analysis of the two point correlations of different sets of objects (from galaxies to superclusters). The relation

$$\xi_i^{(2)}(r) \approx (r/r_i)^{-1.8} \quad (3.13)$$

sufficiently interpolates the 2-point correlation for all classes of objects, each one characterized by a correlation length r_i and by an interval of distances where (3.13) holds. Moreover, there are indications that r_i increases with the richness of the system (Davis & Peebles 1983; Bahcall & Soneira 1983; Klypin & Kopilov 1983; Schectman 1985; Bahcall & Burgett 1986; Plionis & Borgani 1991).

Galaxies

The observed 2-point correlation for the galaxies has the form (see e.g. Peebles 1980)

$$\xi_g^{(2)}(r) = (r/r_g)^{-\gamma} , \quad (3.14)$$

$$\gamma = 1.77 \pm 0.4 , \quad (3.15)$$

$$r_g = 5.4 \pm 0.1 h^{-1} Mpc , \quad (3.16)$$

with $0.1 h^{-1} Mpc \lesssim r \lesssim 10 h^{-1} Mpc$ and $\xi_g^{(2)}(r) \ll 1$.

Hierarchical models reproduce this reasonably well in N-body simulations (Frenk *et al.* 1983; Davies *et al.* 1985; White *et al.* 1987; Frenk *et al.* 1988). The Durham deep-redshift sample (Shanks *et al.* 1989) indicates a correlation function with scale length $\sim 7 h^{-1} Mpc$, beyond which a break in the slope appears. There is persistent evidence that the correlation function is not a power law, but has a “shoulder” on scales $\sim 2 \div 5 h^{-1} Mpc$ (see also Dekel & Aarseth 1984; Guzzo *et al.* 1991), although this could arise because the data are in redshift space rather than true position (Kaiser 1987). There is also persistent evidence that the correlation function becomes negative at $20 h^{-1} Mpc$ never turning positive again, but this may be because the survey appears to avoid notable galaxy clusters; the newly compiled APM catalogue of more than 2 million galaxies reveals a strictly positive $\xi_g^{(2)}$ up to $\sim 50 \div 100 h^{-1} Mpc$, which is unexpected within the popular (biased) CDM model (Chapter VI). Peacock and Nicholson (1991), using an all-sky sample of *radio* galaxies at redshifts $z \leq 0.1$, find $\xi \approx (r/11 h^{-1} Mpc)^{-1.8}$ on scales up to several hundred Mpc; this strength of clustering is hardly surprising, since radio galaxies are elliptical and tend to reside in clusters.

In the case of the higher order galaxy correlation function, the results are essentially relative to 2-dimensional catalogs and they have pointed out an approximately hierarchical form for the connected correlations, in the sense that $\xi_g^{(3)}$ and $\xi_g^{(4)}$ can be expressed as sums of products of $N - 1$ ($N = 3, 4$) 2-point correlation functions; respectively (Groth & Peebles 1977; Fry and Peebles 1978; see also Peebles 1980)

$$\xi_g^{(3)}(1, 2, 3) \approx Q \left[\xi_g^{(2)}(12) \xi_g^{(2)}(23) + \xi_g^{(2)}(12) \xi_g^{(2)}(13) + \xi_g^{(2)}(13) \xi_g^{(2)}(23) \right] , \quad (3.17)$$

$$Q \approx 1.29 \pm 0.21 , \quad (3.18)$$

$$\xi_g^{(4)}(1, 2, 3, 4) \approx \sum_{ijkl} \left[R_a \xi_g^{(2)}(ij) \xi_g^{(2)}(jk) \xi_g^{(2)}(kl) + R_b \xi_g^{(2)}(ij) \xi_g^{(2)}(ik) \xi_g^{(2)}(il) \right] , \quad (3.19)$$

$$R_a \approx 2.5 \pm 0.6 ; \quad R_b \approx 4.3 \pm 1.2 . \quad (3.20)$$

Note that these hierarchical forms are symmetric in their arguments and go to zero if one or more objects are far from those remaining .

Fry (1984) showed that the above forms are originated by nonlinear evolution starting from Gaussian primordial conditions. The form of Eq.(3.17) appears in hydrodynamics, where the three-point complete correlation function is given by the Kirkwood superposition relation (Huang 1963; Ichimaru 1974). Melott & Fry (1986) extract a reasonable value of ζ from a big N-body simulation. Szalay (1988), in the biased scenario, computed the scaling coefficient Q in terms of the Hermite expansion of a general non linear thresholding function.

It has been attempted to obtain from the Zwicky Catalogue the 5-point correlation function, but with poor success, because the errors have the tendency to become comparable with the measurable quantities (Sharp, Bonometto & Lucchin 1984).

Clusters

Since the first quantitative analysis of (rich) cluster correlations (Hauser & Peebles 1973), showing that clusters are clumped on scales at least as large as $\sim 25 h^{-1} Mpc$ and possibly larger, it was known that the 2-point correlation function for the rich Abell clusters (number of galaxies $N_g > 65$) has the form (Bahcall & Soneira 1983; Klypin & Kopilov 1983; Postman, Geller & Huchra 1986)

$$\xi_c^{(2)}(r) \approx \left(\frac{r}{25 h^{-1} Mpc} \right)^{-1.8}, \quad (3.21)$$

out to separations of order $\sim 100 h^{-1} Mpc$, although this upper limit is controversial (Olivier *et al.* 1990; Sutherland & Efstathiou 1991). Note that this implies that $\xi_c^{(2)} \approx 20 \xi_g^{(2)}$ and the rich clusters of galaxies are observed to have greater amplitude than could be expected for the galaxy distribution on the same large scales.

Recently many controversies have grown about the first thought well established clustering of Abell clusters. Firstly, the Bahcall & Soneira sample (1983) is very small (only 104 clusters) and the statistical uncertainties are correspondingly large. A realistic analysis of the likely errors is given in Ling, Frenk & Barrow (1986). Secondly, there are considerable doubts as to the reliability of Abell's catalogue; in particular the visual method used to obtain the richness classes of clusters can lead to large systematic effects (Lucey 1983; Efstathiou *et al.* 1992). A careful analysis of a larger three dimensional cluster catalogue (Struble & Rood 1987) has, moreover, revealed clear evidence for projection effects in the Abell catalogue (Sutherland 1988) that, once allowed, reduce the amplitude of $\xi_c^{(2)}$ to ~ 1 at $14 h^{-1} Mpc$ rather than $25 h^{-1} Mpc$ (see also Dekel,

Blumenthal & Primack 1988)

$$\xi_c^{(2)}(r) \approx \left(\frac{r}{14 h^{-1} Mpc} \right)^{-1.8}. \quad (3.22)$$

This trend seems confirmed also by recent determinations of cluster correlation for the new APM cluster catalogue (Dalton *et al.* 1992; Efstathiou *et al.* 1992; see also Postman, Huchra & Geller 1992) and for ACO catalog (Mc Gill & Couchman 1989; Batuski *et al.* 1989).

In addition, the correlation length for the Abell clusters increases with cluster richness (Bahcall & Soneira 1983; Bahcall, Soneira & Burgett 1986). This can be understood qualitatively just because the richer clusters are rarer. Shectman (1985) determined the 2-point correlation for the identified poor clusters for the Lick catalog and confirmed the previous results: richer and more luminous systems are more strongly correlated (see also Plionis & Borgani 1991).

The Kirkwood relation for the three-point spatial correlation for the rich clusters has been analitically obtained by Politzer & Wise (1984) and, in a more general way, Matarrese, Lucchin & Bonometto (1986). The problem of estimating the 3-point correlation function of galaxy clusters has been recently addressed by several authors, both considering angular samples (Jing & Zhang 1989; Toth, Hollosi & Szalay 1989), three dimensional samples (Jing & Valdarnini 1991) and numerical simulations (Gott, Gao & Park 1991). All these analyses converge to indicate that the hierarchical model of Eq.(3.17) is consistent with data. However, although similar values of Q are worked out from such analyses, remarkably different estimates of the relative uncertainties were given, according to the different method used for the correlation and error analysis; these questions are summarized and addressed in Borgani, Jing & Plionis (1992).

Superclusters

Analyses like these have been extended to the supercluster scale. Bahcall & Burgett (1986) have studied the Supercluster Sample of Bahcall & Soneira (1984) and they found a positive correlation on scales of the order of $\gtrsim 10 h^{-1} Mpc$. If this correlation is quantified by the usual power law,

$$\xi_{sc}^{(2)}(r) \approx \left(\frac{r}{r_{sc}} \right)^{-\gamma}, \quad (3.23)$$

one has $r_{sc} \approx 60 h^{-1} Mpc$ (Bahcall & Burgett 1986), higher than r_c . The law (3.23) holds in the range $50 h^{-1} Mpc \lesssim r \lesssim 150 h^{-1} Mpc$.

These results, even more than those relative to the clusters, must be considered with caution, because of the smallness and the peculiarity of the statistical sample examined.

Richness-Correlation Relation

As suggested previously, there exists a tendency for the correlation between homogeneous systems of rising richness and scale (galaxies, clusters and superclusters) to increase. This fact is shown e.g. in Fig.1 and Fig.2 in Bahcall & Burgett (1986). A universally accepted theoretical justification of this does not exist, but some authors have attempted to explain such a tendency in the framework of the biased galaxy formation scenario (classical references are e.g.: Kaiser 1984; Politzer & Wise 1984; Schaeffer & Silk 1985; Fry 1986; BBKS 1986; Jensen & Szalay 1986; Matarrese, Lucchin & Bonometto 1986), where high peaks of the mass density field are taken as the sites where bright galaxies or rich clusters of galaxies form. The consequences of such a hypothesis are discussed in Chapter VI.

3.3 Power Spectra

Cosmological information is stored not only in the N -point correlation functions, but also, in a complementary way, in their Fourier transform, the *power spectra* (see e.g. Baumgart & Fry 1991; Peacock 1991).

Furthermore, to follow the ultimate gravitational collapse into condensed systems of initially small (Gaussian) perturbations, one must first determine an initial spectrum for density perturbations in the very early Universe.

The main physical observable connected with density perturbations, indeed, is the root-mean-square relative mass fluctuation $\sigma_M = \sqrt{\langle \delta_{\lambda M}^2 \rangle}$ inside a sphere of radius R ; cosmologists estimate it by e.g. the r.m.s. fluctuation in galaxy counts, $(\delta N/N)_g$. Such an observable can be expressed in terms of the relative density perturbation $\bar{\delta}(\mathbf{k})$ in Fourier space, which in turn can be expressed in terms of the 2-point correlation function

$$\sigma_M^2 = \frac{\langle M^2 \rangle - \langle M \rangle^2}{\langle M \rangle^2} = \frac{1}{2\pi^2} \int_0^\infty dk k^2 \langle |\bar{\delta}(\mathbf{k})|^2 \rangle \widetilde{W}^2(kR), \quad (3.24)$$

where $M \equiv \frac{4}{3}\pi\rho R^3$ is the mass inside the R -sphere and $\widetilde{W}(y) \equiv 3(\sin y - y \cos y)/y^3$, which is zero if $y \gg 1$ and one if $y \ll 1$: essentially all the perturbations with wavelength $\lambda \approx k^{-1} > R$ contribute to the variance σ_M^2 . Another important physical observable is the rms peculiar velocity on a given scale R (see e.g. Gorski 1988; Kashlinsky 1992 and references therein)

$$\sigma_v^2(R) = \langle v(R)^2 \rangle = \frac{H^2 f(\Omega)^2 a^2}{2\pi^2} \int_0^\infty dk \langle |\bar{\delta}(\mathbf{k})|^2 \rangle \widetilde{W}^2(kR), \quad (3.25)$$

where $f(\Omega) \approx \Omega^{0.6}$ (see §4.1).

The *power spectrum* can be defined from the expectation value of the two-point function in Fourier space, as follows (see e.g. Fry 1986; Bertschinger

1991)

$$\langle \bar{\delta}(\mathbf{k}_1) \bar{\delta}(\mathbf{k}_2) \rangle \equiv (2\pi)^3 \delta_D(\mathbf{k}_1 + \mathbf{k}_2) P(k_1). \quad (3.26)$$

If we assume that the density field is continuous, $P(k)$ is the Fourier transform of the 2-point correlation function $\xi(r)$ (Wiener-Kintchine theorem)

$$P(k) = \int d\mathbf{r} \xi(r) e^{i\mathbf{k}\cdot\mathbf{r}} = 4\pi \int_0^\infty dr r^2 \xi(r) \frac{\sin kr}{kr}, \quad (3.27)$$

$$\xi(r) = \frac{1}{(2\pi)^3} \int d\mathbf{k} P(k) e^{-i\mathbf{k}\cdot\mathbf{r}} = \frac{1}{2\pi^2} \int_0^\infty dk k^2 P(k) \frac{\sin kr}{kr}. \quad (3.28)$$

Once $\xi(r)$ is given, (3.27) can be considered another definition of $P(k)$; the Dirac delta function is required because of translational invariance: it is reminiscent of the ‘‘momentum conservation’’ in QFT Green’s function. Similarly, isotropy implies that $P(k)$ depends only on the magnitude of the wavevector \mathbf{k} . Instead of (3.24) and (3.25), we can write

$$\sigma_M^2 = \frac{1}{(2\pi)^3} \int d\mathbf{k} P(k) \widetilde{W}^2(kR), \quad (3.29)$$

$$\sigma_v^2 = \frac{H^2 f^2 a^2}{(2\pi)^3} \int d\mathbf{k} \frac{P(k)}{k^2} \widetilde{W}^2(kR). \quad (3.30)$$

We see here one of the several reasons for the importance of the power spectrum: apart from the presence of \widetilde{W} ($\widetilde{W} = 1$ for any \mathbf{k} if the density field is not smoothed out), we see that $P(k)d\mathbf{k}$ is the contribution to the variance of δ_M from modes with wavevectors in the volume element $d\mathbf{k}$ around \mathbf{k} .

Another manner for saying that is stated as follows: $d\sigma_M^2/d\ln k = (1/2\pi^2)k^3 P(k)$ is the contribution to the variance of δ_M per logarithmic interval of k . Moreover, $d\sigma_v^2/d\ln k = (1/2\pi^2)(aHf)^2 k P(k)$. If the power spectrum is peaked at some scale k_{max} , we can say that more energy is injected in correspondence of that scale, and

$$\sigma_M^2 \approx (1/2\pi^2) k_{max}^3 P(k_{max}),$$

$$\sigma_v^2 \approx (1/2\pi^2)(aHf)^2 k_{max} P(k_{max}).$$

Another reason for the importance of the power spectrum is that it completely specifies the statistics of a Gaussian random field (Appendix A; B).

As cosmologists are increasingly realizing (Baumgart & Fry 1991; Peacock 1991; Park 1991), $P(k)$ is a powerful *direct* statistic for describing both large-scale and small-scale structure.

Smoothing

For doing comparisons between observational data and theory, it is *necessary* to filter the fluctuation field $\delta(\mathbf{x})$ by means of a *window function* $W_R(x)$, $x \equiv |\mathbf{x}|$,

$$\delta_R(\mathbf{x}) \equiv \int dy \delta(y) W_R(|\mathbf{x} - y|) = \int dy \delta(\mathbf{x} - y) W_R(y). \quad (3.31)$$

The windowing convolution averages the fluctuation δ over the points y in a volume $\sim R^3$, where one has no interest in the substructure, filtering out the high frequencies corresponding to scales inside this volume: the physical information on scale $\lambda < R$ is completely lost.

The characteristic of $W_R(x)$ is to be essentially constant in the inner regions of radius R and practically zero in the outer regions, with $\int dx W_R(x) = 1$. The introduction of this cut-off is moreover justified by the fact that the high frequency content of the spectrum $P(k)$ can be overlooked, since the microscale fluctuations ($k \gg R^{-1}$) are not observable and also not relevant in cosmology (see e.g. BBKS).

Usually one assumes R as the typical size of the proto-object considered, and it is related to the mass M of the proto-object through $M(R) = 4\pi \langle \rho \rangle \int_0^\infty dx x^2 W_R(x) = c_{11} \langle \rho \rangle R^3$, c_{11} being a number that depends on the particular choice of the window function.

The result in (3.24) can be now understood in another manner: $\widetilde{W}(y) = 3(\sin y - y \cos y)/y^3$ is the Fourier transform of the “top-hat” window function $W_R(x) = 3\theta(x - R)/4\pi R^3$, introduced just because of the definition of mass given there, $M_{TH} = \frac{4}{3}\pi\langle\rho\rangle R_{TH}^3$. This is not necessarily realistic, an observational sample has indeed a complicated boundary determined by observational selection; moreover galaxies and clusters of galaxies do not have sharp edges.

An alternative assumption is that of a Gaussian window (see BBKS)

$$W_R(x) = (2\pi R^2)^{-3/2} \exp\left(-\frac{x^2}{2R^2}\right), \quad (3.32)$$

$$\widetilde{W}(kR) = \exp\left(-\frac{R^2 k^2}{2}\right), \quad (3.33)$$

for which $M_G = (2\pi)^{3/2}\langle\rho\rangle R_G^3$; $M_{TH} = M_G$ if $R_G = 0.64 R_{TH}$.

The arbitrariness of the smoothing procedure means one must be cautious about making quantitative predictions, particularly when these are sensitive to R . However, the filtering is not only a purely formal concept, but it can correspond to real physical processes (see Peebles 1980; BBKS).

All properties of $\delta(\mathbf{x})$ are inherited by $\delta_R(\mathbf{x})$ and for each observable relative to $\delta(\mathbf{x})$, there exists the correspondent relative to $\delta_R(\mathbf{x})$. In such a manner, the 2-point correlation of the filtered density field $\delta_R(\mathbf{x})$ is

$$\xi_R^{(2)}(\mathbf{x}_1 - \mathbf{x}_2) \equiv \langle \delta_R(\mathbf{x}_1) \delta_R(\mathbf{x}_2) \rangle = \int \int \left\{ \prod_{h=1}^2 d\mathbf{y}_h W_R(|\mathbf{x}_h - \mathbf{y}_h|) \right\} \xi^{(2)}(\mathbf{y}_1 - \mathbf{y}_2). \quad (3.34)$$

The Wiener-Kintchine relation reads

$$\xi_R^{(2)}(r) = \frac{1}{2\pi^2} \int_0^\infty dk k^2 \frac{\sin kr}{kr} P(k) \widetilde{W}_R^2(k). \quad (3.35)$$

One can say that

$$P_R(k) \equiv P(k) \widetilde{W}_R^2(k) \quad (3.36)$$

is the power spectrum of the fluctuation $\delta_R(\mathbf{x})$. In this context, δ_R represents the mass fluctuation in a volume of radius R , suitably smoothed by the chosen W_R .

The relation (3.29) can be written in the more general form as

$$\sigma_o(R) = \xi_R^{(2)}(0). \quad (3.37)$$

Origin

The most common choice of the wave-number analytical dependence of $P(k)$ is

$$P(k) \propto k^n. \quad (3.38)$$

n is the *primordial spectral index*, where $n > -3$ to provide convergence of the rms density fluctuation as $k \rightarrow 0$ (ie. asymptotic homogeneity) and $n < 4$ is imposed by the discreteness of matter (*minimal spectrum*; see Peebles 1980; Peacock 1991). The power-law form is chosen because we have no physical reason for picking out any characteristic scale: it is therefore a statement of our ignorance more than anything else.

The assumption (3.38) can be written in terms of primordial mass variance on scale M as

$$\sigma_M \propto M^{-(n+3)/6} \quad (3.39)$$

changing, because of evolution, to $\sigma_M \propto M^{-(n-1)/6}$ upon first coming within the horizon (see e.g. Peebles 1980): the *Harrison-Zel'dovich* $n = 1$ spectrum is characterized by a constant variance at the horizon crossing, independent of the scale; it is the most natural primordial power spectrum (Harrison 1970; Peebles & Yu 1970; Zel'dovich 1972), predicted in inflationary models too (Brandenberger 1985, 1990; Mukhanov, Feldman & Brandenberger 1992 and references therein).

The Zel'dovich spectrum also arises automatically if the fluctuations are due to cosmic strings (Zel'dovich 1980; Vilenkin 1981; see however Albrecht & Stebbins 1992) or to the more updated global textures (see Cen *et al.* 1991; Gooding *et al.* 1991). Other nomenclature which is worth mentioning is the *flicker-noise* spectrum ($n = -3$), and the *white-noise* spectrum ($n = 0$). Spectra with $n < 0$ ($n > 0$) imply more power on large (small) scale.

Evolution of the fluctuations after the inflation epoch modifies the spectrum. While the fluctuations are still linear the modification is simply a linear filtering, with transfer function $T(k, a) = P(k, a)/P(k, a_i)$. For a discussion of the transfer function in various cosmological models see Efstathiou (1990).

With a power-law model

$$P(k) = Ak^n e^{-k/k_c}, \quad (3.40)$$

where k_c is a short wavelength cut-off that is necessary if $n \geq 0$ (see Peebles 1980, § 42), some insights into $\xi(r)$ are obtained.

The autocorrelation function simplifies to

$$\xi(r) = \frac{A \Gamma(3+n)}{2\pi^2 (2+n)} \sin\left(\frac{(2+n)\pi}{2}\right) r^{-(3+n)}. \quad (3.41)$$

For $0 < n < 2$, ξ becomes anticorrelated at large r , approaching zero as r^{-3-n} , and first becomes negative at

$$r_o = k_c^{-1} \operatorname{tg}\left(\frac{\pi}{2+n}\right). \quad (3.42)$$

Therefore, sign and slope of ξ_{gg} on linear scales should provide direct information about the power spectrum there.

Normalization

Although inflation generically predicts the slope of the initial power spectrum, the overall amplitude is effectively a free parameter that cannot be calculated with any confidence because it is highly model dependent: it is usually assumed to be fixed by observations. However, there are, as yet, no observations that can be related unambiguously to the amplitude of linear fluctuations in the density field. Two prescriptions for fixing the normalization have been applied relatively widely.

The first is based on the second moment of the mass correlation function

$$J_3(R) \equiv \int_0^R dr r^2 \xi(r) = \frac{R^3}{6\pi^2} \int dk P(k) \widetilde{W}^2(kR), \quad (3.43)$$

compared with estimates from galaxy redshift surveys. There are several problems with this type of comparison (see e.g. Efstathiou 1990). By an analysis of the spatial correlation function from the CfA redshift survey (Huchra *et al.* 1983), Davis & Peebles (1983) find $J_3(10 h^{-1} Mpc) = 277 (h^{-1} Mpc)^3$ and $J_3(25 h^{-1} Mpc) = 780 (h^{-1} Mpc)^3$, although $10 h^{-1} Mpc$ is about the largest scale on which a reliable estimate of J_3 can be derived from the CfA survey (see Efstathiou 1990).

Another prescription for matching theoretical power spectrum with observations is similar and involves the variance of the galaxy distribution when sampled with randomly placed spheres of radius R (see Eq.(3.24)). Normalization now corresponds to specifying σ_R for some R . For $R = 8 h^{-1} Mpc$, the rms relative mass fluctuation is also denoted σ_8 . Galaxy number counts give $\sigma_8 \approx 1$ (Peebles 1982); if galaxies trace mass on scales of several Mpc and if nonlinear

effects do not modify σ_8 appreciably, then $\sigma_8 = 1$ is reasonable. In practice, this method of normalizing theoretical spectra is similar to the J_3 method.

If instead of assuming that galaxies accurately trace the mass distribution we adopt the less restrictive assumption that fluctuations in the galaxy distribution are proportional to fluctuations in the mass distribution, $(\delta\rho/\rho)_g = b(\delta\rho/\rho)$, $b = \text{const.} > 1$, then $\xi_g \approx \xi_\rho$ (see Kaiser 1984) and $\sigma_8 = b^{-1}$. In the $\Omega = 1$ adiabatic CDM model, which we discuss in detail in § 5.3, a “biasing” parameter of $b \approx 2$ is required for consistency with the observed peculiar velocities of galaxies and then the mass density fluctuations on scales $\gtrsim 8 h^{-1} Mpc$ are expected to be linear.

Other normalization prescriptions are based on measurements of peculiar velocity fields (see Eq.(3.25)) and of fluctuations of the microwave background radiation (Peebles 1982; Abbott & Wise 1984).

High Order Spectra

We can also evaluate higher order spectra. The *bispectrum* B is defined by the irreducible part of the 3-point correlation function in Fourier space

$$\langle \tilde{\delta}(\mathbf{k}_1) \tilde{\delta}(\mathbf{k}_2) \tilde{\delta}(\mathbf{k}_3) \rangle_c \equiv (2\pi)^3 \delta_D(\mathbf{k}_1 + \mathbf{k}_2 + \mathbf{k}_3) B(k_1, k_2) \quad (3.44)$$

ie.

$$B(k_1, k_2) = \int dr ds \zeta(\mathbf{r}, \mathbf{s}) e^{i\mathbf{k}_1 \cdot \mathbf{r} + i\mathbf{k}_2 \cdot \mathbf{s}} , \quad (3.45)$$

where, in the continuous case, ζ is the connected three point correlation function.

Fry & Seldner (1982) showed that if the three-point function is of hierarchical form (see Eq.(3.17)), then the bispectrum

$$B(k_1, k_2, k_3) = Q [P(k_1)P(k_2) + P(k_1)P(k_3) + P(k_2)P(k_3)] , \quad (3.46)$$

with the same value of Q , which can be also estimated by the simple gravitational instability picture in perturbation theory (Fry 1984).

Similarly, for the fourth moment we have

$$\langle \bar{\delta}(\mathbf{k}_1) \bar{\delta}(\mathbf{k}_2) \bar{\delta}(\mathbf{k}_3) \bar{\delta}(\mathbf{k}_4) \rangle_c \equiv (2\pi)^3 \delta_D \left(\sum_i \mathbf{k}_i \right) T(k_1, k_2, k_3) \quad (3.47)$$

where, by extension, T is the *trispectrum*

$$T(k_1, k_2, k_3) = \int d\mathbf{r} d\mathbf{s} d\mathbf{z} \eta(\mathbf{r}, \mathbf{s}, \mathbf{z}) e^{i\mathbf{k}_1 \cdot \mathbf{r} + i\mathbf{k}_2 \cdot \mathbf{s} + i\mathbf{k}_3 \cdot \mathbf{z}}, \quad (3.48)$$

and η is the connected 4-point correlation function. In the hierarchical model (see Eq.(3.18)), the trispectrum is the product of three power spectra

$$\begin{aligned} T(k_1, k_2, k_3, k_4) &= R_a [P(k_1) P(|\mathbf{k}_1 + \mathbf{k}_2|) P(k_3) + \text{c.p. (12 terms)}] \\ &+ R_b [P(k_1) P(k_2) P(k_3) + \text{c.p. (4 terms)}] . \end{aligned} \quad (3.49)$$

Recently, Baumgart & Fry (1991) claimed a strong detection of a third moment from CfA catalogue data (Huchra *et al.* 1983) and from a compilation of galaxy redshifts in the Perseus-Pisces supercluster region (Giovanelli & Haynes 1985; Giovanelli, Haynes & Chincarini 1986; Haynes *et al.* 1988). The observed bispectrum obeys the hierarchical pattern. The trispectrum, though weakly detected at best, still follows the hierarchical pattern.

Nonvanishing higher order ($N \geq 3$) moments imply that the galaxy distribution is decidedly non Gaussian, even on those large scales where correlations are very weak. This should not be surprising: in a nonlinear theory, even an initially Gaussian primordial distribution soon develops higher order correlations (Chapter VII).

CHAPTER IV

Growth of Perturbations

Cosmologists reasonably believe that observed structures grew from general small perturbations of the homogeneous and isotropic background in the energy density of the universe at early times.

The most largely accepted scenario to approach the structure formation is the so called *gravitational instability scenario*, which treats essentially noise amplification; ie. linear (small) perturbations at some early time grow to non linearity under their own self gravitation.

Since the beginning of modern cosmology, the role of gravity in developing the departures from homogeneity into structures like galaxies and clusters of galaxies has been at the center of exciting discussions (Einstein 1917; Jeans 1928; Lemaitre 1933a; 1933b; 1934). Curiously, Lifshitz, who developed the general analysis of linear perturbation in a Friedmann-Lemaitre model (Lifshitz 1946a; 1946b), stated that “we can apparently conclude that gravitational instability is not the source of condensation of matter into separate nebulae” (Lifshitz 1946b). Why Lifshitz’s statement was not quite correct was first pointed out by Novikov (1964a; 1964b).

Another problem is to understand the physical mechanism which could generate these fluctuations. Peebles (1980, §17) takes in consideration primeval magnetic fields, perhaps present at the time of the big bang, as possible sources

of mass density fluctuations.

Actually, cosmologists tend to solve the problem of the *origin* of the primordial fluctuations by accepting inflation: perturbations are generated during the epoch of vacuum energy domination, when the Universe is in an exponentially expanding de Sitter phase; primordial scalar fields placed in de Sitter space exhibit quantum fluctuations, generating perturbations to the matter density (Bardeen 1980; Guth & Pi 1982; Hawking 1982; Starobinsky 1982; Bardeen, Steinhardt & Turner 1983; Abbott & Wise 1984; Brandenberger 1985; Mukhanov, Feldman & Brandenberger 1992).

These quantum fluctuations manifest themselves as *curvature fluctuations* with a constant amplitude on the horizon scale as long as the inflation persists. Therefore it is a “natural” prediction of the inflationary model that the Universe should contain primordial fluctuations of scale-invariant form, as apparently confirmed by the more recent COBE measurements (Smoot *et al.* 1992).

Because these were generated by fluctuations in spatial curvature, they are *adiabatic* in nature, affecting the matter density and radiation density fluctuations equally, namely

$$\delta_r = \frac{4}{3} \delta_m . \quad (4.1)$$

A solution orthogonal to curvature fluctuation is conceivable: it is termed *isocurvature fluctuation*. This mode results from isothermal initial conditions, in which the matter density is perturbed, but not the radiation density

$$\delta_r = -\frac{\rho_m}{\rho_r} \delta_m , \quad (4.2)$$

where, in the radiation-dominated era, $\rho_m \ll \rho_r$: this generates no perturbations in the curvature, just because matter is a negligible constituent of the very early universe, instead modifying the number of photons per particle (entropy per

baryon), leading to the alternative name of *entropy perturbations*.

It is more natural to produce adiabatic fluctuations than isocurvature fluctuations, namely any GUT model, in which the baryon asymmetry of the Universe is generated via baryon number violation, will produce a constant entropy per baryon (Kolb & Turner 1990). Models have been suggested in which later phase transitions (e.g. quark-hadron transition) generate entropy fluctuations, but there is not clear evidence for them to be scale-invariant. Moreover, isothermal fluctuations generate adiabatic perturbations of the same magnitude, at horizon crossing time; this point has been further clarified by careful investigation of isothermal fluctuations through the epoch of decoupling (Suto, Sato & Kodama 1985): even initially isothermal perturbations give rise to temperature fluctuations in later stages comparable with those of initially adiabatic perturbations. This seems to rule out isothermal perturbations as a solution to the galaxy formation problem, but the possibility for them should not be rejected (Barrow & Turner 1981; Bond, Kolb & Silk 1982; Kofman & Linde 1987). For a detailed discussion of isocurvature perturbations using general relativity, see Kodama & Sasaki (1986). A recent fine review on cosmological perturbations is given by Mukhanov, Feldman & Brandenberger (1992).

4.1 Equations of Motion for Matter

We want now to describe in some detail the motion of nonrelativistic matter in the Universe; galaxies and clusters of galaxies are possibly tracing it now. Namely we present here the fundamental equations describing the growth of matter perturbations. We assume the (adiabatic) instability scenario: perturbations generated somehow in the early stages of the Universe start to grow

when (nonrelativistic) matter begins to dominate the density of the Universe; we assume the existence of post-recombination density fluctuations in nonrelativistic components of matter; it contains nucleonic matter as well as a collisionless dark matter component clustered around galaxies and clusters of galaxies.

We treat the matter as a pressureless ($p \equiv 0$) ideal fluid, ie. the particles' paths do not cross. The standard equations for an ideal fluid are the classical Poisson equation, Euler equation and continuity equation, ie. respectively, in Eulerian formulation

$$\nabla^2 \phi = 4\pi G a^2 (\rho - \rho_b) , \quad (4.3)$$

$$\frac{\partial \mathbf{v}}{\partial t} + \frac{1}{a} (\mathbf{v} \cdot \nabla) \mathbf{v} + \frac{\dot{a}}{a} \mathbf{v} = -\frac{1}{a} \nabla \phi , \quad (4.4)$$

$$\frac{\partial \rho}{\partial t} + 3 \frac{\dot{a}}{a} \rho + \frac{1}{a} \nabla \cdot \rho \mathbf{v} = 0 . \quad (4.5)$$

All the observables, potential ϕ , peculiar velocity \mathbf{v} and density ρ are functions of the comoving coordinates $\mathbf{x} = \mathbf{r}/a(t)$; the cosmic scale factor is not an unknown here, it is solution of the Friedmann equation (1.2).

The Poisson equation (4.3) states that (matter) density fluctuations originate, and are originated by, metric perturbations given by the Newtonian gravitational potential ϕ . The Euler equation (4.4) and the continuity equation (4.5) state respectively the momentum and the energy conservation during the evolution of the perturbations.

If we define the (mass) fluctuation $\delta(\mathbf{x}, t)$ as

$$\rho(\mathbf{x}, t) \equiv \rho_b(t) [1 + \delta(\mathbf{x}, t)] , \quad (4.6)$$

the previous system of equations takes the more familiar form in the literature

$$\nabla^2 \phi = 4\pi G \rho_b a^2 \delta , \quad (4.7)$$

$$\frac{\partial \mathbf{v}}{\partial t} + \frac{1}{a} (\mathbf{v} \cdot \nabla) \mathbf{v} + \frac{\dot{a}}{a} \mathbf{v} = -\frac{1}{a} \nabla \phi, \quad (4.8)$$

$$\frac{\partial \delta}{\partial t} + \frac{1}{a} \nabla \cdot (1 + \delta) \mathbf{v} = 0. \quad (4.9)$$

Essentially any relativistic component contributes negligibly to the density fluctuations, therefore *fluctuations* means *mass fluctuations*.

Sometimes, looking for δ solutions, a second order differential equation is introduced, obtained combining (4.8) and (4.9); explicitly it is given by (see e.g. Peebles 1980, § 9; Fry 1984)

$$\partial_0^2 \delta + 2\dot{a}a^{-1} \partial_0 \delta = a^{-2} \left[\partial_\alpha (1 + \delta) \partial_\alpha \phi + \partial_\alpha \partial_\beta (1 + \delta) v^\alpha v^\beta \right], \quad (4.10)$$

ie., from (4.7)

$$\begin{aligned} & \partial_0^2 \delta + 2\dot{a}a^{-1} \partial_0 \delta - 4\pi G \rho_b \delta = \\ & = 4\pi G \rho_b \delta^2 + a^{-2} \partial_\alpha \delta \partial_\alpha \phi + a^{-2} \partial_\alpha \partial_\beta (1 + \delta) v^\alpha v^\beta, \end{aligned} \quad (4.11)$$

where $\partial_0 \equiv \partial/\partial t$, $\partial_\alpha \equiv \partial/\partial x^\alpha$ and summation over repeated indices is understood.

The Eulerian fluid equations may also be derived by taking velocity moments of the Vlasov equation for the time evolution of the phase space distribution function $f(\mathbf{x}, \mathbf{v}, t)$: the streaming velocity of the fluid is defined as the local mean momentum per unit mass of the particles (for this alternative approach see Peebles 1980, §9A).

We stress that the comoving Euler and continuity equations hold *even* for large δ ; to apply Eq. (4.11) one must find some technique for dealing with the right-hand term: in the *linear* approximation such a term is just dropped.

Linear Solutions

The lowest order solutions of the fluid equations are recovered linearizing (4.7), (4.8) and (4.9): we assume that the amplitude of the matter fluctuations is very small ($\delta \ll 1$), so that the rms particle velocity about the zeroth-order Hubble flow solution is small too. The main reason for looking for linear solutions is that surely at early times $\delta \ll 1$ (because of CBR constraints), or, in other words, the linear description may be good for describing the large scale phenomena, even if $\delta \gg 1$ on small scales.

(i) Linear δ Solution

δ is solution of the equation (just dropping the right hand side of (4.11))

$$\partial_0^2 \delta + 2\dot{a}a^{-1} \partial_0 \delta - 4\pi G \rho_b \delta = 0 . \quad (4.12)$$

This equation has been discussed at length (Meszaros 1974; Groth & Peebles 1975).

The general growing mode (the decaying mode disappears rapidly: we'll not consider it) is given by

$$\delta(\mathbf{x}, t) = \delta_1(\mathbf{x}) D(t). \quad (4.13)$$

Therefore the δ solution is *self-similar* in the linear regime (in fact the Eq. (4.12) does not depend on spatial derivatives): δ evolve only in amplitude, preserving their original shape. Thus in the linear regime *structure retains a memory of its origin*.

The function $D(t)$, which satisfies the ordinary equation corresponding to (4.12)

$$\ddot{D} + 2\dot{a}a^{-1} \dot{D} - 4\pi G \rho_b D = 0 , \quad (4.14)$$

takes different forms depending on the model of Universe. For instance, in an Einstein-de Sitter universe ($\Omega = 1$, $\Lambda = 0$), we have $a \propto t^{2/3}$ and $4\pi G\rho_b = 2/3t^2$; therefore (4.14) reduces to

$$\ddot{D} + \frac{4}{3t}\dot{D} = \frac{2}{3t^2}D. \quad (4.15)$$

One finds

$$\delta(\mathbf{x}, t) = \delta_1(\mathbf{x})t^{2/3}. \quad (4.16)$$

Solutions for open or closed universes are given in Peebles (1980, § 11): usually they are much more complicated.

We stress the fact that the solution (4.16) is *local* even though the peculiar gravitational field \mathbf{g} depends on an integral over the mass distribution

$$\phi(\mathbf{x}, t) = -Ga^2\rho_b \int dx' \frac{\delta(\mathbf{x}', t)}{|\mathbf{x}' - \mathbf{x}|}, \quad (4.17)$$

$$\begin{aligned} \mathbf{g}(\mathbf{x}, t) &= -\frac{1}{a}\nabla\phi = Ga\rho_b \int dx' \delta(\mathbf{x}', t) \frac{\mathbf{x}' - \mathbf{x}}{|\mathbf{x}' - \mathbf{x}|^3} \\ &= Ga \int dx' \rho(\mathbf{x}', t) \frac{\mathbf{x}' - \mathbf{x}}{|\mathbf{x}' - \mathbf{x}|^3}; \end{aligned} \quad (4.18)$$

in fact, what is relevant is the divergence of \mathbf{g} ($\nabla \cdot \mathbf{g} \propto \nabla^2\phi$), which of course depends on local density.

The evolution of δ is non-local ie. non-selfsimilar to second order perturbation expansion.

(ii) Linear \mathbf{v} Solution

In the linear regime, the peculiar velocity field satisfies the equations

$$\partial_o(a\mathbf{v}) = a\mathbf{g}, \quad (4.19)$$

$$\nabla \cdot \mathbf{v} = -a\partial_o\delta. \quad (4.20)$$

By solving the last equation

$$\mathbf{v} = a\partial_o\left(\frac{\mathbf{g}}{4\pi G\rho_b a}\right), \quad (4.21)$$

which, once substituted in (4.19), gives us

$$\partial_o \left(a^2 \partial_o \frac{\mathbf{g}}{\rho_b a} \right) = 4\pi G a \mathbf{g} . \quad (4.22)$$

This is another form of the Eq.(4.12). The growing mode of the velocity field \mathbf{v} corresponds to the growing mode of the density field in (4.16):

$$\mathbf{v} = \frac{\mathbf{g}}{4\pi G \rho_b} \frac{d \ln D}{dt} . \quad (4.23)$$

In an Einstein-de Sitter universe we recover the classical $\mathbf{v} = \mathbf{g} t$ ($\sim t^{1/3}$).

Eq.(4.23) is usually known in the form (e.g. Peebles 1980, Eq.(14.8))

$$\mathbf{v} = \frac{H f}{4\pi G \rho_b} \mathbf{g} = \frac{2f}{3H\Omega} \mathbf{g} , \quad (4.24)$$

where

$$f = f(\Omega) \equiv \frac{d \ln D}{d \ln a} \quad (4.25)$$

is the logarithmic growth rate. The approximation $f(\Omega) \approx \Omega^{0.6}$ is commonly used (Peebles 1980); more accurately, the leading term near $\Omega = 1$ is $f(\Omega) = \Omega^{1/7}$ (Lightman & Schechter 1990; actually the first one to work out this result was Fry, in a not well known paper (Fry 1985b)). We stress the fact that \mathbf{v} is parallel to the acceleration \mathbf{g} (since (4.19)).

Eq.(4.24) is extremely important in observational cosmology; it offers the possibility of determining the density parameter Ω : this is usually done by measuring the infall velocity of the Local Group towards the Local Supercluster (see Davis & Peebles 1983).

We'll often use alternative expressions of the linear velocity; defining the Newtonian potential

$$\Delta \equiv \frac{\phi}{4\pi G \rho_b a^2} = -\frac{1}{4\pi} \int dx' \frac{\delta(\mathbf{x}', t)}{|\mathbf{x}' - \mathbf{x}|} , \quad (4.26)$$

for which

$$\nabla^2 \Delta = \delta , \quad (4.27)$$

$$\mathbf{g} = -4\pi G \rho_b a \nabla \Delta , \quad (4.28)$$

we get

$$\mathbf{v} = -\frac{1}{4\pi G \rho_b a} \frac{\dot{D}}{D} \nabla \phi = -a \partial_o \nabla \Delta = -a \frac{\dot{D}}{D} \nabla \Delta . \quad (4.29)$$

It is evident from these expressions that \mathbf{v} has zero vorticity.

It is often convenient, especially for instance when going to higher orders in perturbation theory, to work in \mathbf{k} -space, where one wins simplicity, since derivatives become simple algebraic operations.

The linear (growing) solutions of the equations of matter in \mathbf{k} -space look, respectively

$$-k^2 \bar{\Delta}(\mathbf{k}) = \bar{\delta}(\mathbf{k}) , \quad (4.30)$$

$$\bar{v}^\alpha(\mathbf{k}) = i a \frac{\dot{D}}{D} \bar{\delta}(\mathbf{k}) \frac{k^\alpha}{k^2} . \quad (4.31)$$

This simplification is not obtained at no cost, however; for instance the simple products in \mathbf{x} -space (\cdot) become *convolutions* ($*$) in the transform formulation

$$F\left(\prod_{h=1}^N f_h(\mathbf{x})\right) \equiv \left(\ast\right)_{h=1}^N \tilde{f}_h(\mathbf{k}_h) = \frac{1}{(2\pi)^{3N}} \int d\mathbf{k}_1 \cdots \int d\mathbf{k}_N \left[(2\pi)^3 \delta_D\left(\sum_{h=1}^N \mathbf{k}_h - \mathbf{k}\right) \right] \prod_{h=1}^N \tilde{f}_h(\mathbf{k}_h) .$$

Typical Scales: Critical Jeans Length

We have seen how the matter perturbations in an expanding universe grow; effectively, processes other than gravity can modify our simple description. Competing effects of gravity and pressure gradient force are in fact important

before the recombination or in correspondence of small scales: the more important result of taking into account the radiation pressure is that not all the matter perturbations are destined to grow, but only those above a precise scale.

Before recombination, matter is Compton radiation dragged and the matter plus radiation fluid can be treated as an ideal fluid.

Modifying the Euler equation to consider the pressure contribution, one finds that perturbation amplitudes of comoving wavelength $\lambda/a = 2\pi/k$ are described by a linear acoustic wave equation with Hubble dragging and gravitational driving terms (Peebles 1980)

$$\partial_{\circ}^2 \tilde{\delta}(\mathbf{k}, t) + 2\dot{a}a^{-1} \partial_{\circ} \tilde{\delta}(\mathbf{k}, t) = 4\pi G \rho_b \left[1 - \frac{\lambda_J}{\lambda} \right] \tilde{\delta}(\mathbf{k}, t). \quad (4.32)$$

At very long wavelengths (very large scales), $\lambda \rightarrow \infty$, this equation reduces to the zero pressure case discussed previously; but, at small scales, $\lambda \rightarrow 0$, the pressure term is dominant and the primordial plasma simply oscillates just like an acoustic wave. The balance between the pure gravitational regime and the acoustic regime occurs at the scale

$$\lambda = \lambda_J \equiv c_s \sqrt{\pi/G\rho_b}, \quad (4.33)$$

$c_s^2 = dp/d\rho$ being the square of the adiabatic sound speed. λ_J is called the *Jeans length*; it defines equivalently the *Jeans mass*

$$M_J = \frac{4}{3} \pi \rho_b \left(\frac{\lambda_J}{2} \right)^3 = \frac{\pi}{6} \rho_b \lambda_J^3. \quad (4.34)$$

M_J (ie. λ_J) fixes the smallest scale on which gravitational instability can be expected. At the recombination z_{rec} , M_J drops from its highest value $\approx 2.2 \times 10^{17} (\Omega h)^{-2} M_{\odot}$ to the much smaller $\approx 1.27 \times 10^6 (\Omega h)^{-1/2} M_{\odot}$, just because c_s drops from $c/\sqrt{3}$ to $\sqrt{5k_B T/3m_p}$ ($\approx 10 \text{ km s}^{-1}$), then $M_J \propto a^{-3/2}$ as the temperature falls down.

We know that the perturbations with $\lambda > \lambda_J$ grow as a power t^α of the cosmic time t (in a flat universe); those with $\lambda < \lambda_J$ behave like oscillating waves: in the limit $p \ll \rho c^2$ the cosmic expansion damps their amplitude (but not in the case $p = \rho c^2/3$) according to the law

$$\delta \sim [c_s(t) a(t)]^{-1/2} e^{-i \int^t dt c_s k/a} . \quad (4.35)$$

We could reconstruct at this point the history and the fate of a relevant sized fluctuation, say on a galaxy scale $M_G \sim 10^{11} M_\odot$, but the picture is effectively complicated by another process that we have not considered, the *Silk damping* (Silk 1968): the photon diffusion indeed damps out very efficiently the adiabatic baryon fluctuations below the Silk scale during the radiative era. The Silk scale can be estimated as follows. The photon mean free path is given by $l \sim (\sigma_T n_e)^{-1}$, where σ_T is the Thomson scattering cross-section and n_e is the number density of electrons. A photon diffuses a distance λ in the time $\tau_d(\lambda) \sim \lambda^2/lc$; the Silk damping scale is found if we equal $\tau_d(\lambda)$ to the Hubble time t ie. $\lambda_S \sim (lct)^{1/2}$, and the Silk mass is defined by

$$M_S = \frac{\pi}{6} \rho_m \lambda_S^3 . \quad (4.36)$$

Detailed calculations show that, at recombination (Silk 1968; Peebles & Yu 1970; Bonometto & Lucchin 1976; Press & Vishniac 1980; Wilson & Silk 1981; Peebles 1980; 1981)

$$M_S \approx 10^{12} (\Omega h^2)^{-5/4} . \quad (4.37)$$

All the fluctuations $\lambda < \lambda_S$ are damped by photon diffusion, since $\tau_d < t$; the damping rate, determined also by the fractional ionization of the hydrogen, increases for decreasing scales.

Depending on the spectrum of the primordial perturbation, the cutoff at M_S may fix the size of the first generation of objects to form after recombination. If $\Omega h^2 = 1$, $M_S \approx 10^{12} M_\odot$; if $\Omega h^2 = 0.03$, $M_S \approx 10^{14} M_\odot$ and

it is very interesting that one can find a reasonable interpretation for either of these numbers: the mass in the visible parts of the largest galaxies is $\sim 10^{12} M_{\odot}$ and the nominal mass in a rich cluster is $\sim 10^{14} M_{\odot}$. Thus, typical galaxies, $\sim 10^{11} M_{\odot}$, can form only by *fragmentation* of larger collapsed perturbations. This opens another problem. The value of the Silk cutoff, extrapolated to the present epoch is

$$\lambda_S \approx 2/(0.036 + \Omega h^2) Mpc, \quad (4.38)$$

which is uncomfortably large for any acceptable baryonic universe: if the amplitude at recombination is large enough to make bound systems of size M_S form, then we should also see density fluctuations of large amplitude on the scale λ_S . This *strongly* contradicts the observations that the galaxy 2-point correlation function is less than unity at $r \gtrsim r_0 \sim 4 h^{-1} Mpc$.

A way to solve the problem is to consider the isocurvature modes. In such a case, there is no Silk damping, just because the radiation is smoothed, and fluctuations on scales below the baryon Jeans mass (now $10^6 M_{\odot}$) can grow after recombination: in this picture, the larger structures form by hierarchical merging of sub smaller scale structures. This scenario, popular in the 1970's, is not actually so favoured, mainly because of small scale anisotropy constraints from CBR (Bond & Efstathiou 1984; Vittorio & Silk 1984), detailed N-body studies (Frenk 1986) and, overall, the requirement that Ω should take the value unity: this can occur only in non-baryonic dark matter universes, as we'll discuss in a next section.

4.2 An Application of Linear Theory: The Local Group Motion

The strongest evidence for a peculiar motion of the Local Group (LG) of galaxies is provided by the observations of the CBR.

Since the first convincing detection of anisotropy in the CBR (Fabbri *et al.* 1980), it was realized that a dipole anisotropy characterizes the microwave sky map: the dipole, amplitude $\Delta T/T \approx 1.2 \times 10^{-3}$, points roughly towards 45° away from the Virgo Cluster (namely, in galactic coordinates: $l = 268^\circ$, $b = 27^\circ$). The usual interpretation is that such a dipole is not a cosmological phenomenon, instead it is originated by the fact that the Earth is moving with respect the CBR rest frame. The recent spectacular COBE measurements confirm that $\Delta T/T = 1.2 \pm 0.03 \times 10^{-3}$ and $v_{LG} = 622 \pm 20 \text{ km s}^{-1}$ towards $(l, b) = (277^\circ \pm 2^\circ, 30^\circ \pm 2^\circ)$ (Smoot *et al.* 1991).

Using determinations of solar motion relative to the LG (Yahil, Tamman & Sandage 1977), Davis and Peebles (1983) quantified one component of the LG velocity, precisely the LG infall velocity towards the Virgo Cluster, located roughly at the center of the Local Supercluster ($\sim 10 h^{-1} \text{ Mpc}$ far from us). Knowing this, Davis and Peebles (1983) did the first determination of Ω_o from large scale dynamics. Adopting a simple spherical model, the LG infall velocity at distance R from the Virgo Cluster is related to the excess of mass δM located there by the linear equation (4.24)

$$v_V = \frac{2 G f(\Omega_o)}{3 H_o R^2 \Omega_o} \delta M , \quad (4.39)$$

or

$$v_V = \frac{1}{3} H_o R \Omega_o^{0.6} \frac{\delta M}{M} . \quad (4.40)$$

Assuming the Local Supercluster to be a fair indicator of the distribution of matter ie. estimating $\delta M/M = \delta N/N = \delta$, where $\delta N/N$ is the concen-

tration of bright galaxies in the LSC, one obtains

$$\Omega_o^{0.6} = 3 \left(\frac{v_V}{v_H} \right) \delta, \quad (4.41)$$

$v_H = H_o r$ being the Hubble flow velocity. Measurements in the LSC give $\delta N/N = 2.2 \pm 0.3$; $v_V = 400 \pm 60 \text{ km s}^{-1}$ and (Davis & Peebles 1983)

$$\Omega_{o,LSC} \approx 0.2. \quad (4.42)$$

The uncertainty on $\Omega_{o,LSC}$ is essentially due to the uncertainty in v_V ; on the other hand, a simple spherical model does not seem quite adequate, in view of the fact that the LG peculiar motion with respect to the rest frame of the MWB has other components besides v_V .

Many efforts are actually devoted to understanding the peculiar motion of the LG and its origin. Further modifications of the smooth Hubble flow have been revealed, and there is evidence that the LG motion is shared by the whole local volume within $30 \div 40 h^{-1} \text{ Mpc}$ (Staveley-Smith & Davies 1987; 1988).

An innovative suggestion has been advanced that the local galaxy bulk motions are caused by enormous mass concentrations just beyond $\approx 40 h^{-1} \text{ Mpc}$ (Dressler *et al.* 1987; Burstein 1989; Kaiser 1990a; Dressler 1991), this opening the era of the huge “attractors” (see e.g. Scaramella *et al.* 1989).

Another open question is the determination of Ω_o from large scales. Among others, an elegant technique consists in calculating the peculiar acceleration acting on the LG from the distribution of objects like galaxies and clusters of galaxies, as sampled by flux-limited catalogues (optical, IRAS, Abell, ACO, etc.): applying Eq.(4.39) one can obtain, in principle, estimates of Ω_o , namely $\Omega_o^{0.6}/b$, where b is a linear “bias” factor (see Chapter VI), from the deepest depths until now sampled (e.g. $\approx 300 h^{-1} \text{ Mpc}$ in Scaramella, Vettolani &

Zamorani (1991)). All these analyses seem to suggest the existence of a huge mass concentration towards the Centaurus region at $\sim 150 h^{-1} Mpc$, which could contribute to originate the LG motion, but the reliability of the estimated Ω_0 value is controversial, both for the biasing scheme dependence and/or statistical incompleteness of the available catalogues; moreover, the clustering pattern in redshift space may be strongly distorted by peculiar velocities (Kaiser 1987; McGill 1990; Strauss *et al.* 1992).

The existence of a large scale anisotropy towards Centaurus is confirmed by a recent analysis (Plionis, Coles & Catelan 1992) of the all-sky QDOT-IRAS redshift survey of galaxies (see Kaiser 1990b), where the questions of biasing dependence, statistical catalogue incompleteness and redshift distortion in doing Ω_0 determinations are discussed; we present the forthcoming paper in Appendix C.

In the next chapter we'll review other techniques with which it is possible to estimate the value of the density parameter Ω_0 .

CHAPTER V

The Mean Mass Density in the Universe

Measuring the mass density of the Universe is one of the most important tasks in observational cosmology, but it is not easy at all. In the previous section we showed how the value of the density parameter Ω_0 can be estimated by the Local Group infall to Virgo. Here we review other dynamical techniques for estimating Ω_0 (a fine review is in Peebles 1986). The missing mass problem is then discussed.

5.1 Dark Matter in Spiral Galaxies

From the fact that the rotation curves of spiral galaxies are flat (but see Persic & Salucci 1991 and references therein) from few kpc to distances well beyond the point where the light emission ceases (by observing the rare stars or 21-cm emission from neutral H, or HI, gas clouds; see e.g. Bosma 1981) it follows that the mass of *dark* halos is much larger than the entire visible mass. In particular, the mass-to-light ratio M/L can increase by a factor 100 in 10 kpc (Faber & Gallagher 1979; Carignan & Freeman 1985). From dynamical studies of the Milky Way's satellites (see Primack 1984), it is possible to set lower limits of $r_{halo} \gtrsim 70$ kpc and correspondingly $M/M_{lum} \gtrsim 10$ and $M \gtrsim 2 \times 10^{12} M_\odot$ for our own Galaxy. This mass is comparable to that suggested by studies of the dynamics of the LG of galaxies (Einasto, Koasik & Sear 1974).

A dark matter component is present also in large cosmic structures, like Abell clusters and superclusters; moreover the DM fraction increases with the scale. Indeed, the first one to show the presence of DM in the Universe was Zwicky (1933; 1937); analyzing the velocity dispersion of galaxies in Coma Cluster, Zwicky demonstrated that $M_{COMA,dyn}/M_{COMA,tum} \gtrsim 100$.

The presence of DM in spiral galaxies translates into a DM contribution to Ω_0 .

To quantify it, we remember that the observed galaxy luminosity density is roughly (see e.g. Peebles 1980)

$$\langle L \rangle \approx 1.8 \times 10^8 h L_\odot Mpc^{-3} , \quad (5.1)$$

where $L_\odot = 3.83 \times 10^{33} \text{ erg } s^{-1}$. With this, we can evaluate the mean mass-to-light ratio of the Universe

$$M/L = \Omega \rho_c / \langle L \rangle \approx 1500 \Omega h M_\odot / L_\odot . \quad (5.2)$$

Typically, in the central regions of galaxies (Efstathiou & Silk 1983)

$$M/L \approx 14 h M_\odot / L_\odot , \quad (5.3)$$

then

$$\Omega_{gal} = \rho_{gal} / \rho_c \approx 0.02 , \quad (5.4)$$

if we take into account the entire visible mass.

On the other hand, if the *dynamical* galactic mass, including that of the halo, is about ten times greater, as previously discussed, then

$$\Omega_{dyn} = \rho_{dyn} / \rho_c \approx 0.2 . \quad (5.5)$$

This is the strongest evidence that the *observed* Universe is open and that 90% of the dynamical mass in the Universe is *dark*.

Remembering that hot big bang primordial nucleosynthesis and the observed light element cosmic abundances constrain the baryonic contribution Ω_b of the matter density (Yang *et al.* 1984; Walker *et al.* 1991)

$$\Omega_b \lesssim 0.1 , \quad (5.6)$$

we conclude that essentially all the dynamical mass can be in baryonic form. However, an Einstein-de Sitter (or inflationary) $\Omega = 1$ Universe cannot be baryonic.

5.2 Correlation Analysis

Galaxy correlation data, combined with estimates of the relative *peculiar* velocity between pairs of galaxies, can be used to give dynamical estimates of Ω . In order to use these data to estimate the mean content of matter in the Universe, it is fundamental to assume that the luminous matter distribution coincides with the underlying mass distribution. However this is not the case; it is known that the rich clusters are more correlated than galaxies (Kaiser 1984), therefore they cannot *both* be good tracers of the mass, perhaps neither are. For the moment we ignore the problem (however it will come up again in Chapter VI), and assume that the galaxies are good tracers of the mass, with $\delta\rho/\rho \sim \xi_g(r) = \xi(r)$ (Efstathiou & Silk 1983).

Peculiar Galaxy Dynamics

According to Peebles (1980), the rms of the peculiar velocity field $\mathbf{v}_{12} \equiv \mathbf{v}_1 - \mathbf{v}_2$ of a pair of galaxies at comoving separation $\mathbf{u} = \mathbf{u}_1 - \mathbf{u}_2$ is

$$\langle v_{12}^2(r) \rangle = \frac{6 G \rho_b}{\xi^{(2)}(r)} \int_r^\infty \frac{dr}{r} \int d\mathbf{z} \frac{\mathbf{r} \cdot \mathbf{z}}{z^3} \xi^{(3)}(r, z, |\mathbf{r} - \mathbf{z}|) , \quad (5.7)$$

where $\mathbf{r} = a(t)\mathbf{u}$, \mathbf{z} is a fixed position relative to the pair of galaxies. By Eqs.(3.14) and (3.17), the previous relation reduces to the form (Peebles 1980)

$$\langle v_{12}^2(r) \rangle = \frac{6\pi G\rho_b Q r_g J(\gamma)}{(\gamma - 1)(2 - \gamma)(4 - \gamma)} r^{2-\gamma}, \quad (5.8)$$

where $J(1.8) = 3.70$. Eq.(5.8) is known as the *Cosmic Virial Theorem*. It can be understood also remembering that the mass of a typical aggregation of matter with $r \ll r_g$ is

$$M(r) \approx \rho r^3 \approx \rho_b \xi_g^{(2)}(r) r^3 \approx \rho_b r_g^\gamma r^{3-\gamma} \quad (5.9)$$

and therefore the currents on scale r are

$$v(r)^2 \approx GM(r) r^{-1} \approx G\rho_b r_g^\gamma r^{2-\gamma}; \quad (5.10)$$

we observe that $\langle v_{12}^2(r) \rangle$ is the sum of the contributions of motions on all the scales $\lesssim r$ interior to the subclusters. Since $\gamma < 2$, the main contribution to this sum is given by the currents in correspondence of the scale r , so that Eq.(5.10) coincides with Eq.(5.8).

We can rewrite Eq.(5.8) as

$$\Omega \equiv \rho_b/\rho_c \approx Q^{-1} \left(\frac{\sqrt{\langle v_{12}^2(r) \rangle}}{800 \text{ km s}^{-1}} \right)^2 \left(\frac{1 \text{ h}^{-1} \text{ Mpc}}{r} \right)^{2-\gamma}. \quad (5.11)$$

Observationally, from estimates of redshifts (Davis & Peebles 1983; Bean *et al.* 1983)

$$\sqrt{\langle v_{12}^2 \rangle} = 300 \pm 50 \text{ km s}^{-1} \quad (5.12)$$

on scales $\sim 1 \text{ h}^{-1} \text{ Mpc}$, with a slight dependence on r compatible with Eq.(5.8).

By the Cosmic Virial Theorem with $Q \approx 0.7 \div 1.3$, one has

$$\Omega \approx 0.1 \div 0.2. \quad (5.13)$$

Cosmic Energy Equation

Another estimate of Ω can be obtained by applying the *Cosmic Energy Equation* (Layzer 1963; 1964; Dmitriev & Zel'dovich 1964; Irvine 1965)

$$\frac{d}{dt}(T + W) + \frac{1}{a} \frac{da}{dt} (2T + W) = 0 . \quad (5.14)$$

Eq.(5.14) relates the cosmic potential energy per unit mass W with the cosmic kinetic energy per unit mass T due to the gravitational interaction with the rest of the Universe. In particular, Eq.(5.14) relates the velocity dispersion along a fixed direction, say \bar{v}_p , of a galaxy, with the potential energy stored in the mass fluctuations (see Peebles 1980).

The differential equation (5.14) can be approximated by an algebraic relation (Davis & Peebles 1983)

$$\bar{v}_p^2 \approx \frac{2}{7} H_o^2 J_2(\infty) \Omega , \quad (5.15)$$

where $J_2(\infty) = \int_0^r d\tilde{r} \xi_g^{(2)}(\tilde{r})$ and H_o is the Hubble constant. If $\xi_g^{(2)}$ is negligible at $r \gtrsim 20 h^{-1} Mpc$ one has $J_2(\infty)h^2 \approx 150 Mpc^2$, from which

$$\Omega \approx \left(\frac{\bar{v}_p}{660 \text{ km/s}} \right)^2 , \approx 0.25 , \quad (5.16)$$

where $\bar{v}_p \approx 330 \text{ km s}^{-1}$ (Davis & Peebles 1983).

Statistical Equilibrium

An estimate of Ω due to Davis & Peebles (1983) is based on the assumption that the matter clustering on scales less than $1 h^{-1} Mpc$ is statistically stable, ie. the Hubble flow and the processes of gravitational collapse are compensated *on average*. This condition can be written as

$$\sigma_v(r)^2 \approx 4.13 Q (H_o r)^2 \xi_g^{(2)}(r) \Omega , \quad (5.17)$$

where $\sigma_v(r)$ is the line of sight rms fluctuation of the difference of the peculiar velocities of correlated pairs of galaxies at separation r ; such a quantity is measured precisely on scales $hr < 5 Mpc$:

$$\sigma(r) = \sigma_o \left(\frac{hr}{1 Mpc} \right)^{(0.13 \pm 0.04)} km s^{-1}, \quad (5.18)$$

$$\sigma_o = 340 \pm 40 km s^{-1}, \quad (5.19)$$

$$10 kpc \lesssim hr \lesssim 1 Mpc. \quad (5.20)$$

Finally we obtain

$$\Omega \approx Q^{-1} \left(\frac{\sigma_o}{900 km s^{-1}} \right)^2 = 0.20 e^{\pm 0.4}, \quad (5.21)$$

compatible with previous results.

We have to stress that all these methods, estimating the mean mass clustered on scale $\sim 1 h^{-1} Mpc$, are insensitive to a possible component of dark matter that is not clustered on such a small scales, but instead distributed rather uniformly in the Universe (see Dekel & Rees 1987). The ‘biased’ galaxy formation scenario, according to which the galaxies form where the high peaks of the field $\delta\rho/\rho$ are, can reconcile the observed value of Ω with the larger theoretical value.

Conclusions:

The accurate measurement of the cosmological density parameter is difficult, but it probably lies in the range $0.1 \lesssim \Omega \lesssim \text{few}$. Large Ω , such as the Einstein-de Sitter value $\Omega = 1$, are excluded, unless mass density is distributed considerably more broadly than luminosity.

Arguments for $\Omega = 1$

As we have seen, the value of Ω is of course an observational question. Despite of the dynamical estimates of Ω , we review some theoretical arguments which have been advanced in support of $\Omega = 1$. A more detailed discussion is given in Peebles (1986 and references therein).

- (i) In Guth's inflation model (Guth 1984), the expansion of the Universe can be traced back to a phase transition before which the energy density would have had a large nearly constant term (which behaves like a large Λ -term) that would have caused space to expand as an exponential function of time (instead of the power-law expansion of the usual models). If this exponential *inflationary* phase lasted long enough, it could have stretched all characteristic lengths. This implies that the curvature term in Friedmann equation (Eq.(1.2)) is negligibly small. This brings us to $\Omega = 1$
- (ii) Galaxy formation seems to be easier to understand if $\Omega = 1$. Actually in a purely baryonic universe, $\Omega = \Omega_b \approx 10^{-1}$, the adiabatic perturbations cannot collapse in cosmic proto-objects without violation of the CBR isotropy: indeed at recombination their amplitudes should be $\delta_b(z_{rec}) \gtrsim (\Omega z_{rec})^{-1} \gtrsim 10^{-2}$. On the contrary, if $10^{-1} \approx \Omega_b < \Omega = 1$ then $\delta_b(z_{rec}) \approx 10^{-3}$ compatible with the CBR constraints $\delta T/T < 10^{-4}$ (Bond & Efstathiou 1984; Vittorio & Silk 1984).
- (iii) Galaxy biased clustering (Chapter VI).

The amount of (dark) matter in the Universe is strictly related to the age of the Universe. If one assumes the existence of a non baryonic component weakly interacting with the other components and closing the Universe, formed by (unspecified) massive particle, say X , such that $\Omega_b < \Omega_X \approx \Omega \approx 1$, it is possible to fix the following constraint.

Remembering that, for a matter dominated model with $\Omega = 1$, the age of the Universe is given by

$$t_o = \frac{2}{3} H_o^{-1} \approx 6.5 h^{-1} Gyr , \quad (5.22)$$

and, since the oldest stars in globular clusters formed at least $10 \div 13 Gyr$ ago, it must be that $h \lesssim 0.5 \div 0.65$, from which

$$\Omega_X h^2 \lesssim 0.25 \div 0.425 . \quad (5.23)$$

We remember that the parameter Ωh^2 is very often present in the cosmological expressions. We stress that, if a cosmological term is absent, the values $\Omega = 1$ and $H_o = 100 km s^{-1} Mpc^{-1}$, which is the maximum value of H_o , are incompatible, since for a such a type of universe $t_o \approx 6.5 Gyr$; instead, it must be $H_o \lesssim 60 km s^{-1} Mpc^{-1}$ ie. $h \lesssim 0.6$. Standard CDM model assumes $\Omega = 1$ and $h = 0.5$.

5.3 Non Baryonic Dark Matter in the Universe

The particle candidates to constitute the cosmological dark matter are essentially divided in three classes: Hot, Warm and Cold DM particles. The classification has been introduced by Bond, Primack & Blumenthal (Primack & Blumenthal 1983; Primack 1984), in terms of the *free-streaming* of the DM particles. The free-streaming distance is the mean distance covered by the DM particles, since the decoupling with the other components of the primordial plasma to the moment in which they are not longer relativistic. Collisionless particles, as the DM particles, rapidly dissipate the fluctuations with wavelength below the free-streaming distance. Essentially, the fluctuations on a typical galactic scale ($\approx 10^{11} M_\odot$) are dissipated by hot particles, but preserved with warm particles;

all the cosmologically significant fluctuations survive in universes dominated by cold dark particles.

Of course, there is the possibility that the dark matter is a mixture of, for instance, “jupiters” plus neutrinos (Schramm & Steigman 1981). Some models even include unstable DM that decays into relativistic particles (Sciama 1990a; 1990b; Splinter & Melott 1992).

For brevity, we’ll consider in more detail the cosmological implications of two types of particles, the hot and cold DM particles, since these seem the more promising scenarios. The WDM scenario shows considerable intrinsic difficulties; for instance, there is at present no obvious warm DM candidate elementary particle, in contrast to the hot and cold DM cases.

Hot Dark Matter (HDM)

‘Hot’ dark matter is any form of non-baryonic dark matter that has a relativistic velocity at the time of equal matter and radiation ($z \sim 10^4$). The standard candidate is the massive neutrino, which has to have a mass $m_\nu \approx 30 \text{ eV}$ for being cosmologically important (Gershtein & Zel’dovich 1966; Bond, Efstathiou & Silk 1980). There is no conclusive evidence that there actually exists a species of neutrino with the required mass.

The important fact about neutrinos (or other HDM particles) is that they are expected to be relativistic at decoupling, with neutrino decoupling temperature $T_{d,\nu} \approx M_{Pl}^{-1/3} G_F^{-2/3} \approx 1 \text{ MeV}$, where the Planck mass $M_{Pl} = 1.22 \times 10^{19} \text{ MeV}$ and the Fermi constant $G_F \approx 10^{-5} \text{ GeV}^{-2}$; they remain relativistic until the matter temperature drops to $\approx m_\nu$. During this interval of time, the neutrinos stream freely over a distance $\lambda_\nu = \lambda_h(T = m_\nu) \sim M_{Pl} m_\nu^{-2}$, where $\lambda_h \sim (G\rho)^{-1/2} \sim M_{Pl} T^{-2}$. In order to survive this free streaming, a neutrino

fluctuation must have linear size $> \lambda_\nu$. Correspondingly, the minimum mass in neutrinos of a surviving fluctuation is $M_{J,\nu} \approx \lambda_\nu^3 m_\nu n_\nu(T = m_\nu) \approx M_{Pl}^3 m_\nu^{-2}$. Thus, even collisionless particles effectively exhibit a Jeans mass (*free-streaming Jeans mass*). Careful calculations (Bond, Efstathiou & Silk 1980; Bond & Szalay 1984) give

$$\lambda_\nu = 41 \left(\frac{m_\nu}{30 \text{ eV}} \right)^{-1} (1+z)^{-1} \text{ Mpc} , \quad (5.24)$$

or $\lambda_\nu = 41 (m_\nu/30 \text{ eV}) \text{ Mpc}$ in *comoving coordinates*. The corresponding neutrino Jeans mass is

$$M_J = 1.77 M_{Pl}^3 m_\nu^{-2} = 3.2 \times 10^{15} (m_\nu/30 \text{ eV})^{-2} M_\odot , \quad (5.25)$$

which is the mass scale of superclusters; objects of this size are the first to form in a ν -dominated universe, so that galaxies must form by fragmentation of early larger structures.

Note that when a fluctuation of total mass $\approx 10^{15} M_\odot$ enters the horizon at the equivalence epoch $z \approx 10^4$, the photon-baryon fluid perturbations cease growing, starting to oscillate as an acoustic wave, while those of the massive neutrinos continue to grow linearly with rate $(1+z)^{-1}$. At recombination, $z \approx 10^3$, $\delta_{r-m}/\delta_\nu \lesssim 10^{-1}$, with an eventual additional suppression of δ_{r-m} by Silk damping (see Primack 1984, Fig. 3.4). Thus the hot DM scheme with adiabatic primordial fluctuations predicts small-angle fluctuations in the CBR somewhat below observational limits (Uson & Wilkinson 1984). Similar arguments apply in the CDM scenario (Bond & Efstathiou 1984; Vittorio & Silk 1984).

There exist however a number of problems with the neutrino dominated universe.

- (i) From dynamical studies of non-linear clustering, $\lambda \lesssim 10 \text{ Mpc}$, and bulk velocities in the linear regime, the supercluster formation is not an ancient

event: $z_{SC} < 2$ in any case (Frenk, White & Davis 1983; Kaiser 1983). On the other hand, limits on galaxy ages from globular clusters (Faber 1984), and determinations of high redshift quasars (Warren *et al.* 1987) and radio sources (Lilly 1988; Chambers, Miley & van Breugel 1990), indicate that $z_{GF} \gtrsim 3$. This *timing-scaling problem* has severe implications for the neutrino pancake model. However, since a recent radio detection of neutral H at redshift $z = 3.4$ (Uson, Bagri & Cornwell 1991), claimed as the first observational evidence of a Zel'dovich pancake, the timing-scaling problem could be not so acute.

- (ii) Another problem regards the ratio mass *vs.* baryonic mass at small and large scales. Large clusters ($\geq 10^{14} M_{\odot}$) should contain a larger amount of neutrino component than the galaxies ($\approx 10^{12} M_{\odot}$), and M/M_b should increase by a factor ~ 5 from galactic scale to supercluster scale (Bond, Szalay & White 1983). Such a trend is not observed.
- (iii) Both theoretical arguments related to the dwarf spheroidal (*dS*) galaxies around the Milky Way (Faber & Lin 1983) and data on Draco, Carina and Ursa Minor (Aaronson 1983; Aaronson & Olszewski 1988) imply that dark matter is present in exceptionally large amounts in these systems. The phase-space constraint (Tremaine & Gunn 1979) then sets a lower limit $m_{\nu} > 500 \text{ eV}$ (Lin & Faber 1983), which is completely incompatible with the cosmological constraints (Gershtein & Zel'dovich 1966). Viceversa, for reasonable neutrino mass, ($\approx 30 \text{ eV}$), phase-space limits would then require very large core radii ($\sim 10 \text{ kpc}$) and masses ($\sim 4 \times 10^{11} M_{\odot}$): objects of such enormous masses would have spiraled into and merged with the Milky Way long ago (Gerhard & Spergel 1992).

The general problem with HDM is that it may possess too little power

on small scales, just due to its own free streaming scale. One possible way to correct that problem is to produce density fluctuations not from inflation but from *seed* perturbations. Seeded hot dark matter models have been recently studied by a large numbers of people (Scherrer, Melott & Berschinger 1989; Villumsen, Scherrer & Bertschinger 1991; Cen *et al.* 1991). Traditionally, in these studies the seeded perturbations have been taken to be either primordial black holes, cosmic strings or global textures, and have been quite successful at improving the small scale power relative to the standard hot dark matter models.

Cold Dark Matter (CDM)

Whereas HDM is characterised by a free-streaming mass $M_J \sim 10^{15} M_\odot$, cold dark matter has a free streaming mass very much smaller than the mass of a galaxy ($< 10^8 M_\odot$), since the CDM particles decouple and become non relativistic much earlier than the hot particles. There are a host of plausible particle physics candidates for CDM including *axions* of mass $\sim 10^{-5}$ eV (Weinberg 1978; Wilczek 1978; Ipser & Sikivie 1983; Sikivie 1983); a heavy, weakly interacting, stable *photino*, with a mass $\gtrsim \frac{1}{2}$ GeV (Goldberg 1983; Ellis *et al.* 1984); and *primordial black holes* with $10^{17} g \lesssim M \lesssim M_\odot$ (Carr 1978; Stecker & Shafi 1983; Freese, Price & Schramm 1983; Mac Gibbon 1987). These and other CDM candidates are reviewed in e.g. Primack (1984). None of these candidates has yet been detected, although experiments are capable of detecting cosmological abundances of some of them (Smith 1988; Ellis 1991).

Assuming that the primordial fluctuations are adiabatic, when the Universe is radiation-dominated, the perturbations in the CDM grow as $\delta \sim R^2$ on scales larger than the horizon. When a fluctuation crosses the horizon in this era, the photons and charged particles oscillate as an acoustic wave and the neutrinos,

assumed to be massless in this scenario, stream away. This means that the driving term for the growth of the CDM perturbations disappears and the growth consequently *stagnates* until we reach the transition to matter-domination at $z \approx 10^4$ (Blumenthal *et al.* 1984), after which all linear modes grow with the same rate; as a consequence, the fluctuation power spectrum has a discontinuity at the horizon scale. The detailed growth of fluctuations in this scenario must be handled essentially numerically, although it is possible to make substantial analytic progress using a gauge-invariant formalism (Peebles 1982a; 1982b; Vittorio & Silk 1984; Bond & Efstathiou 1984; Efstathiou 1990 and references therein). The detailed solutions are obviously complicated, but they are characterized by limiting forms. The initial power spectrum $P(k) \propto k^n$ is modified so that

$$P(k) \propto k^{n-4} \ln k. \quad (5.26)$$

Thus, for mass scales much less than the horizon mass at the matter-radiation equivalence ($M_{eq} \approx 10^{15} M_\odot$), we get

$$\frac{\delta M}{M} \sim (\ln M)^{3/2}, \quad (5.27)$$

so that the spectrum is rather flat for $M \ll M_{eq}$. If $n = 1$, the spectrum steepens to

$$\frac{\delta M}{M} \sim M^{-2/3}, \quad (5.28)$$

for $M \gg M_{eq}$. A more detailed discussion of the growth of perturbations in this scenario is given in a fine review by Blumenthal *et al.* (1984).

In this scenario, as in the HDM case, the CDM perturbations can start to grow *before* the baryons decouple from the radiation. After recombination ($z \approx 10^3$), the baryon fluctuations grow rapidly to match the CDM fluctuations (they tend to fall into the potential well created by the CDM perturbations): in this model the first structures to form will be of the order of the baryon Jeans

mass after recombination, $\sim 10^6 M_\odot$ (“bottom-up” scenario).

The CDM model has been considered, during the last years, the most successful theory for the formation of structure in the Universe (Davis *et al.* 1992). However it has recently suffered some setbacks from observational evidence suggesting that there is more large-scale power than it can explain.

The most serious of these observational challenges has come from statistical studies of the galaxy distribution on large scales ($\gtrsim 10 h^{-1} Mpc$). The recent APM catalogue of more than 2 million galaxies reveals indeed more large-scale structure than predicted by simple versions of the theory (Maddox *et al.* 1990). Further evidence has come from infrared galaxies detected with the IRAS satellite (Efstathiou *et al.* 1990; Saunders *et al.* 1991), from clusters of galaxies (Bahcall & Soneira 1983) and from radio galaxies (Peacock & Nicholson 1991).

Possible fixes for the CDM model involve decaying particles or departures from the scale-invariant fluctuations predicted by simple inflationary models. For instance, the predictions for large-scale structures can be boosted if 17-keV neutrinos (Simpson 1985; Hime & Jelley 1991) really do exist (in addition to CDM) and decay on a timescale of $\sim 1 \div 5$ years (Bond & Efstathiou 1991). Alternatively, one can construct models of inflation that are tuned (for example, by involving multiple scalar fields) to produce seed fluctuations with a large-scale characteristic length (Salopek, Bond & Bardeen 1989). A third possibility is that primordial fluctuations do not arise from quantum processes during inflation, but rather reflect the gravitational effect of topological defects generated at a different phase transition. Recent work, however, indicates that the cosmic string model, for a long time the most promising of its kind, actually produces less large-scale structure than standard CDM (Albrecht & Stebbins 1992)! Cosmic textures, a type of topological knot that unties itself as it shrinks,

may provide a more successful model (Turok 1991). Notice that each of these proposals requires both CDM and a flat universe; the *only* differences from the standard theory concern the nature of the seeding perturbations.

There may be less exotic ways of producing extra large-scale structures, which require nothing more than low-energy astrophysics. As we'll note in the next chapter the relation between the distribution of galaxies and mass is uncertain and is poorly constrained by current observations; although it is a *convenient* model, the “high-peak” biasing scheme may be a poor representation of where galaxies actually form. Possibly, the galaxy formation process could itself introduce structure in the galaxy distribution on large scales (Bower *et al.* 1992).

CHAPTER VI

Biased Galaxy Formation

Until fairly recently cosmologists tacitly assumed that the luminous matter traces the matter distribution ie. the mass-to-light ratios M/L of different cosmic structures were the same. However, there is a great deal of observational and theoretical evidence that this is not the case. Such a evidence leads in a natural way to the concept of *biased* galaxy formation ie. galaxy formation (or, more in general, cosmic structure formation) occuring in such a way that galaxies do not fairly trace the underlying mass distribution. In most of biased scenarios, one is able to relate luminous matter and *dark matter* by involving a very specific form of bias (Kaiser 1984), although such a prescription is not unique (Bower *et al.* 1992).

In this section we review the motivations for biasing the galaxy distribution, possible physical mechanisms and the types of bias expected in various cosmological scenarios. A more detailed discussion is in Dekel & Rees (1986).

6.1 Missing Mass Problem: Can the Universe Be Flat?

Mass estimates on very large scales are obtained using knowledge of the statistical properties of galaxy clustering and/or linear theory of overdensities, using galaxy counts to estimate the overdensity (§ 4.2). If one assumes that

galaxies trace mass, on the scale r (Eq.(5.8))

$$\Omega \approx \rho_c^{-1} G^{-1} \xi(r)^{-1} \left(\frac{v(r)}{r} \right)^2, \quad (6.1)$$

where $\xi(r)$ is the two-point correlation function, v is the mean pair-velocity and/or (Eq.(4.41))

$$\Omega \approx \delta^{-1.7} \left(\frac{3v}{Hr} \right)^{1.7}, \quad (6.2)$$

where δ is the density enhancement within the LG radius r , and v is the infall velocity at r . The results apparently suggest $\Omega \approx 0.2$. The crucial point is that they are obtained using observables corresponding to *galaxies*: their number overdensity δ_g or the galaxy-galaxy correlation function $\xi_g(r)$. If, indeed, the galaxies cluster more than the underlying matter, such that $\delta_g = b \delta$ ie. $\xi_g(r) = b^2 \xi(r)$, the real value of Ω , as obtained by (6.1) and (6.2) is larger by a factor $b^{1.7} \div b^2$. The data would be compatible with $\Omega = 1$ if the degree of bias corresponds to $b \approx 2 \div 3$.

6.2 Voids

“Voids” $\sim 50 h^{-1} Mpc$ in diameter in the galaxy distribution are actually quite common (Hoffman, Salpeter & Wasserman 1982; De Lapparent, Geller & Huchra 1986; Oemler 1987; Geller 1987). It is difficult to reconcile the existence of such a voids with the CBR isotropy, if the galaxy formation is not biased. The number density of bright galaxies in these “voids” is typically less than 10% of the mean, and, according to spherical model (Hoffman, Salpeter & Wasserman 1982), such an underdensity in the mass distribution corresponds, at decoupling z_{dec} , to $|\delta| \leq 10^{-2}$ if $\Omega \approx 1$, and to $|\delta| \leq 5 \times 10^{-2}$ if $\Omega \approx 0.1$, evidently too large. The existence of void-regions so large (like the Great Void in Botes) contradicts the results of large scale N-body simulations too; even in the “pancake” scenario

(White, Frenk & Davis 1983; Centrella & Melott 1983; Dekel & Aarseth 1984) such large regions are never found with an underdensity less than 25% of the mean. Moreover, voids cannot be dynamically so evacuated (by the only gravity), even harder if $\Omega < 1$.

For estimating the real mass in the voids, let consider a simple model of universe in which superclusters and voids have uniform density, both in luminous and dark matter, and

$$\left(\frac{\delta_g}{\delta_{DM}}\right)_{void} = \left(\frac{\delta_g}{\delta_{DM}}\right)_{SuperCluster} = b. \quad (6.3)$$

If we assume that structures like the Local SuperCluster (LSC) and the Botes Void (BV) are quite common, we can adopt the corresponding observed values for the *galaxies* $\delta_{g,SC} \approx \delta_{g,LSC} \approx 2.5$ and $\delta_{g,V} \approx \delta_{g,BV} \approx -0.9$. On the other hand, if $\Omega = 1$ ($b = 3$), we get, from the previous relations $\delta_{DM,SC} \approx \delta_{DM,LCS} \approx 0.85$ and $\delta_{DM,V} \approx \delta_{DM,BV} \approx -0.32$. It is not difficult to see that the fractional volume of voids is 0.73 and the fractional mass in voids is 0.5. The obtained mass densities in superclusters and in voids are both compatible with $|\delta| \approx 10^{-3}$, at z_{dec} , which corresponds to $\delta_T \approx 3.5 \times 10^{-5} (\Omega h^{-1})$, if most of the dark matter is non-baryonic, which is compatible with the observed isotropy constraints if $\Omega h^2 = 1$. An open universe with $\Omega \approx 0.2$ ($b = 1$) would require a real mass underdensity of $\sim 10\%$ in the voids ie. $\delta_T \approx 5 \times 10^{-3}$, too large.

6.3 Difficulties in Cosmogonic Scenarios

Simulations of the two most popular scenarios (see e.g. Primack 1984), in which the Universe is either dominated by “cold” DM or by massive neutrinos, have led to the conclusion that (if $\Omega \approx 1$) neither can reproduce the observed large-scale distribution of galaxies unless galaxy formation is biased.

- CDM. The CDM N-body simulations of Davis *et al.* (1985) are not compatible with the observed Universe unless bright galaxies formed at the top of high peaks of matter distribution. Assuming that light traces mass, Davis *et al.* (1985) found that $r_g = 1.27 h^{-2} Mpc$ in an Einstein-de Sitter universe, too small if compared directly with the $r_o = 5 h^{-2} Mpc$ observed for galaxies, except for the case $h = 0.25$. The specific scenario of CDM with $\Omega = 1$ would require an enhanced clustering of the galaxies relative to CDM such that $\xi_g(r) = 5 \div 20 \xi(r)$, $h = 0.5 \div 1$, which is consistent with the values of b deduced above from more general considerations.
- HDM. In the case of $30 eV$ neutrinos, N-body simulations (Centrella & Melott 1983; White, Frenk & Davis 1983) show that the neutrino correlation length is $r \approx 8(\Omega h^2)^{-1}$, too large in comparison with r_o unless $\Omega h^2 > 1$. If the galaxies form only in the collapsed regions, these constraints become even tighter, so the bias required here is of an opposite sense: the galaxies should somehow be less clustered than the neutrinos. This seems to make a “biased” neutrino model rather difficult to accept: we require an anti-bias to get the correct $\xi_{gg}(r)$, but a positive bias to resolve the problems of missing mass and voids.

To summarize:

- (i) A large-scale segregation between galaxies and the dominant mass seems inevitable.
- (ii) Large regions of low density as observed in the “voids” cannot form by the present, especially if $\Omega < 1$.
- (iii) If $\Omega = 1$, as favoured by theory, most of the (non-baryonic) mass must hide in the “voids” to escape detection in clusters and superclusters.

- (iv) Neither the CDM scenario nor the HDM scenario can match the observed large-scale galaxy distribution unless galaxy formation is biased i.e. restricted to the peaks of the density field.

6.4 Physical Bias Mechanism

We review here some physical mechanisms that could originate galaxies in correspondence of high peaks of density field. Such a type of bias mechanism could be classified in three general types (see e.g. Rees 1985).

- (i) The voids may be filled with a *uniform* component of ‘missing-mass’ of a different nature from the clustered DM.
- (ii) There is one important kind of DM, but the baryonic component is segregated from the non-baryonic DM even on scales $\sim 30 h^{-1} Mpc$, providing supply for galaxy formation only in certain regions (density peaks).
- (iii) The large-scale baryon distribution traces the DM on scales $> 1 h^{-1} Mpc$, but the efficiency with which baryons turn into luminous galaxies is sensitive to other environmental effects.

In particular the bias mechanism could be *autonomously* determined in each protogalaxy, when the intrinsic properties of a protogalactic perturbation determine its final state (galaxy or no galaxy), or it may be a result of feedback interaction, not only gravitational, among more galaxies. The result might be destructive, suppressing galaxy formation locally (causing underclustering) or far away, but it could also be constructive, enhancing galaxy formation in the neighborhood of other galaxies (e.g. explosions).

Recently, Bower *et al.* (1992) have considered a feedback biased model, in which galaxy formation occurs at high peaks of the mass density field, as in the standard biased picture, but is further enhanced by the presence of nearby galaxies. Such a modification produces enough additional clustering to fit the angular correlation function of the APM galaxy survey (Maddox *et al.* 1991).

6.5 Uniform Component

A hypothesis that might hopefully ease the voids problem previously discussed is to suppose that the Universe is dynamically dominated by a uniform unclustered component of dark matter with different properties than the clustered dark matter. For example, the spread DM may be non baryonic and the clumped DM all baryonic.

One way that this could happen is in an Universe dominated by ‘ultra-hot’ dark matter particles which are still relativistic today, or at least they have velocity $> 10^3 \text{ km s}^{-1}$, the estimated peculiar velocity among clusters (Bahcall 1988), and therefore do not cluster at all. Hoffman & Bludman (1984) have shown that if such particles formed at an early stage of the evolution of the Universe, they would always be dynamically dominant over the baryons, and would have prevented any gravitational clustering. This would also yield an unacceptably fast expansion timescale during nucleosynthesis. Further possibilities are that the particles are generated by the decay of heavy particles with lifetimes comparable to the age of the Universe (Turner, Steigman & Krauss 1984; Gelmini, Schramm & Valle 1984; Olive, Seckel & Vishniac 1985; Daly 1987; 1988).

Apart from the *ad hoc* fine-tuning of particle lifetimes in these scenarios,

the main observational constraints on such models arise from the isotropy of the microwave background and from the effects of the decay on the dynamics of structures (Turner 1985; Efstathiou 1985). For instance, Flores *et al.* (1986) find that the galactic rotation curves would not have remained flat if the Universe were dominated by relativistic decay products.

6.6 High Peak Biasing

An enhanced clustering of galaxies or rich clusters over the background matter can arise in a ‘bottom-up’ scenario if galaxies formed only from *high peaks* of the density distribution smoothed on galactic scales or cluster scales; peaks are characterized by an overdensity δ above a threshold $\nu\sigma_0$, where $\sigma_0^2 \equiv \langle \delta^2 \rangle$. Kaiser (1984) showed that, in the case where the density field is Gaussian distributed, in correspondence of scales where $\xi \ll 1$, the enhanced correlation function of high ν -peaks is approximated by

$$\xi_\nu^{(2)}(r) \approx \left(\frac{\exp(-\nu^2/2)}{\int_\nu^\infty dx \exp(-x^2/2)} \right)^2 \frac{\xi^{(2)}(r)}{\xi^{(2)}(0)} \approx \left(\frac{\nu}{\sigma_0} \right)^2 \xi^{(2)}(r). \quad (6.4)$$

This relation shows that, while $\xi_\nu^{(2)}$ has the same form of $\xi^{(2)}$, higher peaks (ie. richer systems) have an *amplified* autocorrelation.

The result (6.4), which determines precisely the bias parameter b , suggests a *statistical* interpretation of the clustering properties of rich Abell clusters (we’ll rederive it in a detailed manner in a later section).

This suggestion motivated a number of detailed mathematical analyses of the properties of high level regions in Gaussian random field (e.g. BBKS 1986; Couchman 1987a; 1987b) following previous discussions in a rather different context (Rice 1954; Cartwright & Longuet-Higgins 1956; Doroshkevich 1970; Adler 1981; Vanmarcke 1983).

It is argued that for rich clusters this form of biasing is very natural: clusters form very recently in bottom-up models and they are clearly very rare; they are plausibly identified with high peaks. The lower peaks on cluster scales either have not yet collapsed or have collapsed but have not produced a final object identified as a rich cluster.

The crucial question one has to answer for applying this idea to *galaxies* is what astrophysical mechanism prevents lower-amplitude peaks from turning into galaxies as well? Such a mechanism would produce a fairly sharp *cut off* in the efficiency of (bright) galaxy formation at $\nu \approx 2 \div 3$, the number density of such peaks being comparable to that of bright galaxies (see the papers by Bardeen, Kaiser and White, 1986).

The most obvious thing about high ν peaks is that they could collapse earlier and have a higher turn around density than the typical fluctuations on a given mass scale ¹. Rees (1985) argue that, in principle, this might be enough to create the biasing if star formation were highly sensitive to, for instance, the ratio of the cooling time, $\tau_{cool} \sim \rho^{-1}$, to the collapse time, $\tau_{coll} \sim \rho^{-1/2}$; collapse and fragmentation of gas clouds to form stars are faster when this ratio is small. If high ν peaks collapse at $z \geq 10$, Compton scattering off MWB photons would produce very efficient cooling. If lower peaks form after this time, Compton cooling would be unimportant and cooling much less efficient. It is still an open question if these effects can produce a cutoff sharp enough at ν .

The bias may result from processes *intrinsic* to the protogalaxies. For instance, Dekel & Silk (1986) have argued that protogalaxies formed from high

¹The height of the peak is correlated with the time of collapse. Modeled as a spherical, uniform density "top-hat" with a density excess δ_{TH} extrapolated to the present by linear perturbation theory, the peak collapses to infinite density at a redshift z_c such that

$$1 + z_c = \delta/1.68 .$$

A threshold in δ corresponds to a threshold in time, in that only peaks which collapse before a certain time (above a certain redshift) form the galaxy or cluster.

ν fluctuations would have higher velocity dispersions and escape velocities than low ν peaks. High ν peaks are more able to retain gas that might be blown out of low ν peaks by e.g. explosive processes (supernovae); they argue that bright galaxies *must* originate from high density peaks ($2\sigma_0 \div 3\sigma_0$) in the initial fluctuation field, while typical peaks ($\sim 1\sigma_0$) either cannot produce a luminous galaxy at all, or they make very faint dwarf galaxies with very low gas content. This would lead to a selective bias, in which bright galaxies are biased but dwarf galaxies do trace accurately the DM distribution. There is, as yet, no definitive observational evidence to confirm or reject the assumption that ξ_{gg} for bright galaxies is different than ξ_{gg} for dwarfs.

6.7 Bias in a ‘Top-Down’ Scenario (Neutrinos)

A bias mechanism is generated *automatically* in any top-down scenario where the perturbations below $\sim 30 h^{-1} Mpc$ have all damped out, as in neutrino universe. Motions of the baryonic matter from proto-voids to proto-pancakes are followed by collapses into flattened structures (‘pancakes’) accompanied by streaming toward their intersections (‘filaments’) and knots where rich clusters form; there the gas collapses dissipatively into high density regions, within which cooling and galaxy formation start. Galaxies are thus limited to very specific ‘biased’ regions. However, if the efficiency of galaxy formation is similar in all the collapsed regions, this natural bias just makes the timing-scaling problems more severe; one has to invoke a mechanism that would suppress the formation of galaxies in the high density regions, or enhance their formation in the low density regions, but such a mechanism is not a natural outcome of a dissipative pancake scenario.

Dekel (1983) proposed an alternative *non-dissipative* pancake scenario, which would arise from a *hybrid scenario*: if galaxies form independently of pancakes, e.g. from another component of density perturbations, the timing-scaling constraint becomes irrelevant: galaxies could have formed at $z \geq 3$ and large scale pancakes at $z \sim 1$. Therefore galaxies would not be limited to pancakes but rather be present everywhere, subject to the biasing mechanisms that are relevant in general bottom-up scenario. Such a hybrid scenario could consist of two types of DM, baryonic and/or non-baryonic, and of two types of initial fluctuations, adiabatic and isothermal (see e.g. Valdarnini & Bonometto 1985).

6.8 The Kaiser Biased Model

As we mentioned previously (see e.g. § 3.2), according to the observations, the rich clusters of galaxies are strongly correlated at distances where the correlation functions of the single galaxies have negligible amplitude, and the correlation length increases with the scale of the system. Kaiser (1984) suggested that the origin of such enhancement is primarily statistical and it is not due to an underlying substantial power spectrum on cluster scales. By assuming that the (rich) clusters of galaxies condense where the primordial (smoothed) Gaussian fluctuations exceed a suitable level $\nu\sigma_0$, then they exhibit a 2-point correlation amplified with respect to the mass correlation, and moreover this amplification increases when the scale is increased. We outline the mathematical details. We want now deduce the 2-point correlation of the up-crossing *regions* above the threshold $\nu\sigma_0(R)$ in the case in which δ_R is Gaussian distributed. In the simplest version of the Kaiser biasing scheme the galaxies trace the mass, therefore

$$\xi(r) = \xi_{gg}(r).$$

The 2-point correlations of the enhanced regions can be calculated as follows: by choosing at random a point, the probability $P_1^{(\nu)}$ that the Gaussian fluctuation δ_R exceeds the sharp threshold $\nu\sigma_o(R)$ at that point is given by

$$P_1^{(\nu)} = \int_{\nu\sigma_o(R)}^{\infty} d\alpha p(\alpha) = \frac{1}{2} \operatorname{erfc}(\nu/\sqrt{2}), \quad (6.5)$$

where $p(\alpha)$ is showed in Eq.(A.1). $P_1^{(\nu)}$ is the fraction of space where $\delta_R > \nu\sigma_o(R)$. The probability $P_2^{(\nu)}(\mathbf{x}_2, \mathbf{x}_2)$ that in the points (in the neighborhood of the points) \mathbf{x}_1 and \mathbf{x}_2 is $\delta_R > \nu\sigma_o(R)$ is given by

$$P_2^{(\nu)}(\mathbf{x}_2, \mathbf{x}_2) = \int_{\nu\sigma_o(R)}^{\infty} d\alpha_1 \int_{\nu\sigma_o(R)}^{\infty} d\alpha_2 p(\alpha_1, \alpha_2), \quad (6.6)$$

where $p(\alpha_1, \alpha_2)$ is the bivariate Gaussian in Eq.(A.8).

Finally, the 2-point correlation function for the enhanced ($> \nu\sigma_o$) regions, $\xi_\nu^{(2)}$, is

$$1 + \xi_\nu^{(2)}(r) = \frac{P_2^{(\nu)}(\mathbf{x}_2, \mathbf{x}_2)}{[P_1^{(\nu)}]^2}, \quad (6.7)$$

if $r \equiv |\mathbf{x}_1 - \mathbf{x}_2|$. The integral in (6.6) is difficult. The original approximation by Kaiser (1984) for large ν and small $\xi_\nu^{(2)}(r)$ (linear regime) was

$$\xi_\nu^{(2)}(r) \approx \frac{\nu^2}{\sigma_o(R)^2} \xi_R^{(2)}(r). \quad (6.8)$$

A suitable choice of ν can therefore explain, as statistical enhancement, the amplification of the 2-point cluster correlation function and the trend of increasing r_c with richness by identifying richer clusters with higher levels. Other authors have analyzed the model in more detail. Politzer & Wise (1984) obtained the 2-point biased correlation in the form

$$1 + \xi_\nu^{(2)}(r) \approx e^{\nu^2 \omega^{(2)}(r)}, \quad (6.9)$$

$\omega^{(2)}(r) \equiv \xi_R^{(2)}(r)/\sigma_o(R)$, which generalizes (6.8). They also computed N-point

correlations in this approximation

$$1 + \xi_\nu^{(N)} = \exp \left(\nu^2 \sum_{j>h}^N \omega_{jh}^{(2)} \right) = \prod_{j>h}^N \left(1 + \xi_\nu^{(2)}(jh) \right), \quad (6.10)$$

similar to the Kirkwood superposition. Politzer & Wise's result is only an approximation, obtained on the linear expansion of the exponent in the bivariate (multivariate) Gaussian distribution. The exact result for sharp clipping was obtained by Jensen & Szalay (1986), using a series expansion for any ν

$$\xi_\nu^{(2)}(r) = \sum_{m=1}^{\infty} \frac{\omega(r)^m}{m!} A_m^2, \quad (6.11)$$

$$A_m(\alpha) \equiv \frac{2 e^{-\alpha^2} H_{m-1}(\alpha)}{\sqrt{\pi} \sqrt{2}^m \operatorname{erfc}(\alpha)}, \quad (6.12)$$

where $\alpha = \nu/\sqrt{2}$, H_n is a Hermite polynomial of order n , erfc is the complementary error function; the leading term of the series corresponds to the Kaiser approximation.

All these results are obtained in the case of sharp threshold function, say $G(\delta) = \theta(\delta - \nu\sigma_0)$, where θ is the step function. Szalay (1988) considered the effects on the biased N-point correlations of a general nonlinear biasing function $G(\delta)$.

In the next section we'll consider a new "weighted" biasing scheme and analyze preliminary results (Catelan *et al.* 1992): as we'll see, generalizations of the previous expression can be obtained.

The calculation of ξ_ν we showed is physically meaningful when the two points with field values α_1 and α_2 lie in the disjoint regions of the field above the threshold, since only in such a case the two points correspond to different proto-objects, but no condition is given to ensure that \mathbf{x}_1 and \mathbf{x}_2 actually lie in different enhanced regions.

Coles (1986) showed that, unless ν is larger than ≈ 3 , typical sizes of the regions are rather large, with a high probability of exceeding even $15 \div 20 h^{-1} Mpc$. Some clusters are effectively counted more than once. This means that the simple calculation presented previously will seriously overestimate the two point cluster-cluster correlations at distances of this order (see Peacock & Heavens 1985; BBKS). For very high threshold ($\nu > 3$), the problem is not so acute, because the regions are then much smaller (see Coles 1986).

Another question is that all calculations based on the high-level region approximation predict that $\xi_{cc}(r) = 0$ whenever the underlying matter correlation function is zero (our ‘weighted’ biased scheme shows the same behaviour). Monte-Carlo simulations of 3D noise by Otto, Politzer & Wise (1986a) reveal that true maxima do not possess this property. Unfortunately, their analytic expressions for the correlations of peaks are incorrect (Otto, Politzer & Wise 1986b) and they give no explanation of that. This point is particularly relevant to the CDM model, in which context biasing is usually discussed; the CDM correlation function goes to zero at $r \sim 18 h^{-1} Mpc$ if $\Omega = 1$ (Otto, Politzer & Wise 1986a), but the observed cluster-cluster 2-point correlation is non-zero at this distance.

In spite of the likely errors in the details of the statistical enhancements predicted by the simple Kaiser model, the qualitative explanation of such enhancements in terms of peaks of the density field above some level is extremely plausible. To avoid problems like those mentioned previously, what is required is a calculation of the 2-point correlation function of local maxima, not just regions above some level. The reason for studying true peaks rather than high regions is that peaks define a true spatial point process, with no disjointness problem of the sort discussed here.

Unfortunately, the statistical properties of maxima of 3D random fields are extremely difficult to compute rigorously. BBKS (1986) obtained asymptotic expressions for the correlation function of peaks of Gaussian random noise $\xi_{pk-pk}(r)$ as $r \rightarrow \infty$, but these expressions can only be accurate for monotonically decreasing covariance functions. Further progress with peaks of 3D fields, by handling fairly cumbersome relations, is given in Cline *et al.* (1987). The clustering of local maxima of random Gaussian fields is also analyzed in Couchman (1987a; 1987b), Coles (1989) and Lumsden, Heavens & Peacock (1989).

6.9 Weighted Bias and Galaxy Clustering

A weighted biasing scheme for galaxy clustering is considered. Contrary to previous treatments, the biased density field coincides with the background mass-density whenever the latter exceeds a given threshold. All the observables in this approach can be continuously defined down to the unbiased case. The two-point function of biased objects, which is computed for underlying Gaussian density fluctuations, turns out to be quite different from that obtained in previous treatments even at large distances and for high threshold.

A Weighted Biasing Scheme

In this Section we introduce a *Biased Density Field* (hereafter BDF) starting from density fluctuations δ_R exceeding a threshold $\nu\sigma_R$. Specifically, δ_R is the mass density enhancement $\delta_R(\mathbf{x}) \equiv (\rho_R(\mathbf{x}) - \langle\rho\rangle)/\langle\rho\rangle$, filtered on a scale R , defining the typical size of a given proto-object, and σ_R is its *rms* value on that scale. Our BDF is defined as

$$\rho_{\nu,R}(\mathbf{x}) \equiv \rho_R(\mathbf{x}) \theta[\delta_R(\mathbf{x}) - \nu\sigma_R], \quad (6.13)$$

θ being the step function. Note that $\rho_{\nu,R}(\mathbf{x})$ actually represents the true mass-density inside a smoothed sphere of filtering radius R centered on \mathbf{x} for those mass fluctuations which exceed the threshold. It is also useful to define the ratio $\mu_R(\nu) \equiv \langle \rho_{\nu,R} \rangle / \langle \rho \rangle$, which represents the total mass fraction in *excursion regions* (ie. those regions where the mass fluctuation δ_R exceeds the threshold $\nu\sigma_R$). In fact, by considering the brackets as spatial averages over a large (formally infinite) volume V , we find

$$\mu_R(\nu) = \frac{\int_V d\mathbf{x} \rho_R(\mathbf{x}) \theta[\delta_R(\mathbf{x}) - \nu\sigma_R]}{\int_V d\mathbf{x} \rho_R(\mathbf{x})} = \frac{\int_{V_R(\nu)} d\mathbf{x} \rho_R(\mathbf{x})}{\int_V d\mathbf{x} \rho_R(\mathbf{x})} \equiv \frac{M_R(\nu)}{M_{TOT}}, \quad (6.14)$$

where $V_R(\nu)$ is the total volume of the excursion regions. As a consequence, the ratio $\eta_R(\nu) \equiv \mu_R(\nu)/v_R(\nu)$, where $v_R(\nu)$ is the fraction of volume above the threshold, provides an estimate of the *mean density inside an excursion region normalized to the background mean density*. Assuming that the mass fluctuation is a Gaussian random field, we find

$$\mu_R(\nu) = \frac{1}{2} \operatorname{erfc}(\nu/\sqrt{2}) + \frac{\sigma_R}{\sqrt{2\pi}} e^{-\nu^2/2} \equiv [\Phi(\nu) + \nu\sigma_R] \frac{e^{-\nu^2/2}}{\sqrt{2\pi}\nu}, \quad (6.15)$$

where $\operatorname{erfc} x \equiv (2/\sqrt{\pi}) \int_x^\infty dy e^{-y^2}$ is the complementary error function, while the function $\Phi(\nu) \equiv \sqrt{\frac{\pi}{2}} \nu e^{\nu^2} \operatorname{erfc}(\nu/\sqrt{2})$ can be asymptotically expanded as follows

$$\Phi(\nu) \approx 1 + \sum_{n=1}^{\infty} (-1)^n \frac{(2n-1)!!}{\nu^{2n}}. \quad (6.16)$$

We also find

$$\eta_R(\nu) = 1 + \frac{\nu\sigma_R}{\Phi(\nu)}. \quad (6.17)$$

The function $\mu_R(\nu)$ is plotted in Fig.1 for different values of σ_R ; its maximum value, $\mu_R(\nu_m) > 1$, is reached at $\nu_m = -1/\sigma_R$. Both $\mu_R(\nu)$ and $\eta_R(\nu)$ tend to unity as $\nu \rightarrow -\infty$, since in such a case our Gaussian BDF reduces to the mass density field. The presence of negative mass events in the Gaussian statistics causes $\mu_R(\nu)$ to exceed unity for some values of ν . This behaviour is

actually common to any probability distribution $p(\rho_R)$ admitting $\rho_R < 0$ events.

This point can be made more clear by considering the ensemble averages

$$\mu_R(\nu) = \frac{\int_{(\rho)(1+\nu\sigma_R)}^{\infty} d\rho_R \rho_R p(\rho_R)}{\int_{-\infty}^{(\rho)(1+\nu\sigma_R)} d\rho_R \rho_R p(\rho_R) + \int_{(\rho)(1+\nu\sigma_R)}^{\infty} d\rho_R \rho_R p(\rho_R)}. \quad (6.18)$$

The integral $\int_{-\infty}^{(\rho)(1+\nu\sigma_R)} d\rho_R \rho_R p(\rho_R)$ in the denominator always contains a negative contribution coming from $\rho_R < 0$ unphysical events, which is indeed maximized (in absolute value) when $\nu = -1/\sigma_R$.

It then follows that the Gaussian statistics can be consistently applied provided that either $\sigma_R \ll 1$ values are taken, ie. large smoothing scales, which reduces the overall probability of unphysical events, or large threshold values, $\nu \gg 1/\sigma_R$, are considered for a given smoothing scale, so that negative mass events have little effects on observables such as $\mu_R(\nu)$, $\eta_R(\nu)$ and BDF correlations functions.

In order to study the behaviour of the observables $\mu_R(\nu)$ and $\eta_R(\nu)$, we have computed these two quantities for an underlying *lognormal* distribution of density fluctuation (e.g. Coles & Jones 1991), namely

$$p(\delta_R) = \frac{(1 + \delta_R)^{-1}}{\sqrt{2\pi \ln(1 + \sigma_R^2)}} \exp\left(-\frac{\ln^2[(1 + \delta_R)\sqrt{1 + \sigma_R^2}]}{2\ln(1 + \sigma_R^2)}\right). \quad (6.19)$$

In such a case we find

$$\mu_R(\nu) = \frac{1}{2} \operatorname{erfc}\left(\frac{\ln[(1 + \nu\sigma_R)/\sqrt{1 + \sigma_R^2}]}{\sqrt{2\ln(1 + \sigma_R^2)}}\right), \quad (6.20)$$

which consistently takes its maximum value $\mu_R(\nu_m) = 1$ at $\nu_m = -1/\sigma_R$, corresponding to the unbiased case. The function $\eta_R(\nu)$ is immediately obtained dividing the above expression by the volume fraction above the threshold

$$v_R(\nu) = \frac{1}{2} \operatorname{erfc}\left(\frac{\ln[(1 + \nu\sigma_R)\sqrt{1 + \sigma_R^2}]}{\sqrt{2\ln(1 + \sigma_R^2)}}\right). \quad (6.21)$$

BDF Two-Point Correlation Function

The next step is to obtain the BDF two-point correlation function, which is defined as $\xi_{\nu,R}(r) \equiv \langle \delta_{\nu,R}(\mathbf{x}_1) \delta_{\nu,R}(\mathbf{x}_2) \rangle$, where $r \equiv |\mathbf{x}_1 - \mathbf{x}_2|$ and $\delta_{\nu,R}$ is the BDF fluctuation

$$\delta_{\nu,R}(\mathbf{x}) = \mu_R(\nu)^{-1} [1 + \delta_R(\mathbf{x})] \theta[\delta_R(\mathbf{x}) - \nu\sigma_R] - 1. \quad (6.22)$$

One has

$$\begin{aligned} & \mu_R^2(\nu) [1 + \xi_{\nu,R}(r)] = \\ & = \left\langle [1 + \delta_R(\mathbf{x}_1) + \delta_R(\mathbf{x}_2) + \delta_R(\mathbf{x}_1) \delta_R(\mathbf{x}_2)] \theta[\delta_R(\mathbf{x}_1) - \nu\sigma_R] \theta[\delta_R(\mathbf{x}_2) - \nu\sigma_R] \right\rangle. \end{aligned} \quad (6.23)$$

It is straightforward to show that, in the Gaussian case,

$$\begin{aligned} & \mu_R^2(\nu) [1 + \xi_{\nu,R}(r)] = \int_{\nu}^{\infty} \int_{\nu}^{\infty} d\alpha d\beta \\ & \left[(1 + \sigma_R^2 \omega) - 2\sigma_R(1 + \omega) \frac{\partial}{\partial \alpha} + 2\sigma_R^2 \omega \frac{\partial^2}{\partial \alpha^2} + \sigma_R^2(1 + \omega^2) \frac{\partial^2}{\partial \alpha \partial \beta} \right] p(\alpha, \beta; \omega), \end{aligned} \quad (6.24)$$

where ω is the ratio of the background correlation function $\xi_R(r)$ (for the smoothed field) to the variance, namely $\omega(r) \equiv \xi_R(r)/\sigma_R^2$. The joint probability $p(\alpha, \beta; \omega)$ is a bivariate Gaussian for the normalized field δ_R/σ_R , namely $p(\alpha, \beta; \omega) = (2\pi\sqrt{1-\omega^2})^{-1} \exp[-(\alpha^2 + \beta^2 - 2\omega\alpha\beta)/2(1-\omega^2)]$.

Some of the integrals in Eq.(6.24) can be performed leading to the following expression

$$\begin{aligned} & \mu_R^2(\nu) [1 + \xi_{\nu,R}(r)] = \frac{1 + \sigma_R^2 \omega}{2\sqrt{2\pi}} \int_{\nu}^{\infty} d\alpha e^{-\alpha^2/2} \operatorname{erfc} \left(\frac{\nu - \alpha\omega}{\sqrt{2(1-\omega^2)}} \right) + \\ & + [1 + \omega(1 + \nu\sigma_R)] \frac{\sigma_R e^{-\nu^2/2}}{\sqrt{2\pi}} \operatorname{erfc} \left(\frac{\nu}{\sqrt{2}} \sqrt{\frac{1-\omega}{1+\omega}} \right) + \frac{\sigma_R^2 \sqrt{1-\omega^2}}{2\pi} e^{-\nu^2/(1+\omega)}. \end{aligned} \quad (6.25)$$

The expression for the standard bias (Kaiser 1984) is easily recovered from the latter equation, by taking the $\sigma_R \rightarrow 0$ limit at fixed ν and ω ,

$$1 + \xi'_{\nu,R}(r) = \frac{\sqrt{2}}{\sqrt{\pi} [\operatorname{erfc}(\nu/\sqrt{2})]^2} \int_{\nu}^{\infty} d\alpha e^{-\alpha^2/2} \operatorname{erfc} \left(\frac{\nu - \alpha\omega}{\sqrt{2(1-\omega^2)}} \right). \quad (6.26)$$

Note that, as $\nu \rightarrow -\infty$, the BDF correlation function reduces to the background one, $\xi_R(r)$.

The formula in Eq.(6.25), in the limit of zero lag, ie. for $\omega \rightarrow 1$, yields an exact expression for the BDF variance

$$\sigma_{\nu,R}^2 = \frac{(1 + \sigma_R^2)\Phi(\nu) + \nu\sigma_R(2 + \nu\sigma_R)}{[\Phi(\nu) + \nu\sigma_R]^2 (e^{\nu^2/2}\sqrt{2\pi}\nu)} - 1, \quad (6.27)$$

which in the limit $\nu \rightarrow -\infty$ reduces to the background mass variance, σ_R^2 .

Weighted Biasing Factor

An interesting approximation can be obtained in the limit of large distances, ie., for $\omega \ll 1$. By Taylor expanding Eq.(6.25) up to first order in ω , which involves expressions such as $e^{-\nu^2/(1+\omega)} \approx (1 + \nu^2\omega) e^{-\nu^2}$ and

$$\operatorname{erfc}\left(\frac{\nu}{\sqrt{2}}\sqrt{\frac{1-\omega}{1+\omega}}\right) \approx \operatorname{erfc}(\nu/\sqrt{2}) + \sqrt{\frac{2}{\pi}}\nu\omega e^{-\nu^2/2}, \quad (6.28)$$

one gets

$$\xi_{\nu,R}(r) \approx b_R(\nu)^2 \xi_R(r), \quad (6.29)$$

where we have introduced the *linear biasing factor*

$$b_R(\nu) = \frac{\sigma_R\Phi(\nu) + \nu(1 + \nu\sigma_R)}{\sigma_R\Phi(\nu) + \nu\sigma_R^2}. \quad (6.30)$$

This result can be compared with the Kaiser's expression (1984)

$$b'_R(\nu) = \frac{\nu}{\sigma_R\Phi(\nu)}. \quad (6.31)$$

Contrary to Eq.(6.31), our biasing factor in Eq.(6.30) reduces to unity in the unbiased Gaussian case, $b_R(-\infty) = 1$. Also, note that Eq.(3.9) gives $b_R(\nu) \approx \nu/\sigma_R$ in the high- ν limit.

High Threshold Limit

High threshold ($\nu \gg 1$) relations can be obtained both for $\mu_R(\nu)$ and for the BDF correlation function, provided that $\omega \neq 1$. The first integral on the r.h.s. of Eq.(6.25) can be approximated, using Mehler's formula (e.g. Bateman 1953), by the asymptotic expression

$$\frac{1}{2\sqrt{2\pi}} \int_{\nu}^{\infty} d\alpha e^{-\alpha^2/2} \operatorname{erfc} \left(\frac{\nu - \alpha\omega}{\sqrt{2(1-\omega^2)}} \right) \approx \frac{e^{-\nu^2}}{2\pi\nu^2} e^{\nu^2\omega}, \quad (6.32)$$

while in the second term $\operatorname{erfc} x \approx (\pi x^2)^{-1/2} e^{-x^2}$, for $x \rightarrow \infty$. One therefore obtains $\mu_R(\nu) \approx (2\pi\nu^2)^{-1/2} (1 + \nu\sigma_R) e^{-\nu^2/2}$, and

$$1 + \xi_{\nu_R} \approx \frac{(1 + \sigma_R^2\omega) e^{\nu^2\omega}}{(1 + \nu\sigma_R)^2} + \frac{(2 + \nu\sigma_R)\nu\sigma_R}{(1 + \nu\sigma_R)^2} \sqrt{\frac{(1 + \omega)^3}{1 - \omega}} e^{\nu^2\omega/(1+\omega)}. \quad (6.33)$$

In the limit $\sigma_R \rightarrow 0$ (actually for $\sigma_R \ll 1/\nu$) at fixed ν and ω we recover the Politzer & Wise (1984) relation

$$1 + \xi'_{\nu_R} \approx \exp(\nu^2\omega). \quad (6.34)$$

On the contrary, for $\sigma_R \gg 1$, we get

$$1 + \xi_{\nu_R} \approx \sqrt{\frac{(1 + \omega)^3}{1 - \omega}} \exp[\nu^2\omega/(1 + \omega)], \quad (6.35)$$

which is clearly not affected by the negative mass events of the Gaussian statistics. This also reduces to Eq.(6.34) at large distances ($\omega \ll 1$).

The cosmological implications of this new biasing scheme have yet to be explored. The results seem promising. To weight a proto-structure with its own mass above a given threshold permits one to recover the unbiased observables simply by taking the limit $\nu \rightarrow -\infty$, contrary to previous treatments. New observables, like the mass fluctuation *in* the excursion regions, can be defined. In general, the weighted peak-peak correlation functions are *enhanced* with respect

to the classical Kaiser peak-peak correlations, overall at small and intermediate scales ($\omega \sim 1$), while the standard expressions of the biased two-point correlation functions are recovered at very large separations ($\omega \rightarrow 0$), essentially because the intermediate scale information is lost there.

CHAPTER VII

Non Linear Gravitational Evolution: Perturbative Theory

The linear growth laws discussed in Chapter IV hold until $\delta \approx 1$. When the perturbation amplitudes approach unity, non linear gravitational effects become important. For instance, by using a simple spherical top hat model, it is easy to show that collapse to a point of infinite density occurs at a time when (if $\Omega = 1$) the *linear* density contrast is $\delta \approx 1.68$ (see Peebles 1980). However, to follow the non-linear stage of the gravitational collapse is undoubtedly very hard to do in an analytical way and the interest in such a type of analysis is drastically reduced. People are forced to resort to N-body techniques (Hansel *et al.* 1985; Sugimoto *et al.* 1991. Davis *et al.* 1985; Efstathiou *et al.* 1985; White *et al.* 1987a; 1987b, in the CDM framework), or various analytical approximations, as the *Zel'dovich approximation* (Zel'dovich 1970; Buchert 1989; 1992), leading to another ones, the *adhesion approximation* (see e.g. Gurbatov, Saichev & Shandarin 1989; Kofman & Shandarin 1989; Shandarin & Zel'dovich 1989; Kofman, Pogosyan & Shandarin 1990) and, more able to follow the development of structures beyond the epoch of first caustic formation, the *frozen-flow approximation* (Matarrese *et al.* 1992); these approximations are useful for developing intuition, but they are not a substitute for exact or numerical non linear solutions.

A very interesting new general-relativistic algorithm to study the non-linear evolution of density perturbations of collisionless matter is given by Matarrese, Pantano & Saez (1992).

Recently the interest in the analytical treatment of non-linear gravity has grown and many efforts are devoted to understand the results.

The basic technique is the perturbative theory, the systematic development of the perturbative expansion being obtained by writing

$$\delta = \sum_n \delta^{(n)}, \quad (7.1)$$

where $\delta^{(n)} = 0(\delta^{(1)n})$, $\delta^{(1)}$ corresponding to the linear solution. Comparing terms of equal order in Eq.(4.11), one constructs the differential equation for the n-th term $\delta^{(n)}$, lower order solutions providing source terms for the higher orders.

The published literature on the perturbative approach is considerably growing.

The evolution of cosmological adiabatic perturbations in the so called weakly non-linear regime, when the second order contribution $\delta^{(2)}$ in (7.1) is not negligible, was analyzed by Juszkiewicz (1981): he showed that second order effects could induce tidal processes leading to the disruption of large scale inhomogeneities into smaller units; the articles of Vishniac (1983) and Juszkiewicz, Sonoda & Barrow (1984) treat in detail the consequences on the galaxy clustering pattern.

Fry (1984) calculates the evolution of cosmological density correlation functions to lowest non vanishing order in perturbative theory for an initially random Gaussian distribution; an extrapolation of the observed hierarchical form of the two-, three- and four-point correlation functions ξ , ζ and η (Groth & Peebles 1977; Fry & Peebles 1978; Sharp, Bonometto & Lucchin 1984) emerges quite generally. The form of the connected correlations induced by non-linearities in the time evolution of primordial Gaussian fluctuations is discussed also in Goroff *et al.* (1986). Fry (1986) stresses that the enhancement of clustering, proper of the biased scenario, is a general feature of non-linear processing of the galaxy

distribution. The non-linear gravitational evolution is essential to predict a correct interpretation of large-scale deviations from the Hubble flow, as showed in Grinstein *et al.*(1987). The predictions of the Zel'dovich approximation, often used to mimic the effects of non-linear gravitational time evolution, are compared with those of the true non-linear regime in Grinstein & Wise (1987). More recently, Coles (1990) uses perturbative technique to explore the possibility of originating more power on large scales in the standard CDM cosmogony. Suto & Sasaki (1991) found that, even when fluctuations are in linear regime, a non-linear correction might significantly affect the result for the corresponding velocity field predicted in the framework of linear theory. They show also that nonlinear effects either suppress or *enhance* the growth of perturbations on large scales, depending on the spectrum shape; the second order perturbations are analytically tractable for all power-law spectra (see also the very recent Makino, Sasaki & Suto 1992). Moutarde *et al.* (1991) in a rigorous Lagrangian perturbative theory (at the end of calculations physical observables are known in the rest frame of each fluid element), whose first order corresponds to the Zel'dovich approximation, found that density contrasts up to $\delta \sim 50$ could be appropriately described analytically. Bernardeau (1992b), using results of Bernardeau (1992a), derives the exact relationship between the density and the divergence of the velocity field, including *all* non-linear features.

The first direct observational suggestion that gravitational instability in the perturbative regime operates on large scales is in Baumgart & Fry (1991); the observed bispectrum obeys the hierarchical pattern, with a reduced three point amplitude that is consistent with gravitational instability in perturbative theory starting from Gaussian initial conditions. The trispectrum, marginally detected, is again consistent with the hierarchical pattern.

More emphasis was showed claiming the measurement of another second

order effect: the distribution of IRAS galaxies out to $140 h^{-1} Mpc$ is such that the inferred underlying distribution of density is found to be positive skewed, physically meaning that the superclusters (positive fluctuations) are smaller than the voids (negative fluctuations), but depart more from the mean density (Saunders *et al.* 1991). This result, with the detection of new superclusters and voids, “rule out the standard CDM model at least the 97% confidence limit” (previous reference, pag. 37), already seriously challenged by the large-scale power detected in IRAS (Efstathiou *et al.* 1990) and APM (Maddox *et al.* 1990) catalogues.

7.1 Second and Third Order Perturbations

Second order perturbative theory has been discussed in a more general context (e.g. pressure included) by Hunter (1964) and Tomita (1967; 1971; 1972). Peebles (1980) indicates how to compute the growth of skewness (the third central moment) in second order approximation; positive skewness has been recently detected in IRAS data (Saunders *et al.* 1991) and analyzed by Park (1991); the importance of the sign of the skewness of the linear (non-Gaussian) density field as a predictor of the non-linear evolution has recently been emphasized by Moscardini *et al.* (1991), Matarrese *et al.* (1991) and Messina *et al.* (1992 and references therein) in the framework of CDM scenario (see also Weinberg & Cole 1992).

Gaussian fields have zero skewness, but the presence of a non-zero skewness in the e.g. IRAS data, does not necessarily imply non-Gaussian initial conditions: even if the initial probability distribution of the mass density contrast δ is Gaussian then symmetric, an asymmetry will inevitably develop later, as a second order effect, under the influence of gravity. Indeed, δ can grow indefi-

nately in regions where it was initially positive, whereas in the voids it can never decrease below -1 .

We show here how gravity can induce skewness in an initially Gaussian distribution, computing and solving the second order solutions of the equations of motion of matter. Next, we calculate the skewness in density field, assumed Gaussian at early time (e.g. at recombination), also suggesting how to work out the skewness in the more general case in which δ is non-Gaussian at the beginning. We conclude discussing how the observations can be used to distinguish “conventional” models from an intrinsically non-Gaussian alternative. If someone is interested in the subject we advise Silk & Juszkiewicz (1991), Juszkiewicz & Bouchet (1991), Martel & Freudling (1991), Coles & Frenk (1991) and Bouchet *et al.* (1992).

Second Order Equations: Solutions

In comoving coordinates, the equations of motion for the pressureless self-gravitating fluid are Eq. (4.7), Eq.(4.8) and Eq.(4.9).

The perturbative series for δ and \mathbf{v} may be written as

$$\delta = \delta^{(1)} + \delta^{(2)} + \dots, \quad (7.2)$$

$$\mathbf{v} = \mathbf{v}^{(1)} + \mathbf{v}^{(2)} + \dots, \quad (7.3)$$

where $\delta^{(n)}$ and $\mathbf{v}^{(n)}$ are of order n ; $\delta^{(1)}$ and $\mathbf{v}^{(1)}$ are the linear solutions.

In particular, we consider only the growing mode $\delta^{(1)} \propto D$. The second order contribution $\delta^{(1)} + \delta^{(2)}$ is a solution of the differential equation (4.11), reducing to, once (4.12) is taken into account

$$\begin{aligned} & \partial_0^2 \delta^{(2)} + 2\dot{a}a^{-1} \partial_0 \delta^{(2)} - 4\pi G \rho_b \delta^{(2)} = \\ & = 4\pi G \rho_b \delta^{(1)2} + a^{-2} \partial_\alpha \delta^{(1)} \partial_\alpha \phi^{(1)} + a^{-2} \partial_\alpha \partial_\beta v^{(1)\alpha} v^{(1)\beta}; \end{aligned} \quad (7.4)$$

$\delta^{(2)}$ is related to the second order peculiar potential $\phi^{(2)}$ by

$$\nabla^2 \phi^{(2)} = 4\pi G a^2 \rho_b \delta^{(2)}. \quad (7.5)$$

A common way to write (7.4) is

$$\begin{aligned} \partial_o^2 \delta^{(2)} + 2\dot{a}a^{-1} \partial_o \delta^{(2)} - 4\pi G \rho_b \delta^{(2)} &= \left[4\pi G \rho_b + \left(\frac{\dot{D}}{D} \right)^2 \right] \delta^{(1)2} + \\ \left[4\pi G \rho_b + 2 \left(\frac{\dot{D}}{D} \right)^2 \right] \partial_\alpha \delta^{(1)} \partial_\alpha \Delta^{(1)} &+ \left(\frac{\dot{D}}{D} \right)^2 \partial_\alpha \partial_\beta \Delta^{(1)} \partial_\alpha \partial_\beta \Delta^{(1)}, \end{aligned} \quad (7.6)$$

where $D = D(t)$ is a solution of (4.14) and $\Delta^{(1)}$ is the linear gravitational potential defined in (4.26). We can see that each side of Eq.(7.6) is homogeneous in powers of t ; we solve (7.6) in an Einstein-de Sitter universe: noting that $D^2 \propto \delta^{(2)} \equiv \delta_2(\mathbf{x}) D(t)^2$,

$$\partial_o^2 D^2 + 2\dot{a}a^{-1} \partial_o D^2 - 4\pi G \rho_b D^2 = \frac{1}{2} f(\mathbf{x}, t) \left(\frac{\dot{D}}{D} \right)^2, \quad (7.7)$$

where, since $4\pi G \rho_b = 2/3t^2$ and $\dot{D}/D = \dot{a}/a = 2/3t$,

$$\delta_2(\mathbf{x}) f(\mathbf{x}, t) \equiv 5 \delta^{(1)2} + 7 \partial_\alpha \delta^{(1)} \partial_\alpha \Delta^{(1)} + 2 \partial_\alpha \partial_\beta \Delta^{(1)} \partial_\alpha \partial_\beta \Delta^{(1)}$$

ie. by (7.7),

$$\left[4\pi G \rho_b + 2 \left(\frac{\dot{D}}{D} \right)^2 \right] D^2 = \frac{1}{2} \left(\frac{\dot{D}}{D} \right)^2 f$$

or

$$f = 7D^2.$$

Therefore the solution of (7.7) is given by (Peebles 1980, Eq.(18.8))

$$\delta^{(2)} = \frac{5}{7} \delta^{(1)2} + \partial_\alpha \delta^{(1)} \partial_\alpha \Delta^{(1)} + \frac{2}{7} \partial_\alpha \partial_\beta \Delta^{(1)} \partial_\alpha \partial_\beta \Delta^{(1)}. \quad (7.8)$$

It is not difficult to show that $\langle \delta^{(2)} \rangle = 0$, ie. mass is conserved.

We see from (7.8) that, to second order, the behaviour of δ is non local (and in fact it depends on spatial derivatives): the mass fluctuation at the position \mathbf{x} depends on initial perturbations at other positions via $\Delta^{(1)}$ (Eq.(4.26)).

Physically this means that, differently from the linear local case, when density fluctuation grows in amplitude, its spatial dependence, in comoving coordinates, changes. Thus the gravity field does change direction and particles are not accelerated in a fixed direction, as occurs in linear regime; the last term in right-hand side of Eq.(7.8) corresponds to the linear peculiar velocity shear contribution: indeed, if we write this, apart from a multiplicative factor, in the form $\sigma_{\alpha\beta} = (\frac{1}{3} \delta_{\alpha\beta} \nabla^2 - \partial_\alpha \partial_\beta) \phi^{(1)}$, we get $(\partial_\alpha \partial_\beta \Delta^{(1)})^2 = \sum_{\alpha,\beta=1}^3 (\sigma_{\alpha\beta})^2$.

Finally, if $\delta^{(1)}$ is Gaussian distributed, $\delta^{(2)}$ is no longer Gaussian distributed.

The second order velocity $\mathbf{v}^{(2)}$ is solution of the equations

$$\partial_\circ(a \mathbf{v}^{(2)}) = (\mathbf{v}^{(1)} \cdot \nabla) \mathbf{v}^{(1)} = a \mathbf{g}^{(2)}, \quad (7.9)$$

$$\partial_\circ \delta^{(2)} + a^{-1} \nabla \cdot (\mathbf{v}^{(2)} + \delta^{(1)} \mathbf{v}^{(1)}) = 0, \quad (7.10)$$

where $\mathbf{g}^{(2)} \equiv -a^{-1} \nabla \phi^{(2)}$ is the second order peculiar acceleration. From (7.10)

$$\mathbf{v}^{(2)} = a \partial_\circ \left(\frac{\mathbf{g}^{(2)}}{4\pi G \rho_b a} \right) - \delta^{(1)} \mathbf{v}^{(1)}. \quad (7.11)$$

Substituting in (7.9) and taking the divergence,

$$\begin{aligned} & \partial_\circ^2 \delta^{(2)} + 2\dot{a} a^{-1} \partial_\circ \delta^{(2)} - 4\pi G \rho_b \delta^{(2)} = \\ & = -a^{-1} \nabla \cdot \left[(\partial_\circ + \dot{a} a^{-1}) \delta^{(1)} \mathbf{v}^{(1)} - a^{-1} (\mathbf{v}^{(1)} \cdot \nabla) \mathbf{v}^{(1)} \right], \end{aligned} \quad (7.12)$$

which is another form of (7.4).

Because $\delta^{(2)} \propto D^2$, we have $\mathbf{g}^{(2)} \propto \rho_b a D^2$; alternative forms of (7.11) are therefore

$$\mathbf{v}^{(2)} = a \frac{\dot{D}}{D} \left[\frac{2 \mathbf{g}^{(2)}}{4\pi G \rho_b a} + \delta^{(1)} \nabla \Delta^{(1)} \right]$$

$$\begin{aligned}
&= a \frac{\dot{D}}{D} \left[\delta^{(1)} \nabla \Delta^{(1)} - 2 \nabla \Delta^{(2)} \right] \\
&= a \frac{\dot{D}}{D} \nabla \left[\frac{1}{2} (\nabla \Delta^{(1)})^2 - 2 \Delta^{(2)} \right], \tag{7.13}
\end{aligned}$$

where $\Delta^{(2)} \equiv \phi^{(2)}/4\pi G\rho_b a^2$ is the second order gravitational potential.

In an Einstein-de Sitter universe $\mathbf{v}^{(2)} \sim t$, slower than $\delta^{(2)} \sim t^{1/3}$. $\nabla \wedge \mathbf{v}^{(2)} = 0$. We stress the fact that $\mathbf{v}^{(2)}$ is *not* parallel to the second order acceleration $\mathbf{g}^{(2)}$: this is a consequence of the non locality.

Finally, we remember that $\mathbf{v}^{(2)}$ is known only once $\delta^{(2)}$ is known. The equation (7.6) can be solved exactly only if $\Omega = 1$, in which case all terms in right-hand side have the same time dependence, making the equation separable. For $\Omega \neq 1$ the equation (7.6) is not separable, and thus cannot be directly integrated.

Approximate expressions of $\delta^{(2)}$ in non-flat universes are given in Fry (1984) and in Martel & Freudling (1991), but the Eq.(7.6) is really solved, for a general Ω universe, only in Bouchet *et al.* (1992): using an elegant perturbative theory in Lagrangian representation, they find

$$\delta^{(2)} = \frac{1}{2} \left[1 - E(\Omega)/D^2 \right] \delta^{(1)2} + \partial_\alpha \delta^{(1)} \partial_\alpha \Delta^{(1)} + \frac{1}{2} \left[1 + E(\Omega)/D^2 \right] \partial_\alpha \partial_\beta \Delta^{(1)} \partial_\alpha \partial_\beta \Delta^{(1)} \tag{7.14}$$

where $E(\Omega)$ is a very complicated function of Ω , but in vicinity of $\Omega = 1$, effectively in the range $0.05 \lesssim \Omega \lesssim 3$,

$$E(\Omega) = -\frac{3}{7} \Omega^{-2/63} D^2 + 0 \left[(\Omega - 1)^2 \right], \tag{7.15}$$

from which (0.4% accuracy)

$$\delta^{(2)} = \frac{1}{2} \left[1 + \frac{3}{7} \Omega^{-2/63} \right] \delta^{(1)2} + \partial_\alpha \delta^{(1)} \partial_\alpha \Delta^{(1)} + \frac{1}{2} \left[1 - \frac{3}{7} \Omega^{-2/63} \right] \partial_\alpha \partial_\beta \Delta^{(1)} \partial_\alpha \partial_\beta \Delta^{(1)}. \tag{7.16}$$

Therefore, the $\Omega \neq 1$ solutions scale with time almost exactly like D^2 , since $\delta^{(1)} \propto \Delta^{(1)} \propto D(t)$, and $E(\Omega)$ is *extremely weakly* sensitive to Ω . This property has been also noticed by Martel & Freudling (1991), who have integrated an approximate time evolution equation for $\delta^{(2)}$ with $\Omega = 0.2$.

We stop a bit for computing the Fourier transforms of $\delta^{(2)}$ and $\mathbf{v}^{(2)}$; although Peebles in his book (1980, §18) derives for an Einstein-de Sitter universe the induced-by-gravity skewness of an initially Gaussian density field directly in \mathbf{x} -space, it is much more simple to do that in \mathbf{k} -space.

We can obtain $\tilde{\delta}^{(2)}$ directly Fourier transforming the differential equation (7.6) (* indicates convolution)

$$\begin{aligned} & \partial_0^2 \tilde{\delta}^{(2)} + 2\dot{a}a^{-1} \partial_0 \tilde{\delta}^{(2)} - 4\pi G\rho_b \tilde{\delta}^{(2)} = \\ & = \left[4\pi G\rho_b + \left(\frac{\dot{D}}{D} \right)^2 \right] \tilde{\delta}^{(1)} * \tilde{\delta}^{(1)} + \left[4\pi G\rho_b + 2 \left(\frac{\dot{D}}{D} \right)^2 \right] (k^\alpha \tilde{\delta}^{(1)}) * \left(\frac{k^\alpha}{k^2} \tilde{\delta}^{(1)} \right) + \\ & \quad + \left(\frac{\dot{D}}{D} \right)^2 \left(\frac{k^\alpha k^\beta}{k^2} \tilde{\delta}^{(1)} \right) * \left(\frac{k^\alpha k^\beta}{k^2} \tilde{\delta}^{(1)} \right). \end{aligned} \quad (7.17)$$

In the Einstein-de Sitter case, the left-hand side becomes $14 \tilde{\delta}^{(2)}/9t^2$; therefore,

$$\tilde{\delta}^{(2)} = \frac{5}{7} \tilde{\delta}^{(1)} * \tilde{\delta}^{(1)} + (k^\alpha \tilde{\delta}^{(1)}) * \left(\frac{k^\alpha}{k^2} \tilde{\delta}^{(1)} \right) + \frac{2}{7} \left(\frac{k^\alpha k^\beta}{k^2} \tilde{\delta}^{(1)} \right) * \left(\frac{k^\alpha k^\beta}{k^2} \tilde{\delta}^{(1)} \right), \quad (7.18)$$

which is just the Fourier transform of (7.8).

Explicitly (time dependence is understood)

$$\tilde{\delta}^{(2)}(\mathbf{k}) = \frac{1}{(2\pi)^3} \int d\mathbf{k}' J_2(\mathbf{k}', \mathbf{k} - \mathbf{k}') \tilde{\delta}^{(1)}(\mathbf{k}') \tilde{\delta}^{(1)}(\mathbf{k} - \mathbf{k}'), \quad (7.19)$$

where we have defined the function

$$\begin{aligned} J_2(\mathbf{k}, \mathbf{k}') & \equiv \frac{5}{7} + \frac{\mathbf{k} \cdot \mathbf{k}'}{k'^2} + \frac{2}{7} \left(\frac{\mathbf{k} \cdot \mathbf{k}'}{kk'} \right)^2 \\ & = \frac{17}{21} + \frac{k}{k'} P_1(\mu) + \frac{4}{21} P_2(\mu), \end{aligned} \quad (7.20)$$

$\mu \equiv \mathbf{k} \cdot \mathbf{k}' / k k'$, $P_1(\mu)$ and $P_2(\mu)$ being Legendre polynomials. Note that, because of mass conservation, $\langle \tilde{\delta}^{(2)}(\mathbf{k}) \rangle = 0$.

For completeness, we give also the Fourier transform of $v^{(2)\alpha}$:

$$\tilde{v}^{(2)\alpha}(\mathbf{k}) = i a \frac{\dot{D}}{D} \frac{k^\alpha}{k^2} \int d\mathbf{k}' \tilde{J}_2(\mathbf{k}', \mathbf{k} - \mathbf{k}') \tilde{\delta}^{(1)}(\mathbf{k}') \tilde{\delta}^{(1)}(\mathbf{k} - \mathbf{k}'), \quad (7.21)$$

where

$$\begin{aligned} \tilde{J}_2(\mathbf{k}, \mathbf{k}') &\equiv 2 J_2(\mathbf{k}, \mathbf{k}') - \frac{(\mathbf{k} + \mathbf{k}') \cdot \mathbf{k}}{k^2} \\ &= \frac{13}{21} + \frac{k}{k'} P_1(\mu) + \frac{8}{21} P_2(\mu). \end{aligned} \quad (7.22)$$

A more general expression of $\tilde{\delta}^{(2)}$, for a general Ω universe, is recovered if one takes the Fourier transform of (7.14).

Third Order Equations: Solutions

$\delta^{(3)}$ is solution of the equation

$$\begin{aligned} &\partial_0^2 \delta^{(3)} + 2\dot{a}a^{-1} \partial_0 \delta^{(3)} - 4\pi G \rho_b \delta^{(3)} = \\ &= 4\pi G \rho_b \left(2\delta^{(1)}\delta^{(2)} \right) + a^{-2} \left(\partial_\alpha \delta^{(1)} \partial_\alpha \phi^{(2)} + \partial_\alpha \delta^{(2)} \partial_\alpha \phi^{(1)} \right) + \\ &+ 2a^{-2} \partial_\alpha \partial_\beta v^{(1)\alpha} v^{(2)\beta} + a^{-2} \partial_\alpha \partial_\beta \delta^{(1)} v^{(1)\alpha} v^{(1)\beta}; \end{aligned} \quad (7.23)$$

however, from the third order on, the advantages of the Fourier transform for computation become more than obvious; we get, from the previous equation,

$$\begin{aligned} &\partial_0^2 \tilde{\delta}^{(3)} + 2\dot{a}a^{-1} \partial_0 \tilde{\delta}^{(3)} - 4\pi G \rho_b \tilde{\delta}^{(3)} = \\ &= 4\pi G \rho_b \left[2 \tilde{\delta}^{(1)} * \tilde{\delta}^{(2)} + (k^\alpha \tilde{\delta}^{(1)}) * \left(\frac{k^\alpha}{k^2} \tilde{\delta}^{(2)} \right) + (k^\alpha \tilde{\delta}^{(2)}) * \left(\frac{k^\alpha}{k^2} \tilde{\delta}^{(1)} \right) \right] + \\ &+ a^{-2} (i k^\alpha)(i k^\beta) \left[2 \tilde{v}^{(1)\alpha} * \tilde{v}^{(2)\beta} + \tilde{\delta}^{(1)} * \tilde{v}^{(1)\alpha} * \tilde{v}^{(1)\beta} \right]. \end{aligned} \quad (7.24)$$

In an Einstein-de Sitter Universe, because $\delta^{(3)} \propto D^2 \propto t^2$, we have $\partial_0^2 \tilde{\delta}^{(3)} + 2\dot{a}a^{-1}\partial_0 \tilde{\delta}^{(3)} - 4\pi G\rho_b \tilde{\delta}^{(3)} = 4\tilde{\delta}^{(3)}/t^2$; using the second order results it is not difficult to show that

$$\begin{aligned} \tilde{\delta}^{(3)}(\mathbf{k}) &= \\ &= \frac{1}{(2\pi)^6} \int d\mathbf{k}_1 d\mathbf{k}_2 d\mathbf{k}_3 \delta_D(\mathbf{k}_1 + \mathbf{k}_2 + \mathbf{k}_3 - \mathbf{k}) J_3(\mathbf{k}_1, \mathbf{k}_2, \mathbf{k}_3) \tilde{\delta}^{(1)}(\mathbf{k}_1) \tilde{\delta}^{(1)}(\mathbf{k}_2) \tilde{\delta}^{(1)}(\mathbf{k}_3), \end{aligned} \quad (7.25)$$

where

$$\begin{aligned} J_3(\mathbf{k}_1, \mathbf{k}_2, \mathbf{k}_3) &\equiv J_2(\mathbf{k}_2, \mathbf{k}_3) \left[\frac{1}{3} + \frac{4}{3} \frac{\mathbf{k}_1 \cdot (\mathbf{k}_2 + \mathbf{k}_3)}{(\mathbf{k}_2 + \mathbf{k}_3)^2} + \frac{4}{9} \frac{\mathbf{k} \cdot \mathbf{k}_1}{k_1^2} \frac{\mathbf{k} \cdot (\mathbf{k}_2 + \mathbf{k}_3)}{(\mathbf{k}_2 + \mathbf{k}_3)^2} \right] + \\ &\quad - \frac{2}{9} \frac{\mathbf{k} \cdot \mathbf{k}_1}{k_1^2} \frac{\mathbf{k} \cdot (\mathbf{k}_2 + \mathbf{k}_3)}{(\mathbf{k}_2 + \mathbf{k}_3)^2} \frac{(\mathbf{k}_2 + \mathbf{k}_3) \cdot \mathbf{k}_3}{k_3^2} + \frac{1}{9} \frac{\mathbf{k} \cdot \mathbf{k}_2}{k_2^2} \frac{\mathbf{k} \cdot \mathbf{k}_3}{k_3^2}. \end{aligned} \quad (7.26)$$

The third order velocity $\mathbf{v}^{(3)}$ is solution of the equations

$$\partial_0 (a\mathbf{v}^{(3)}) + (\mathbf{v}^{(1)} \cdot \nabla) \mathbf{v}^{(2)} + (\mathbf{v}^{(2)} \cdot \nabla) \mathbf{v}^{(1)} = a \mathbf{g}^{(3)}, \quad (7.27)$$

$$\partial_0 \delta^{(3)} + a^{-1} \nabla \cdot (\mathbf{v}^{(3)} + \delta^{(3)} \mathbf{v}^{(2)} + \delta^{(2)} \mathbf{v}^{(1)}) = 0, \quad (7.28)$$

and, in an Einstein-de Sitter universe, $\mathbf{v}^{(3)} \sim t^{5/3}$, slower than $\delta^{(3)}$; its Fourier transform looks like

$$\begin{aligned} \tilde{\mathbf{v}}^{(3)\alpha}(\mathbf{k}) &= i a \frac{\dot{D}}{D} \frac{k^\alpha}{k^2} \int \frac{d\mathbf{k}_1 d\mathbf{k}_2 d\mathbf{k}_3}{(2\pi)^6} \\ &\quad \delta_D(\mathbf{k}_1 + \mathbf{k}_2 + \mathbf{k}_3 - \mathbf{k}) \tilde{J}_3(\mathbf{k}_1, \mathbf{k}_2, \mathbf{k}_3) \tilde{\delta}^{(1)}(\mathbf{k}_1) \tilde{\delta}^{(1)}(\mathbf{k}_2) \tilde{\delta}^{(1)}(\mathbf{k}_3), \end{aligned} \quad (7.29)$$

$$\tilde{J}_3(\mathbf{k}_1, \mathbf{k}_2, \mathbf{k}_3) \equiv 3 J_3(\mathbf{k}_1, \mathbf{k}_2, \mathbf{k}_3) - \frac{\mathbf{k} \cdot \mathbf{k}_1}{k_1^2} J_2(\mathbf{k}_2, \mathbf{k}_3) - \frac{\mathbf{k} \cdot (\mathbf{k}_1 + \mathbf{k}_2)}{(\mathbf{k}_1 + \mathbf{k}_2)^2} \tilde{J}_2(\mathbf{k}_1, \mathbf{k}_2). \quad (7.30)$$

These solutions, although exact, are surely difficult to apply directly, because of the presence of non local terms. In Nusser *et al.* (1991), an approximate interpolation of the contributions up to third order is given.

7.2 An Application of the Non Linear Theory: Skewness as a Cosmological Probe

We have now all the ingredients for calculating the gravitationally induced skewness, starting from an initial Gaussian distributed random field $\delta^{(1)} = \delta_1 D$; the skewness at high redshifts, when the second order effects are negligible, is then

$$\langle \delta^{(1)3} \rangle = \zeta(0) = 0, \quad (7.31)$$

where ζ is the three point correlation function. The lowest order non vanishing term is

$$\langle \delta^3 \rangle = 3 \langle \delta^{(1)2} \delta^{(2)} \rangle. \quad (7.32)$$

To evaluate this quantity, we have to multiply both sides of (7.8) by $\delta^{(1)2}$, than take averages. In \mathbf{k} -space this is easily done; from (7.19) we derive the intermediate result

$$\begin{aligned} & \langle \bar{\delta}^{(1)}(\mathbf{k}_1) \bar{\delta}^{(1)}(\mathbf{k}_2) \bar{\delta}^{(2)}(\mathbf{k}_3) \rangle = \\ & (2\pi)^3 \delta_D(\mathbf{k}_1 + \mathbf{k}_2 + \mathbf{k}_3) \left[\frac{10}{7} + 2 \frac{\mathbf{k}_1 \cdot \mathbf{k}_2}{k_2^2} + \frac{4}{7} \left(\frac{\mathbf{k}_1 \cdot \mathbf{k}_2}{k_1 k_2} \right)^2 \right] P(k_1) P(k_2), \end{aligned} \quad (7.33)$$

where $P(k)$ is the primordial power spectrum, then

$$\langle \delta^3 \rangle_G = \frac{6}{(2\pi)^6} \int d\mathbf{k} d\mathbf{k}' J_2(\mathbf{k}, \mathbf{k}') P(k) P(k'). \quad (7.34)$$

Because of the addition theorem for spherical harmonics

$$\propto \sum_m Y_l^m(\hat{\mathbf{k}}) Y_l^{-m}(\hat{\mathbf{k}}) = \frac{2l+1}{4\pi} P_l(\mu), \quad (7.35)$$

the integral in (7.34) is trivial; we get (Peebles 1980, Eq.(18.8))

$$\langle \delta^3 \rangle_G = \frac{34}{7} \xi(0)^2 \equiv S_3 \langle \delta^2 \rangle^2, \quad (7.36)$$

where ξ is the two-point correlation. The expression for S_3 in \mathbf{k} -space with $\Omega = 1$ was first derived by Fry (1984). Goroff *et al.* (1986) first properly included the

filters W_R in their calculations and pointed out that S_3 may vary with scale when the slope of $P(k)$ changes. Expression (7.36) takes a different form in the case in which the primordial density distribution is non-Gaussian, as we shall see.

The generalization of (7.36) for $\Omega \neq 1$ is given by Bouchet *et al.* (1992): the parameter S_3 depends extremely weakly on Ω

$$S_3 = \frac{34}{7} + \frac{6}{7} (\Omega^{-2/63} - 1) , \quad (7.37)$$

or, in other words, S_3 is a very slowly varying function of time. This property improves the prospects of using observational estimates of $\langle \delta^3 \rangle$ (Saunders *et al.* 1991) to distinguish gravitational instability models with Gaussian initial conditions from more so called exotic scenarios, as pointed out in Silk & Juszkiewicz (1991). The quadratic scaling law (7.36) obtained here from Gaussian initial conditions and small δ , with S_3 expected to be constant in the conventional picture, is favoured by the IRAS data (Saunders *et al.* 1991; Bouchet, Strauss & Davis 1991; Kaiser 1991) and the QDOT data (Park 1991; Coles & Frenk 1991).

Recently, Turok & Spergel (1991), in the framework of global texture models, and Scherrer & Bertschinger (1991), in general intrinsically non-Gaussian models, computed the probability distribution of mass fluctuations δ and explicitly estimate the deviations from a Gaussian distribution in terms of the skewness; what is found is that the skewness scales like

$$\langle \delta^3 \rangle = S'_3 \langle \delta^2 \rangle^{3/2} , \quad (7.38)$$

so that, for having an eventual agreement with data, we need $S'_3 \propto \langle \delta^2 \rangle^{-1/2}$; we see that the power of the test for non conventional models increases with decreasing variance or, in other words, the possibility to detect non-standard

departures from Gaussian distribution improves with the size of the sample. The last generation of catalogues may actually allow to make that detection.

The smoothing operation, necessary to do theoretical predictions comparable to observational estimates, modifies the skewness; for a top hat filter, Juszkiewicz, Bouchet & Colombi (1991) found that, in an Einstein-de Sitter universe, there exists a dependence on the spectral index (see also Fry 1984)

$$S_3 = \frac{34}{7} - (3 + n), \quad -3 \leq n < 1. \quad (7.39)$$

IRAS data (Kaiser 1991) and APM data (Hamilton *et al.* 1991) in the range $20 \div 100 h^{-1}$ seem compatible with (7.39) if $n = -1$; if a Gaussian filter is used, S_3 changes from $34/7 = 4.9$, at $n = 3$, to 3.0 at $n = 1$. $34/7$ seems to be the saturation value of the skewness for the minimal small-scale power, $n = -3$. The skewness S_3 has been also estimated in recent N-body simulations (Bouchet & Hernquist 1991; Weinberg & Cole 1991), with results in agreement with those derived previously in the conventional scheme. We note that (7.39) contradicts a recent claim of Coles & Frenk (1991) which states that the expression for S_3 for the smoothed field “does not involve terms describing the initial spectrum”. The problem is that they adopt as universal the value $S_3 \approx 3$, deduced by Goroff *et al.* (1986, fig.5) in the case $n = 1$ and Gaussian filter.

Skewness of a Primordial Non Gaussian Density Field

All the results previously presented have been obtained assuming that the primordial density distribution is Gaussian. An obvious generalization one may think to do is to extend the same techniques for computing the skewness $\langle \delta^3 \rangle$ starting from a *general* non-Gaussian primordial density field; in this case, we guess immediately, there is a contribution to the skewness from the lowest

perturbative order: this is a ‘primordial’ contribution ie. already contained in the initial conditions. However, because of the difficulty of the calculations (at least for us!), is not so easy at all to compute the contribution to the skewness from the second order terms, which are the terms which take into account the non linear gravitational evolution.

We indicate here a manner for trying to compute the induced-by-gravity skewness starting from a primordial non-Gaussian random field. We do this, extending the previous formalism, by working in \mathbf{k} -space. However, it has been suggested (Fry, private communication) that the same calculation can be probably more easily concluded if one chooses to work in \mathbf{x} -space.

All we need are the previous results up to the second perturbative order,

$$\begin{aligned}\langle \delta^3 \rangle_{nG} &= \langle \delta^{(1)3} \rangle + 3 \langle \delta^{(1)2} \delta^{(2)} \rangle \\ &= \zeta(0) + 3 \langle \delta^{(1)2} \delta^{(2)} \rangle .\end{aligned}\quad (7.40)$$

As in the Gaussian case, we compute the perturbative contribution in \mathbf{k} -space, but now there is the connected contribution from the four point correlation

$$\begin{aligned}\langle \bar{\delta}^{(1)}(\mathbf{k}_1) \bar{\delta}^{(1)}(\mathbf{k}_2) \bar{\delta}^{(2)}(\mathbf{k}_3) \rangle &= \frac{1}{(2\pi)^3} \int d\mathbf{k}_a d\mathbf{k}_b \delta_D(\mathbf{k}_a + \mathbf{k}_b - \mathbf{k}_3) J_2(\mathbf{k}_a, \mathbf{k}_b) \times \\ &\times \left[\langle \bar{\delta}^{(1)}(\mathbf{k}_1) \bar{\delta}^{(1)}(\mathbf{k}_2) \bar{\delta}^{(1)}(\mathbf{k}_a) \bar{\delta}^{(1)}(\mathbf{k}_b) \rangle_c + 2! \langle \bar{\delta}^{(1)}(\mathbf{k}_1) \bar{\delta}^{(1)}(\mathbf{k}_a) \rangle \langle \bar{\delta}^{(1)}(\mathbf{k}_2) \bar{\delta}^{(1)}(\mathbf{k}_b) \rangle \right] .\end{aligned}\quad (7.41)$$

Instead of Eq.(7.34), one finds

$$\begin{aligned}3 \langle \delta^{(1)2} \delta^{(2)} \rangle_{nG} &= \frac{1}{(2\pi)^6} \int d\mathbf{k} d\mathbf{k}' \\ &\left[6 J_2(\mathbf{k}, \mathbf{k}') P(k) P(k') + \frac{1}{(2\pi)^3} \int d\mathbf{k}'' J_2(\mathbf{k}'', \mathbf{k} - \mathbf{k}' - \mathbf{k}'') T(k, k', k'') \right] ,\end{aligned}\quad (7.42)$$

where $T(k, k', k'')$ is the trispectrum.

Finally, the skewness for a general initially non-Gaussian random field is

$$\langle \delta^3 \rangle_{nG} - \zeta(0) = \frac{17}{7} \xi(0)^2 + \frac{17}{21} \langle \delta^{(1)4} \rangle + I, \quad (7.43)$$

where we have defined the quantity I as

$$I \equiv \frac{1}{(2\pi)^9} \int d\mathbf{k} d\mathbf{k}' d\mathbf{k}'' \left[\frac{k''}{\Sigma} P_1(\mu) + \frac{4}{21} P_2(\mu) \right] T(k, k', k'') \quad (7.44)$$

and $\Sigma \equiv \mathbf{k} + \mathbf{k}' + \mathbf{k}''$, $\Sigma \equiv |\Sigma|$, μ the cosine between the vectors \mathbf{k}'' and Σ .

From Eq.(7.44), we see that the skewness induced by gravity is different from the Gaussian case, this implying a deeper discussion about its cosmological significance.

Apart of integration in I , dependence on the Ω value (but we suppose that also in this case it is negligible) and on filtering the underlying field δ has yet to be discussed.

Kurtosis in Density and Velocity Fields

We conclude this section on perturbative techniques by computing the fourth order moment induced by gravity, the kurtosis, in density field and velocity field, initially Gaussian distributed.

The actual catalogues surely are too poor for these observables to be measured; however, Villumsen & Brainerd (1992) analyzing by N-body simulations the highly nonlinear evolution of initially Gaussian perturbations, find that the peculiar velocity field induced by gravity exhibits a strong positive kurtosis. Roughly speaking, this means that the velocity probability distribution $p(\mathbf{v})$ is more strongly peaked near $\mathbf{v} = \mathbf{0}$, but it has larger tails at large values of $|\mathbf{v}|$ than the Gaussian distribution.

A non-Gaussian behaviour in velocity fields reflects the non-Gaussian nature of the underlying density fields (the converse may not be true). Scherrer

(1992) shows that the kurtosis of $p_z(v_z)$ is positive for all seed models with randomly distributed seeds and for all local non-Gaussian models; it is still unclear whether this is a general result which applies to a larger class of non-Gaussian models.

Since δ is initially Gaussian distributed, the lowest order non zero connected part of η_{1234} is of order 6 in $\delta^{(1)}$,

$$\begin{aligned} \eta &= \langle \delta^{(1)}(\mathbf{x}_1) \delta^{(1)}(\mathbf{x}_2) \delta^{(2)}(\mathbf{x}_3) \delta^{(2)}(\mathbf{x}_4) \rangle + \text{c.p. (6 terms)} + \\ &+ \langle \delta^{(1)}(\mathbf{x}_1) \delta^{(1)}(\mathbf{x}_2) \delta^{(1)}(\mathbf{x}_3) \delta^{(3)}(\mathbf{x}_4) \rangle + \text{c.p. (4 terms)}. \end{aligned} \quad (7.45)$$

In particular the density kurtosis is given by (see App. B)

$$k_4 \equiv \eta(0) = 6 \langle \delta^{(1)2} \delta^{(2)2} \rangle + 4 \langle \delta^{(1)3} \delta^{(3)} \rangle. \quad (7.46)$$

It is really much more simple to work in \mathbf{k} -space; we have

$$\begin{aligned} &\langle \bar{\delta}^{(1)}(\mathbf{k}_1) \bar{\delta}^{(1)}(\mathbf{k}_2) \bar{\delta}^{(2)}(\mathbf{k}_3) \bar{\delta}^{(2)}(\mathbf{k}_4) \rangle = \\ &(2\pi)^3 \delta_D(\mathbf{k}_1 + \mathbf{k}_2 + \mathbf{k}_3 + \mathbf{k}_4) \times 4 P(k_1) P(k_2) \times \\ &\times [J_2(-\mathbf{k}_1, \mathbf{k}_1 + \mathbf{k}_3) J_2(\mathbf{k}_2, \mathbf{k}_1 + \mathbf{k}_3) P(|\mathbf{k}_1 + \mathbf{k}_3|) + \\ &+ J_2(\mathbf{k}_2 + \mathbf{k}_3, -\mathbf{k}_2) J_2(\mathbf{k}_2 + \mathbf{k}_3, \mathbf{k}_1) P(|\mathbf{k}_2 + \mathbf{k}_3|)]. \end{aligned} \quad (7.47)$$

We need now for the piece $\langle \delta^{(1)3} \delta^{(3)} \rangle$;

$$\begin{aligned} &\langle \bar{\delta}^{(1)}(\mathbf{k}_1) \bar{\delta}^{(1)}(\mathbf{k}_2) \bar{\delta}^{(1)}(\mathbf{k}_3) \bar{\delta}^{(3)}(\mathbf{k}_4) \rangle = \\ &= (2\pi)^3 \delta_D(\mathbf{k}_1 + \mathbf{k}_2 + \mathbf{k}_3 + \mathbf{k}_4) 3! P(k_1) P(k_2) P(k_3) J_3(\mathbf{k}_1, \mathbf{k}_2, \mathbf{k}_3). \end{aligned} \quad (7.48)$$

Combining these results we get the integral expression of the kurtosis

$k_4(\delta)$,

$$\eta(0) = \frac{24}{(2\pi)^9} \int d\mathbf{k} d\mathbf{k}' d\mathbf{k}'' P(k) P(k') P(k'') [J_3(\mathbf{k}, \mathbf{k}', \mathbf{k}'') +$$

$$+J_2(-\mathbf{k}, \mathbf{k}+\mathbf{k}'')J_2(\mathbf{k}', \mathbf{k}+\mathbf{k}'')P(|\mathbf{k}+\mathbf{k}''|)+J_2(-\mathbf{k}', \mathbf{k}'+\mathbf{k}'')J_2(\mathbf{k}, \mathbf{k}'+\mathbf{k}'')P(|\mathbf{k}+\mathbf{k}''|)] . \quad (7.49)$$

To treat integral expression like this seems not easy at all, except for some naive configurations (see Fry 1984). Goroff *et al.* (1986) treat similar expressions in a CDM framework ($P(k) = k$) using standard Monte Carlo techniques, for Gaussian-filtered density fields: if the normalization of the primordial power spectrum is chosen so that $\langle \delta_R^2 \rangle$ is greater than 1/3 at a distance $Rh^2 = 5 Mpc$, then the connected part of $\langle \delta_R^4 \rangle$ dominates over the disconnected part indicating that for such normalizations the probability distribution for δ_R is still highly non Gaussian at this distance (see their Fig.6).

We can apply the previous results for computing the excess of kurtosis induced by gravitational evolution on the peculiar velocity field. We restrict the analysis along one chosen direction, say $\hat{\alpha}$. The fourth order reduced moment of the velocity field, to lowest perturbative order, is given by

$$k_4(v_\alpha) = \langle v_\alpha^{(1)}(\mathbf{x}_1) v_\alpha^{(1)}(\mathbf{x}_2) v_\alpha^{(2)}(\mathbf{x}_3) v_\alpha^{(2)}(\mathbf{x}_4) \rangle + \text{c.p. (6 terms)} + \\ + \langle v_\alpha^{(1)}(\mathbf{x}_1) v_\alpha^{(1)}(\mathbf{x}_2) v_\alpha^{(1)}(\mathbf{x}_3) v_\alpha^{(3)}(\mathbf{x}_4) \rangle + \text{c.p. (4 terms)} , \quad (7.50)$$

because, due to isotropy, all odd moments are zero.

By using the second and third order perturbative results, we get

$$\eta_v(0) = \frac{24}{(2\pi)^9} \left(\frac{a \dot{D}}{D} \right)^4 \int d\mathbf{k}_1 d\mathbf{k}_2 d\mathbf{k}_3 \frac{k_1^\alpha k_2^\alpha k_3^\alpha (k_1^\alpha + k_2^\alpha + k_3^\alpha)}{k_1^2 k_2^2 k_3^2 |\mathbf{k}_1 + \mathbf{k}_2 + \mathbf{k}_3|^2}$$

$$P(k_1) P(k_2) P(k_3) [\bar{J}_3(\mathbf{k}_1, \mathbf{k}_2, \mathbf{k}_3) + \bar{J}_2(-\mathbf{k}_1, \mathbf{k}_1 + \mathbf{k}_3) \bar{J}_2(\mathbf{k}_2, \mathbf{k}_1 + \mathbf{k}_3) P(|\mathbf{k}_1 + \mathbf{k}_3|) + \\ \bar{J}_2(-\mathbf{k}_2, \mathbf{k}_2 + \mathbf{k}_3) \bar{J}_2(\mathbf{k}_1, \mathbf{k}_2 + \mathbf{k}_3) P(|\mathbf{k}_2 + \mathbf{k}_3|)] . \quad (7.51)$$

APPENDIX A

Gaussian Random Fields

Let consider the homogeneous isotropic Gaussian random field $\delta(\mathbf{x}) \equiv [\rho(\mathbf{x}) - \langle \rho \rangle] / \langle \rho \rangle$, with mean zero and variance $\sigma_{\circ}^2 = \langle \rho \rangle^{1/2}$. The *pdf* of δ with power spectrum $P(k)$ is

$$p(\delta) d\delta = (2\pi\sigma_{\circ}^2)^{-1/2} \exp(-\delta^2/2\sigma_{\circ}^2), \quad (\text{A.1})$$

where (§ 3.3)

$$\sigma_{\circ}^2 = \frac{1}{2\pi} \int_0^{\infty} dk k^2 P(k) = \xi(0), \quad (\text{A.2})$$

$\xi(r)$ being the 2-point correlation function. All statistical properties of δ can be expressed in terms of the correlation function $\xi(r)$ and its derivatives or, alternatively, in terms of integrals over the power spectrum. For instance, one useful moment is

$$\sigma_1^2 = -3\xi''(0) = \frac{1}{2\pi} \int_0^{\infty} dk k^4 P(k), \quad (\text{A.3})$$

which is the mean-square derivative of the field along a line. One may define a related coherence length

$$r_c \equiv \frac{\sigma_{\circ}}{\sigma_1} = \langle k^2 \rangle^{-1/2}, \quad (\text{A.4})$$

which measures the effective range of the correlations present in the field. Many of the power spectra of interest in cosmology lead to a zero coherence length (ie. an infinite mean-square derivative). This happens because such fields have structures on all scales and are therefore not differentiable. The usual approach is to smooth away structure on scales less than some scale of interest R (§ 3.3).

Behind many statistical calculations is the *joint probability distribution* of the values of the field $\delta(\mathbf{x})$ and/or of the derivatives of the field δ in N points $\mathbf{x}_1, \dots, \mathbf{x}_N$, which is a *multivariate gaussian pdf*

$$P_N(\alpha_1, \dots, \alpha_N) = [(2\pi)^N \det M]^{-1/2} \exp \left\{ -\frac{1}{2} \sum_{jh} \alpha_j M_{jh}^{-1} \alpha_h \right\}. \quad (\text{A.5})$$

$M_{jh} \equiv \langle \alpha_j \alpha_h \rangle$ is the $N \times N$ *correlation matrix*. A simple example is the joint probability distribution that δ has a value $\alpha_1 = \delta(\mathbf{x}_1)$ and a value $\alpha_2 = \delta(\mathbf{x}_2) = \delta(\mathbf{x}_1 + \mathbf{r})$. To make things as simple as possible, we use normalized variables $\alpha'_i \equiv \alpha_i / \sigma_o$ and define a normalized correlation function (autocorrelation) $\omega(r) \equiv \xi(r) / \sigma_o^2$. The correlation matrix and its inverse are

$$M = \begin{pmatrix} 1 & \omega \\ \omega & 1 \end{pmatrix}, \quad M^{-1} = \frac{1}{1 - \omega^2} \begin{pmatrix} 1 & -\omega \\ -\omega & 1 \end{pmatrix}, \quad (\text{A.6})$$

therefore,

$$p(\alpha_1, \alpha_2; \omega) = (2\pi\sqrt{1 - \omega^2})^{-1} \exp[-(\alpha_1^2 - 2\omega\alpha_1\alpha_2 + \alpha_2^2)/2(1 - \omega^2)]. \quad (\text{A.7})$$

For those interested in the path-integral approach, we remember that, for a Gaussian scalar random field (Feynman & Hibbs 1965)

$$P[\delta] \propto \exp \left\{ -\frac{1}{2} \int dx dy \delta(\mathbf{x}) K(\mathbf{x}, \mathbf{y}) \delta(\mathbf{y}) \right\}, \quad (\text{A.8})$$

with $\int [d\delta] P[\delta] = 1$, from which it is possible to obtain all the previous relations. K is defined by the relations $K = \xi^{-1}$ and $\int dy K(\mathbf{x}, \mathbf{y}) K^{-1}(\mathbf{y}, \mathbf{z}) = \delta(\mathbf{x} - \mathbf{z})$, as in the usual field theory (see e.g. Negele & Orland 1988; Ramond 1989), and therefore $P(k) = 1/\tilde{K}(k)$, with \tilde{K} the Fourier transform of K . The mathematical theory of Gaussian random fields is given in books by Adler (1981) and Vanmarcke (1983). Many properties are also analyzed in beautiful classical works e.g. Chandrasekhar (1943) and Rice (1954).

APPENDIX B

Cumulant Expansion

A general way of specifying the distribution functional (let suppose that we are treating the *continuous* field case)

$$P[\delta(\mathbf{x})] d[\delta(\mathbf{x})], \quad (\text{B.1})$$

is by (all of) its *moments*

$$\langle \delta(\mathbf{x}_1) \cdots \delta(\mathbf{x}_N) \rangle \equiv \mu_N(\mathbf{x}_1, \dots, \mathbf{x}_N). \quad (\text{B.2})$$

A way for generating automatically these moments is by functional differentiation (e.g. Monin & Yaglom 1971; Zaidi 1983; Fry 1985) of the *moment generating functional* $Z[J]$

$$Z[J] \equiv \left\langle \exp \int d\mathbf{x} \delta(\mathbf{x}) J(\mathbf{x}) \right\rangle = \int d[\delta(\mathbf{x})] \exp \int d\mathbf{x} \delta(\mathbf{x}) J(\mathbf{x}) P[\delta(\mathbf{x})] : \quad (\text{B.3})$$

$$\mu_N(\mathbf{x}_1, \dots, \mathbf{x}_N) = \frac{\delta^N Z[J]}{\delta J(\mathbf{x}_1) \cdots \delta J(\mathbf{x}_N)} \Big|_{J=0}. \quad (\text{B.4})$$

From either the original definition (B.2) or this expression, it is apparent that μ_N is unchanged by interchange of any subset of its arguments.

It is next convenient to introduce the *generating function*

$$K[J] \equiv \ln Z[J] = \left\langle \exp \left(\int d\mathbf{x} \delta(\mathbf{x}) J(\mathbf{x}) \right) - 1 \right\rangle_c, \quad (\text{B.5})$$

from which one can obtain systematically, by functional differentiation, the *connected or reduced moments*

$$k_N(\mathbf{x}_1, \dots, \mathbf{x}_N) \equiv \frac{\delta^N K[J]}{\delta J(\mathbf{x}_1) \cdots \delta J(\mathbf{x}_N)} \Big|_{J=0} = \langle \delta(\mathbf{x}_1) \cdots \delta(\mathbf{x}_N) \rangle_c. \quad (\text{B.6})$$

The k_N are the reduced correlation functions of the distribution $P[\delta(\mathbf{x})]d[\delta(\mathbf{x})]$, also known as *semi-invariants* and/or *cumulants* in probability theory (Monin & Yaglom 1971; Kendall & Stuart 1977) and in statistical studies of liquids (Rice & Gray 1965), and related to the connected Green's function of Quantum Field Theory (Brandenberger 1985; Ramond 1989). In QFT, $Z[J]$ is also known as the *partition functional* or *vacuum-vacuum transition amplitude* in the presence of the external source $J(\mathbf{x})$.

By (B.6), one can state the *cumulant expansion theorem* writing

$$Z[J] = \exp \sum_{N=1}^{\infty} \frac{1}{N!} \left(\prod_{h=1}^N \int d\mathbf{x}_h J(\mathbf{x}_h) \right) \langle \delta(\mathbf{x}_1) \cdots \delta(\mathbf{x}_N) \rangle_c, \quad (\text{B.7})$$

from which, we see, one may reconstruct the generating functional $\ln Z[J]$ from the N -point connected correlation functions $\xi^{(N)}(\mathbf{x}_1, \dots, \mathbf{x}_N) \equiv \langle \delta(\mathbf{x}_1) \cdots \delta(\mathbf{x}_N) \rangle_c$. The probability distribution functional $P[\delta(\mathbf{x})]$ then follows from the (inverse) functional Fourier transform of the functional $Z[iJ]$, often called, in this case, the *characteristic functional* of the distribution (see e.g. Fry 1985): therefore, in principle, *the hierarchy of N -point correlation functions completely specifies the statistics of the homogeneous and isotropic continuous random field $\delta(\mathbf{x})$* (however see Bochner's theorem, Reed & Simon 1980, theorem IX.9).

The cumulant expansion theorem is known in classical (e.g. Ma 1985) and quantum statistical mechanics (e.g. Negele & Orland 1988) as the *linked-cluster theorem*.

The reduced correlation functions k_N have the desirable property that $k_N(\delta + \delta') = k_N(\delta) + k_N(\delta')$ and $k_N(\alpha\delta) = \alpha^N k_N(\delta)$. More importantly, any contribution to μ_N which can be separated as $\langle \delta^M \rangle \langle \delta^{N-M} \rangle$ has been removed from k_N . Thus, $k_N \rightarrow 0$ as any subset of $\{\mathbf{x}_1, \dots, \mathbf{x}_N\}$ is removed to infinite separation.

The first few μ_N and k_N are related by the relations (with $\mu_1 = \langle \delta \rangle = 0$)

$$\begin{aligned}
\mu_2 &= k_2 , \\
\mu_3 &= k_3 , \\
\mu_4 &= k_4 + 3 k_2^2 , \\
\mu_5 &= k_5 + 10 k_2 k_3 , \\
\mu_6 &= k_6 + 15 k_2 k_4 + 10 k_3^2 + 15 k_2^3 , \\
\mu_7 &= k_7 + 21 k_2 k_5 + 35 k_3 k_4 + 105 k_2^2 k_3 , \tag{B.8}
\end{aligned}$$

etc., where, for brevity, labels on the unconnected parts are omitted; one has to take all distinct subgroupings of $\{\mathbf{x}_1, \dots, \mathbf{x}_N\}$, for instance,

$$\mu_4(1, 2, 3, 4) = k_4(1, 2, 3, 4) + k_2(1, 2) k_2(3, 4) + k_2(1, 3) k_2(2, 4) + k_2(1, 4) k_2(2, 3). \tag{B.9}$$

The first few k_N in galaxy clustering are known as $k_2(\mathbf{x}_1, \mathbf{x}_2) = \xi(x_{12})$, the two point function; $k_3(\mathbf{x}_1, \mathbf{x}_2, \mathbf{x}_3) = \zeta_{123}$, the three point function; and $k_4(\mathbf{x}_1, \mathbf{x}_2, \mathbf{x}_3, \mathbf{x}_4) = \eta_{1234}$, the four point function.

Finally, if one assumes that the random field δ is Gaussian distributed, then *all reduced moments k_N of the distribution vanish for $N \geq 3$* ; since we have subtracted out the mean also, this means that the distribution is completely specified by its two-point correlation function $\xi(x)$ (ie. by its Fourier transform, the power spectrum $P(k)$). Thus, the *N th moment*, $\mu_N = \langle \delta^N \rangle$, is obtained by connecting all possible pairs of points: $\mu_N = 0$ if N is odd, or $\mu_N = (N-1)!! \xi^{N/2}$ if N is even.

The particular form of $Z[J]$ in the case of Gaussian field is (Feynman & Hibbs 1965)

$$Z[J] = \int [\delta(\mathbf{x})] \exp \left\{ -\frac{1}{2} \int \int dx dy \delta(\mathbf{x}) K(\mathbf{x}, \mathbf{y}) \delta(\mathbf{y}) + \int dx \delta(\mathbf{x}) J(\mathbf{x}) \right\} . \tag{B.10}$$

Some cosmologists state that the word *non-Gaussian* means nothing, in the same sense that the word e.g. *non-dog* means nothing.

We disagree.

With the generic word *non-Gaussian* we characterize *any* probability distribution with some higher reduced moment different from zero, and this is not a null-statement; of course, this is not sufficient for picking out a specific probability distribution. On the other hand, there exists one exception, namely the distribution $p(x) = \delta_D(x - a)$, with only a mean and no nonvanishing higher irreducible moments.

APPENDIX C

Evidence for Low Ω_0 Universe

The QDOT and Cluster Dipoles: Evidence for a low Ω_0 Universe?

Manolis PLIONIS ¹, Peter COLES ² and Paolo CATELAN ¹

¹ *SISSA - International School for Advanced Studies,
Strada Costiera 11, 34014 Trieste, Italy*

² *Astronomy Unit, School of Mathematical Sciences
Queen Mary & Westfield College, Mile End Road
London E1 4NS, UK*

Summary

We have reanalysed the QDOT survey in order to investigate the convergence properties of the estimated dipole and the consequent reliability of the derived value of $\Omega_0^{0.6}/b$. We find that there is no compelling evidence that the QDOT dipole has converged within the limits of reliable determination and complete-

ness. Therefore the value of Ω_o derived by Rowan-Robinson *et al.* (1990) should be considered only as an upper limit. Furthermore, we find strong evidence that the shell between 140 and 160 h^{-1} Mpc does contribute significantly to the total dipole anisotropy and therefore to the motion of the Local Group with respect to the Cosmic Microwave Background. This shell contains the Shapley concentration, but we argue that this concentration itself cannot explain all the gravitational acceleration produced by it; there must exist a coherent anisotropy which includes this structure, but extends greatly beyond it. With the QDOT data alone, we cannot determine precisely the magnitude of any such anisotropy but any contribution to the Local Group motion from large scales would favour a value of $\Omega_o^{0.6}/b_{IRAS} \leq 0.6$, smaller than previous estimates based on IRAS galaxies; such a result would be consistent with the dipole measured from samples of rich clusters, which are much more complete at large depths.

Key Words: Galaxies: clustering – Infrared: Galaxies – large-scale Structure of the Universe.

C.1 Introduction

Assuming that gravitational instability is the cause of the observed peculiar motions, then the local deviations from a uniform Hubble flow provides a powerful tool to study the *local* mass distribution and therefore to estimate the cosmological density parameter, Ω_o .

Using linear perturbation theory (Peebles 1980), the peculiar velocity can be related to the peculiar acceleration via $\underline{v} \propto f(\Omega_o)\underline{g}$. The local peculiar velocity (\underline{v}) has been determined, to great accuracy, from the dipole anisotropy of the Cosmic Microwave Background Radiation (CMB), which implies a Local Group (LG) motion of $\sim 600 \text{ km/sec}$ towards $l \approx 270^\circ$ and $b \approx 30^\circ$ (Smoot *et al.* 1991 and references therein), while the peculiar acceleration is usually estimated from the dipole moment of the galaxy (or other mass tracer) distribution. To use linear theory one explicitly assumes that the motion of the LG is determined from large scales where non-linear effects can be ignored. It is also necessary to assume that the extragalactic objects, used to determine the peculiar acceleration, trace the underlying mass fluctuations. The latter assumption, however, can be directly tested from the data since the determined peculiar acceleration should be parallel to the peculiar velocity. Note, however, that if the extragalactic objects are *biased* tracers of the mass distribution (Kaiser 1984; Dekel & Rees 1987) then the picture becomes somewhat more complicated. If a simple phenomenological model for the bias is adopted, in which $(\delta\rho/\rho)_g = b(\delta\rho/\rho)_m$, then the dipole moment test constrains a combination of b and Ω_o , namely $\Omega_o^{0.6}/b$ (see Section C.2 below). To deduce the value of Ω_o one therefore needs to know

the value of b so the result is rather model-dependent even for this simple biasing scheme. In more complicated (i.e. more realistic) biasing schemes (e.g. Dekel & Rees 1987; Babul & White 1991; Bower *et al.* 1992) there might be no simple local relationship between galaxy numbers and mass density, making it even more difficult to relate galaxy velocities to density perturbations. We should therefore state at the outset that the weakest link in the chain of reasoning that leads from velocity information to a value of Ω_0 lies in the choice of model for the bias.

Furthermore, it is very important to note that this test can be applied with success only if the galaxy (or other mass tracer) dipole has converged to its *final* value within the limits of the catalogue used. That is to say that the apparent convergence must not be dictated by insufficient sampling of depths from which contributions to the LG acceleration could be significant. Since most catalogues of extragalactic objects are either magnitude/flux or diameter limited there is a significant possibility of this happening. The alignment of the galaxy dipole with the CMB dipole direction and an apparent plateau of the cumulative dipole over some scales should not *a priori* be considered as evidence for the convergence of the acceleration to its final value because it could well be that:

- The structure producing the LG peculiar motion could be very extended and thus the alignment found within a small (inner) volume could just result from the fact that the galaxy catalogue traces only part of a coherent anisotropy which is larger than the sample can probe.
- Beyond an apparent plateau (which in most recent studies coincides with the characteristic depth of the sample !) there could be a further contribution to the dipole. In fact this actually seems to happen in the case

of the cluster dipole; see Plionis & Valdarnini (1991) (hereafter PV91); Scaramella *et al.* (1991), hereafter SVZ. There is no *a priori* reason why the acceleration should grow continuously with depth up to its final value.

Up to now various populations of extragalactic objects have been used to estimate the peculiar acceleration induced on the LG: optical galaxies (Lahav 1987; Plionis 1988), IRAS galaxies (Yahil, Walker & Rowan-Robinson 1986; Meiksin & Davis 1986; Villumsen & Strauss 1987; Strauss and Davis 1988 and references therein; Rowan-Robinson *et al.* 1990, hereafter RR90), X-ray clusters (Lahav *et al.* 1989), X-ray AGNs (Miyaji and Boldt 1990) and Abell clusters (Plionis & Valdarnini 1991; Scaramella *et al.* 1991). Lahav *et al.* (1988) and Lynden-Bell *et al.* (1989) found that the optical and IRAS dipole (using samples with characteristic depths of $\sim 60 h^{-1}$ Mpc) are aligned with the CMB dipole and conclude that the source of the LG motion is within $\sim 40 h^{-1}$ Mpc. However, RR90 using the deeper 0.6 Jy IRAS survey with a characteristic depth of $\sim 120 h^{-1}$ Mpc, find that the dipole continues growing up to $\sim 100 h^{-1}$ Mpc and flattens thereafter while it is also roughly aligned with the CMB dipole. Furthermore, PV91 and SVZ find that the dipole, as traced by Abell clusters, builds up in the same way as that of the optical galaxies (although it misses the local $< 25 h^{-1}$ Mpc contributions) but has a further dipole contribution from depths $> 120 - 150 h^{-1}$ Mpc, while it is aligned with the CMB dipole direction to within only $\sim 5^\circ - 10^\circ$. PV91 have shown that the cluster dipole, estimated in independent equal-volume shells of $\delta V \sim 4 \times 10^6 h^{-3} \text{ Mpc}^3$ out to $160 h^{-1}$ Mpc, is roughly aligned in each shell with the CMB dipole direction which provides evidence for a *coherent* anisotropy over a scale-length (diameter) of $\sim 300 h^{-1}$ Mpc. To ignore the gravitational pull caused by such large correlated structure by assuming the dipole converges at a much smaller depth than $160 h^{-1}$ Mpc,

would lead to a large overestimate of the value of Ω_o .

Under the crucial assumption that the optical (ESO+UGC) and IRAS galaxy distributions contain the source of the LG motion then the amplitude of the optical and IRAS dipoles suggest that $\Omega_o \sim 1$ with $b_{op} \sim 2$ and $b_{IRAS} \sim 1.3$ (but bear in mind the comments above about the simplicity of the bias model adopted in these calculations). However, the value of Ω_o is sensitive to contributions to the dipole from depths beyond the scales sampled by the optical and IRAS catalogues and such contributions can significantly lower its value. In fact, the rich cluster samples, which probe much greater depths than those of galaxies, have led to a much smaller inferred value of $\Omega_o < 0.3$ if the bias factor for galaxies lies in its usual range of 1.6 to 2.5 (PV91; SVZ).

The question of convergence of the dipole has been addressed by other authors (Juszkiewicz, Vittorio & Wyse 1990; Lahav, Kaiser & Hoffman 1990; Strauss *et al.* 1992). These studies have, however, concentrated upon a model-dependent view of the problem; that is to say, given a particular model of clustering – such as CDM – at what depth can one expect the dipole to converge? Or, put another way, how large a sample volume is required to contain the entire source of the Local Group motion in a CDM Universe? Although these are undoubtedly interesting questions to ask, it is in our view better to keep the analyses as data-oriented (rather than model-oriented) as possible. We would prefer to ask the question whether there is any evidence, given the data on galaxy clustering and minimal assumptions about models of structure, whether the dipole has converged within the depths probed by relevant galaxy and cluster samples. With this point of view in mind, we decided to reanalyse the IRAS galaxy dipole inferred from the QDOT survey, and compare the results obtained with the dipole inferred from the distribution of rich clusters. The main questions we shall ask are (i) Out to what depth is the sampling density of the QDOT

survey sufficient to allow a reliable determination of the dipole? (ii) Is there any evidence for a significant contribution to the dipole from scales larger than $\sim 100h^{-1}$ Mpc that would make the QDOT analysis consistent with the results mentioned above obtained from samples of rich clusters?

The layout of the paper is as follows: in Section C.2 we review briefly the method we use for estimating dipoles and relating the result to Ω_o ; in Section C.3 we give some details of the QDOT survey catalogue and apply our dipole method to it; in Section C.4 we discuss the results in the light of other observations; we state the main conclusions in Section C.5.

C.2 Dipole Calculations

C.2.1 FORMALISM

The multipole components of the galaxy (or other extragalactic mass tracer) distribution are calculated by summing moments. The monopole and dipole moments are:

$$M = \frac{1}{4\pi} \sum_{i=1}^n \frac{1}{\phi(r_i)} \frac{1}{r_i^2} = \frac{1}{4\pi} H_o^2 \mu \quad (\text{C.1})$$

$$\underline{D} = \frac{3}{4\pi} \sum_{i=1}^n \frac{1}{\phi(r_i)} \frac{r_i}{r_i^2} = \frac{3}{4\pi} H_o^2 \underline{\gamma}, \quad (\text{C.2})$$

where

$$\phi(r_i) = \int_{L_{min}(r_i)}^{L_{max}} \Phi(L) dL \quad (\text{C.3})$$

is a selection function to take into account the fact that at different distances we sample different portions of the luminosity function. $L_{min}(r)$ is the luminosity

of a source with the limiting flux-density at a comoving distance r , estimated by:

$$r = \frac{cD_L(z)}{H_0(1+z)}, \quad (\text{C.4})$$

with $D_L(z)$ the luminosity distance, $D_L(z) = q_0^{-2} [q_0 z + (q_0 - 1)[(1 + 2q_0 z)^{1/2} - 1]]$.

Throughout this paper we use $q_0 = 0.2$. Different values of q_0 affect the distances only by a small fraction. Note that although in our notation the monopole and dipole moments depend on the value of the Hubble parameter, their ratio does not. Furthermore, it has been shown (PV91), that the relative uncertainties in D/M are significantly smaller than in D , due to the fact that errors have a similar effect on the values of D and M and therefore cancel out in their ratio.

The relatively small size of flux, magnitude or diameter limited galaxy samples, especially at large distances, can introduce a net ‘discreteness’ dipole and large shot noise errors. The shot-noise (discreteness) dipole can be estimated for a uniform population, sampled by N objects each having a weight w_i , by:

$$\langle \underline{\gamma} \cdot \underline{\gamma} \rangle^{\frac{1}{2}} = N^{\frac{1}{2}} \langle w^2 \rangle^{\frac{1}{2}} \quad (\text{C.5})$$

where $w_i = \phi(r_i)^{-1} r_i^{-2}$ and the corresponding shot noise dipole to monopole ratio is $\sigma_{D/M} \simeq 3 \langle w^2 \rangle^{\frac{1}{2}} / N^{\frac{1}{2}} \langle w \rangle$. Although this calculation gives an indication of the order-of-magnitude of the dipole induced by shot-noise effects, it is not accurate for realistic data sets because of the non-uniform nature of the sampling. In order to compute the discreteness dipole and corresponding shot-noise errors in this paper, we use Monte Carlo simulations as described below.

C.2.2 AN ILLUSTRATIVE MODEL

A reliable determination of the dipole from galaxy samples can be used to determine the cosmological density parameter, Ω_0 . We have discussed many

examples of this type of analysis in the Introduction, so we shall not go into much detail here. Here, however, we wish to pay particular attention to the question of convergence of the dipole and consequent uncertainty in the value of Ω_0 . Many authors (e.g. Juszkiewicz *et al.* 1990; Lahav *et al.* 1990; Strauss *et al.* 1992) have discussed how one might expect the dipole to converge given a particular model for the density field, such as CDM. We will take an alternative approach in asking if there is any evidence in the observational data itself that the dipole has either converged or not converged. We stress again that any determination of Ω_0 is only reliable if the total gravitational acceleration of the local group is completely accounted for by structures contained entirely within the sample volume and the value of Ω_0 obtained depends upon the depth at which the cumulative dipole converges to its final value. To show explicitly how this happens we shall apply the formalism introduced in Section C.2.1 to a simple illustrative model.

The gravitational acceleration induced at a point (e.g. the Local Group) by the surrounding density inhomogeneity is

$$\underline{g} = G \int \frac{\rho(\underline{r})\underline{r}}{r^3} d\underline{r} = \frac{4\pi G}{3} \underline{D} \quad (\text{C.6})$$

where $\rho(\underline{r})$ is the continuous mass density and \underline{D} is the dipole moment (C.2) of a set of mass tracers. Using linear perturbation theory (Peebles 1980), we can relate the peculiar velocity of the LG, due to the combined gravitational field of all mass tracers, with the dipole moment and the value of Ω_0 , as follows. We must first assume that the gravitational acceleration has converged to its final value within the limits of the sample and that acceleration and velocity are aligned. We now need to model the density distribution $\rho(\underline{r})$ in (C.6), taking into account the distribution of the mass tracers that are used. To do this, we

first expand the mass density in spherical harmonics:

$$\rho(\underline{r}) = \rho_o + \underline{\delta}(\underline{r}) \cdot \underline{r} + \dots,$$

The dipole vector, $\underline{\delta}(\underline{r})$, is the only term that contributes to the acceleration so this is the term we need to model. For an arbitrary mass distribution, the manner in which the dipole amplitude builds up as a function of depth can be very complicated, but, for illustration, and without loss of generality, we assume that the dipole builds up in two steps (as indicated by the cluster dipole in PV91 and SVZ):

$$\underline{\delta}(\underline{r}) = \underline{\delta}_1(\underline{r})\Theta(R_1 - r) + \underline{\delta}_2(\underline{r})\Theta(R_2 - r)\Theta(r - R_1), \quad (\text{C.7})$$

where $\Theta(x)$ is the Heaviside step function; $\underline{\delta}_1(\underline{r})$ is the dipole due to the distribution of mass-tracers in the sphere $[0, R_1]$; $\underline{\delta}_2(\underline{r})$ is the contribution to the dipole from the shell $[R_1, R_2]$. Assuming for simplicity that $|\underline{\delta}_1(\underline{r})| = \delta_1$ (constant) for $r \leq R_1$, $|\underline{\delta}_2(\underline{r})| = \delta_2$ (constant) for $R_1 < r \leq R_2$ and $|\underline{\delta}(\underline{r})| = 0$ for $r > R_2$ and picking a convenient coordinate system, we can express the density $\rho(\underline{r})$ as:

$$\rho(\underline{r}) = \begin{cases} \rho_o + \delta_1 \cos \theta & r \in [0, R_1] \\ \rho_o + \delta_2(\cos \theta \cos \chi + \sin \theta \sin \phi \sin \chi) & r \in [R_1, R_2] \\ \rho_o & r > R_2 \end{cases}, \quad (\text{C.8})$$

where θ , ϕ are the usual angular coordinates and χ is the angle between δ_1 and δ_2 . θ is also the angle from the CMB dipole direction. The gravitational acceleration is then:

$$|g| = \frac{4}{3}\pi G\Omega_o\rho_c \left[\left(R_1 \frac{\delta\rho_1}{\rho_o} \right)^2 + \left(\Delta R \frac{\delta\rho_2}{\rho_o} \right)^2 + 2 \left(R_1 \frac{\delta\rho_1}{\rho_o} \right) \left(\Delta R \frac{\delta\rho_2}{\rho_o} \right) \cos \chi \right]^{1/2}, \quad (\text{C.9})$$

where $\rho_c (\equiv 3H_o^2/8\pi G)$ is the critical density and $\Delta R = R_2 - R_1$.

If the mass tracer distribution (indicated with suffix t) is modelled in the same way as in Eq. (C.8), we can express the monopole and dipole terms of

the spherical harmonic expansion as:

$$M(\leq z_2) = \frac{1}{4\pi} \int_0^{R_2} \rho_t(\underline{r}) \frac{1}{r^2} d\underline{r} = R_2 \rho_{0t}, \quad (\text{C.10})$$

$$\begin{aligned} |D(\leq z_2)| &= \left| \frac{3}{4\pi} \left[\int_0^{R_1} \rho_t(\underline{r}) \frac{\underline{r}}{r^3} d\underline{r} + \int_{R_1}^{R_2} \rho_t(\underline{r}) \frac{\underline{r}}{r^3} d\underline{r} \right] \right| \\ &= \left[(R_1 \delta \rho_{1t})^2 + (\Delta R \delta \rho_{2t})^2 + 2 (R_1 \delta \rho_{1t})(\Delta R \delta \rho_{2t}) \cos \chi \right]^{1/2} \end{aligned} \quad (\text{C.11})$$

Using the standard “linear” picture of *biassing*, ie., $(\delta\rho/\rho)_t = b(\delta\rho/\rho)$ it is straightforward to show that

$$|g| = \frac{4\pi G R_2 \Omega_o \rho_c}{3b} \frac{|D(\leq z_2)|}{M(\leq z_2)} \quad (\text{C.12})$$

and the resulting relation between v_p and the dipole moment (expressed as the ratio of dipole over monopole M , which is independent of H_o) is:

$$\underline{v}_p = d_{conv} \frac{\Omega_o^{0.6}}{3b} \frac{|D|}{M} (\leq d_{conv}), \quad (\text{C.13})$$

where \underline{v}_p is the LG velocity with respect to the cosmic microwave background radiation rest frame, $d_{conv} = cz_2 \approx R_2 H_o$ is the depth at which the dipole converges to its final value and b is the bias factor that relates galaxy to mass overdensities and which is defined in the introduction. The $\Omega_o^{0.6}$ factor comes in when one uses the theory of linear gravitational instability to relate the peculiar velocity to the gravitational acceleration (Peebles 1980).

C.2.3 COMMENTS

Although that we have worked out Eq. (C.13) on the basis of a two-step model this result is valid whatever model one assumes for the dipole growth, as would be expected from the fact that gravity is a conservative force. (For example, Villumsen & Strauss (1987), Lahav *et al.* (1988) and Miyaji & Boldt

(1990), have all used an even simpler one-step model to derive the same result.) Equation (C.13) therefore holds for *any* continuous distribution $\delta(\underline{r})$ since we can approximate $\delta(\underline{r})$ at each point by an infinitesimal step. Moreover it is valid whether $\delta(\underline{r})$ increases smoothly until it reaches its final value or whether, for example, it increases in finite steps with large plateau between them. We have chosen the two-step model for illustration because it shows explicitly how such a mass distribution could produce a dipole that apparently converges at a depth less than R_2 (which is, by construction the depth at which the dipole actually converges). If one had a data set which samples space poorly in between R_1 and R_2 , one might interpret the plateau as evidence for convergence and thus overestimate the value of Ω_o .

We shall not be attempting to fit this simple model to the data; it serves only as a warning that one must be convinced that the dipole has converged before attempting to infer a value of Ω_o .

RR90 estimated the dipole from the QDOT sample and derived a value of Ω_o using a slightly different formulation from ours. We choose our formulation to highlight the point that the value of Ω_o inferred depends crucially on the value of d_{conv} .

C.3 Application to the QDOT Survey

The QDOT data set is a sparse-sampled (one in six) redshift survey of the IRAS galaxies with $S \geq 0.6$ Jy at 60- μ m. The original IRAS catalogue and the area exclusion mask are described in RR90. Due to *cirrus* emission near the galactic plane we limit our analysis to the $|b| > 10^\circ$ (as in the original work of RR90). To get an idea of the depths traced by the QDOT sample we present in

Figure 1 the space-density of QDOT galaxies evaluated in equal volume shells with $\delta V \simeq 1.2 \times 10^6 h^{-3} \text{ Mpc}^3$. As expected from the fact that the IRAS galaxy sample is flux-limited, the galaxy space-density is a steeply decreasing function of distance. It is evident that at $\sim 100 h^{-1} \text{ Mpc}$ the QDOT galaxy space-density has dropped by a factor > 8 and therefore these depths are very sparsely sampled.

-FIGURE 1-

We have estimated the galaxy weights (C.3) using the parametric form of the luminosity function derived by Saunders *et al.* (1990):

$$\Phi(L) \propto \left(\frac{L}{L_*(z)} \right)^{-\alpha} \exp \left[-\frac{1}{2\sigma^2} \log_{10}^2 \left(1 + \frac{L}{L_*(z)} \right) \right] \quad (\text{C.14})$$

with $\alpha = 1.09 \pm 0.12$, $\sigma = 0.724 \pm 0.031$ and $L_* = 10^{8.47 \pm 0.23} h^{-2} L_\odot$. We prefer to use this parametric form in order to test the stability of the resulting dipole to the details of the weighting scheme adopted (see below). No significant difference is found in the behaviour of the dipole if one uses the non parametric form given by Saunders *et al.* 1990, but this form does not allow one to model the uncertainties as easily.

The QDOT sample we use covers the regions with $|b| \geq 10^\circ$ ($\sim 82\%$ of the sky), while there is still a $\sim 10\%$ area not covered. In calculating the multipole components of the QDOT survey we must take into account the regions not surveyed. Our approach has been to use a composite method:

- The contribution to the dipole and to higher order moments of the excluded region $|b| \leq 10^\circ$ is estimated by expanding the observed surface density of IRAS galaxies using spherical harmonics ($l \leq 2$) and correcting the coefficients of the expansion for the masked region (*cf.* Yahil *et al.* 1986; Lahav 1987; Plionis 1988, 1989; PV91).

- Since the boundaries of the remaining $\sim 10\%$ of unsurveyed sky are rather complicated we estimate its contribution to the dipole by assuming a uniform distribution of IRAS galaxies, having the average weight (as estimated from the rest of the sky).

Note that we have corrected the galaxy velocities to the LG rest frame and we have excluded all galaxies lying within $2 h^{-1}$ Mpc of the LG centroid as well as all galaxies with a luminosity $\leq 10^8 h^{-2} L_{\odot}$ (in accordance with RR90).

Once the weights have been constructed and the correction for missing areas has been performed, one can determine the behaviour of the monopole as a function of radial depth. This is shown in Figure 1 (with an arbitrary vertical scaling). Note that, although the density of galaxies is falling rapidly due to the selection of brighter and brighter galaxies, the monopole *increases* with depth. If the monopole had not carried on increasing in this way, one could have immediately concluded that sampling was too poor to make a reliable statement about the convergence of the dipole (PV91). On the other hand, a given monopole contribution could be made up of a large number of galaxies, each with the same weight, or just a few galaxies each with a much bigger weight. In the first case, the dipole properties would probably be well-defined but, in the second, there will be uncertainties because of small number statistics and also the fact that the weights require accurate knowledge of $\Phi(L)$. Thus, the continued growth of the monopole is a *necessary* condition for a ‘good’ dipole determination but not a *sufficient* one.

We now proceed to estimate the cumulative moments of the QDOT galaxy distribution in 20 distance bins each of width $10 h^{-1}$ Mpc. In the light of the above discussion, we must also estimate the shot-noise dipole produced just by virtue of the small number of galaxies sampled. We do this, using the

same binning, by randomly redistributing the positions of the galaxies found in each bin. In this way we conserve the observed QDOT selection function; RR90 applied a similar method in their analysis but ours is much faster since we do not generate a random 3-d catalogue each time. We perform 50 such Monte-Carlo simulations and we then obtain the net QDOT dipole by subtracting the shot-noise dipole from the raw one. In Figure 2 we present the net QDOT dipole (filled circles), the raw dipole (dashed line) and the shot-noise dipole (open circles); errors are estimated from deviations around the mean simulation dipole. Although the uncertainties are quite large, the dipole certainly seems to have converged to its final value at ~ 90 to $100 h^{-1}$ Mpc (in agreement with RR90): within this range the QDOT dipole points only $\sim 16^\circ$ away from the CMB dipole direction. The corresponding net amplitude ($|D|/M (\leq 100 \text{ Mpc}) \simeq 0.28$) implies $b_{IRAS} \Omega_0^{-0.6} \simeq 1.5$, a value which is about 20% larger than that derived in RR90. We are not quite sure why we get such a different answer but it can probably be attributed to the different way we choose to deal with regions of low galactic latitude ($|b| \leq 10^\circ$). We prefer to extrapolate the structural pattern of the surveyed to the unsurveyed sky, using the spherical harmonic expansion to fill in the missing regions. RR90 replaced the missing regions with a uniform (Poisson) distribution of objects. We believe our method makes a more reasonable estimate of the contribution to the total dipole from the obscured region.

As we have discussed above, since the space density of QDOT galaxies is extremely low at large depths, distant galaxies are assigned an extremely large weight (Eq.(C.3)). The dipole contribution from these depths might therefore be extremely sensitive, to the details of the luminosity function.

-FIGURE 2-

-FIGURE 3-

C.4 Evidence for Contributions from Large Scales: Comparison with the Cluster Dipole

The dipole shown in Figure 2 certainly seems to have converged by around $100 h^{-1}$ Mpc but how strong a statement can we make about whether there is any contribution to the dipole from distances $> 100 h^{-1}$ Mpc when the sampling density and uncertainty in the luminosity function make the convergence of the amplitude of D/M difficult to determine?

To answer this question, we decided to look at the way in which the dipole changes as we increase the integration depth, not just in amplitude but also in *direction*. We find that when we integrate up to $\sim 90 h^{-1}$ Mpc the dipole direction found by successively adding shells of radius $10 h^{-1}$ Mpc is consistently aligned with the CMB dipole direction to an accuracy of $\sim 15^\circ$. However, continuing the integration to larger volumes we find that the dipole direction deviates systematically from the CMB dipole direction by a random-walk only to be pulled back to the vicinity of the CMB dipole when we encompass the shell at $150 \div 160 h^{-1}$ Mpc where the Shapley concentration lies (Shapley 1930; Scaramella *et al.* 1989; Raychaudhury 1989). In Figure 4 we plot the QDOT dipole direction at each step of the volume integration. As we go to greater depths, the deviation from the vicinity from the MWB dipole direction as well as its consequent *realignment* is apparent.

-FIGURE 4-

This is exactly the behaviour we would expect if the LG motion were influenced by structures at these depths. In order to study the significance of the apparent influence to the dipole of the $150 h^{-1} \div 160 h^{-1}$ Mpc shell, we have determined the incremental dipole within equal volume shells of $\delta V \sim 3 \times 10^6 h^{-3} \text{ Mpc}^3$. In other words, we measure the dipole contributed by each shell separately. In order to take into account the direction of each shell dipole, we define a signal to noise ratio (S/N) as follows:

$$\frac{S}{N} = \frac{|\underline{D}|/M \times \cos(\Delta\theta_{cmb})}{\sigma_{D/M}}, \quad (\text{C.15})$$

where $\Delta\theta_{cmb}$ is the angle of deviation between the shell dipole and that of the CMB and $\sigma_{D/M}$ is the shell shot-noise dipole. In Figure 5 we plot S/N for each shell and it is evident that the only significant contributions to the total integrated dipole come, as expected, from the first bin ($\sim 4\sigma$) but also from the fourth bin ($\sim 1.5\sigma$) where the Shapley concentration lies. This finding is in agreement with the results of the cluster dipole (see PV91 and SVZ) which shows that up to 30% - 35% of the total dipole comes from depths $100 \leq r \leq 160 h^{-1} \text{ Mpc}$. It is surprising that we can see anything given the uncertainties at such a distance but, even though we do find evidence of a signal, the QDOT survey samples depths beyond $\sim 100 h^{-1} \text{ Mpc}$ so sparsely (Figure 1) that we cannot determine the precise contribution of fluctuations at such depths to the LG acceleration using this data set.

-FIGURE 5-

What we can do, however, is demonstrate the remarkable agreement between the incremental QDOT dipole and the corresponding results from the

cluster dipole of PV91. Table 1 shows the equal-volume shell limits, the number of clusters and IRAS galaxies respectively in the shell, the directions (in galactic co-ordinates) of the cluster and IRAS dipoles and the mis-match angle between these vectors and the CMB dipole vector. The agreement is remarkable for the $0 \div 99$ and $142.8 \div 157.3h^{-1}$ Mpc bins particularly in the outer shell when one considers the huge drop in the number of IRAS galaxies out to this depth. One could argue that this contribution to the dipole is only aligned with the CMB vector by chance and it is really only a shot-noise effect. However, the probability of two random vectors aligning in this way is less than 3×10^{-4} while the joint random probability that both mass tracers (Abell clusters and IRAS galaxies) are aligned with the CMB dipole within the indicated angles, assuming that their respective distributions are independent of each other, is less than 10^{-7} . Although the two dipoles are aligned at around $150h^{-1}$ Mpc, the difference is that the cluster dipole shows a clear increase in amplitude at this distance whereas the QDOT dipole does not. Without such a clear increase in amplitude our arguments are bound to be based upon circumstantial evidence. On the other hand the shot-noise errors we have estimated are certainly large enough to mask a 25 percent contribution to the QDOT dipole at this distance. It is not unreasonable therefore to interpret our results as evidence that the apparent convergence of the QDOT dipole is just due to poor sampling and that the real mass dipole converges at a much greater depth as indicated by the cluster dipole.

-TABLE 1-

Some indications of the magnitude of the contribution from large scales to the LG motion can be seen in other work. Raychaudhury (1989; 1991) argues

for a contribution $\leq 15\%$, while the cluster dipole analysis (PV91; SVZ) suggested a $\sim 35\%$ contribution. Note, however, that Raychaudhury's limits refer to the contribution to the dipole of one structure only, the Shapley concentration. PV91 estimated that the contribution of this structure is about 20% of the total dipole, which leaves about 15% to be due to other sources on scales $> 100 h^{-1}$ Mpc. In effect what we find from the QDOT sample (Table 1), as well as in PV91, is that the dipole direction of the shell between 142.8 and 157.3 h^{-1} Mpc points towards the CMB direction and not towards the direction of the Shapley concentration. This, in turn, implies that there is a correlated structure at this distance that consists not only of the Shapley concentration but also has considerable extent around the shell. This indicates that the $\sim 15\%$ contribution to v_p , derived by Raychaudhury, should be probably considered as a lower limit. In any case any contribution to the dipole from scales larger than the apparent convergence scale of $\sim 100 h^{-1}$ Mpc implies a lower value of Ω_0 than what we derived in section 4 (and from the RR90 value). For example, a contribution of 20% and 35% to the dipole results in $\Omega_0 \sim 0.4$ and ~ 0.3 respectively (for $b_{IRAS} = 1$). A flat universe would require $b_{IRAS} \geq 1.8$. Additional constraints on b are obviously needed if we are to reach an unambiguous conclusion about the value of Ω_0 . Some steps in this direction were made by Lahav, Nemiroff & Piran (1990) who calculated the correlation functions of galaxies selected by different criteria. The amplitude of the correlation function scales by b^2 in the linear bias model (Kaiser 1984). If different, for example, optical and infra-red selected galaxies possess different bias parameters b then they should therefore have different galaxy-galaxy correlation lengths (defined to be the separation, r_0 , at which $\xi(r_0) = 1$). By comparing the auto- and cross-correlation functions of the ESO/UGC and IRAS samples of galaxies, Lahav *et al.* (1990) find that $b_{opt}/b_{IRAS} \simeq 1.7$. In order to reconcile this and the dipole result with $\Omega_0 = 1$

we require $b_{opt} \simeq 3$; not impossible, but rather large for comfort. All this is predicated on the linear bias model being correct, which is by no means certain.

The picture that is emerging is therefore that there might well be a significant source of gravitational acceleration on a scale of $\sim 150 h^{-1} \text{Mpc}$ which appears clearly in the cluster data but is masked by uncertainties induced by the sampling properties. The actual distribution on large scales might therefore be reasonably well modelled by the simple picture described in Section C.2.2. If this is true then it is an interesting corollary of Eq.(C.10) that, in the shell $[R_1, R_2]$ we have:

$$\left[\frac{\delta\rho}{\rho} \right]_2 \simeq \frac{\beta}{(R_2/R_1) - 1} \left[\frac{\delta\rho}{\rho} \right]_1$$

where β is the fractional contribution to the total dipole from that shell. This implies that the density fluctuation of QDOT galaxies in the shell $[100, 150] h^{-1} \text{Mpc}$ is $\sim 2\beta$ the density fluctuation in the $[0, 100] h^{-1} \text{Mpc}$ shell.

C.5 Conclusions

The main conclusion from this work is that there is no compelling evidence that the QDOT dipole has indeed converged to its final value within the sample volume. Consequently, the value of $\Omega_0^{0.6}/b$ quoted by RR90 should be interpreted only as an *upper limit*. Furthermore, even though the QDOT survey samples the galaxy distribution only very sparsely on scales $> 100 h^{-1} \text{Mpc}$, there is circumstantial evidence of a contribution from distances out to $\sim 160 h^{-1} \text{Mpc}$ because there is a strong alignment of the incremental dipole at that distance with the MWB dipole vector. The most obvious source for this contribution is the Shapley concentration, which is known to contribute around 15 % of the optical dipole (Raychaudhury 1989). But if the Shapley concentra-

tion were the only source of the dipole anisotropy in the relevant distance bin, then the incremental vector in that bin should point in the direction of Shapley. It doesn't; it points in the CMB direction. There must therefore be some correlated structure in this distance bin that includes the Shapley concentration but also has significant extent around the shell. Although this structure is not visually prominent in the QDOT data set because of the low sampling density, we interpret the alignment as strong circumstantial evidence that there is significant structure in the galaxy distribution on scales $\sim 150 h^{-1}$ Mpc; we cannot be more precise about the magnitude of its contribution to the dipole because the sampling is so poor.

We stress again that, in this respect, the QDOT data set possesses similar properties to the cluster catalogues analysed in PV91 and SVZ from which one infers a rather low value of $\Omega_o^{0.6}/b$. Bearing mind the large incompleteness of QDOT and the consequent insensitivity to structures beyond $\sim 100 h^{-1}$ Mpc, it is impossible to derive anything other than an upper limit on $\Omega_o^{0.6}/b_{IRAS} < 0.6$ from this data set if there is such a contribution from this scale. Although the clusters (which are presumably much more biased than IRAS galaxies) suggest a value $\Omega_o^{0.6}/b_{clus} < 0.2$ (PV91) which is consistent with the IRAS dipole as long as we interpret the IRAS dipole as an upper limit rather than an exact determination. We should stress that the reason we get a higher value for the IRAS dipole than clusters might be nothing to do with a different bias for the two sets of objects; it could well be just because the cluster dipole contains the correct contribution from large scales whereas the IRAS data misses this. Thus, the QDOT and cluster data together suggest a low value of Ω_o , unless there is compelling evidence of gross systematic errors in the cluster catalogues and the QDOT dipole alignment at $160 h^{-1}$ Mpc is a fluke.

We stress that this analysis is based on the assumption that any bias

that exists can be modelled by the simple linear model mentioned in the introduction. If the appropriate value of b for IRAS galaxies is around unity, as has been suggested (RR90; Saunders *et al.* 1991) then our results are clearly incompatible with a flat $\Omega_o = 1$ Universe. The simplest interpretation would then be that we live in an open Universe with clusters moderately biased, as expected on simple theoretical grounds (Kaiser 1984). IRAS galaxies may even be less clustered than the total mass distribution if $\Omega_o < 1$. An $\Omega_o = 1$ Universe is not excluded by these results, but the price to be paid is a much more complicated biasing scheme that would require much more detailed modelling.

Acknowledgments

Manolis Plionis and Paolo Catelan have been supported by the Ministero Italiano per la Ricerca Scientifica; Manolis Plionis further thanks SERC for support under the QMW visitors grant. Peter Coles acknowledges support from SERC under the QMW Theory Rolling Grant and thanks SISSA for their hospitality during a short visit when this work was begun. Paolo Catelan acknowledges Enzo Branchini for many stimulating discussions.

References of the Appendix C

- Babul, A. & White, S.D.M., 1991. *Mon. Not. R. astr. Soc.*, **253**, 31P.
- Bower, R.G., Coles, P., Frenk, C.S. & White, S.D.M., 1992. *Astrophys. J.*, in press.
- Dekel, A. & Rees, M.J., 1987. *Nature*, **326**, 455.
- Juszkiewicz, R., Vittorio, N. & Wyse, R.F.G., 1990. *Astrophys. J.*, **349**, 408.
- Kaiser, N., 1984. *Astrophys. J.*, **326**, 19.
- Kaiser, N. & Lahav, O., 1989. *Mon. Not. R. astr. Soc.*, **237**, 129.
- Lahav, O., 1987. *Mon. Not. R. astr. Soc.*, **225**, 213.
- Lahav, O., Edge, A.C., Fabian, A.C. & Putney, A., 1989. *Mon. Not. R. astr. Soc.*, **238**, 881.
- Lahav, O., Kaiser, N. & Hoffman, Y., 1990. *Astrophys. J.*, **352**, 448.
- Lahav, O., Nemiroff, R.J. & Piran, T., 1990. *Astrophys. J.*, **350**, 119.
- Lahav, O., Rowan-Robinson, M. & Lynden-Bell, D., 1988. *Mon. Not. R. astr. Soc.*, **234**, 677.
- Lynden-Bell, D., Lahav, O. & Burstein, D., 1989. *Mon. Not. R. astr. Soc.*, **241**, 325.
- Meiksin, A. & Davis, M., 1986. *As. J.*, **91**, 191.
- Miyaji, T. & Boldt, E., 1990. *Astrophys. J.*, **353**, L3.

- Peebles, P.J.E., 1980. *The Large-Scale Structure of the Universe* Princeton University Press, Princeton.
- Plionis, M., 1988. *Mon. Not. R. astr. Soc.*, **234**, 401.
- Plionis, M., 1989. *Mon. Not. R. astr. Soc.*, **238**, 417.
- Plionis, M. & Valdarnini, R., 1991. *Mon. Not. R. astr. Soc.* **249**, 46. (PV91)
- Raychaudhury, S., 1989. *Nature*, **342**, 251.
- Raychaudhury, S., 1991. In: NATO Advanced Study Institute *Clusters & Superclusters of Galaxies: Contributed Talks and Poster Papers*, eds Colless, M.M., Babul, A., Edge, A.C., Johnstone, R.M. & Raychaudhury, S., pp. 3-4, Institute of Astronomy, Cambridge.
- Rowan-Robinson, M., *et al.*, 1990. *Mon. Not. R. astr. Soc.* **247**, 1. (RR90)
- Saunders, W., Rowan-Robinson, M., Lawrence, A., Efstathiou, G., Kaiser, N., Ellis, R.S., Frenk, C.S., 1990. *Mon. Not. R. astr. Soc.*, **242**, 318.
- Saunders, W. *et al.*, 1991. *Nature*, **349**, 32.
- Scaramella, R., Baiesi-Pillastrini, G., Chincarini, G., Vettolani, G. & Zamorani, G., 1989. *Nature*, **338**, 562.
- Scaramella, R., Vettolani, G. & Zamorani, G., 1991. *Astrophys. J. Lett.*, **376**, L1. (SVZ)
- Shapley, H., 1930. *Harvard Obs. Bull.* **874**, 9.
- Smoot, G.F., *et al.*, 1990. *Astrophys. J. Lett.* **371**, L1.
- Strauss, M.A. & Davis, M., 1988. In *Proceedings of Vatican Study Week on Large-Scale Motions in Universe*, p. 219, eds Rubin, V.C. & Coyne, G., Princeton University Press, Princeton.
- Strauss, M.A., Yahil, A., Davis, M., Huchra, J.P. & Fisher K., 1992. preprint.

Villumsen, J.V. & Strauss, M.A., 1987. *Astrophys. J.*, **322**, 37.

Yahil, A., Walker, D. & Rowan-Robinson, M., 1986. *Astrophys. J.*, **301**, L1.

Shell Limits (h^{-1} Mpc)	IRAS Galaxies				Rich Clusters			
	N	l°	b°	$\Delta\theta$	N	l°	b°	$\Delta\theta$
0.0-99.0	1181	251.9	34.7	15.8	50	247.1	24.5	18.9
99.0-124.8	225	120.2	23.8	120.5	40	325.6	11.3	56.2
124.8-142.8	118	338.7	-47.6	97.9	47	283.6	6.2	25.6
142.8-157.3	74	260.7	39.1	13.6	49	271.5	21.4	6.4
157.3-169.4	50	339.1	-75.5	111.5	36	69.1	5.7	142.5

Table 1. Incremental dipole in each of 5 equal-volume bins for both QDOT IRAS galaxies and Abell and ACO clusters (from PV91). The columns give (i) the radial distance limits of each bin; (ii)-(v) the number of QDOT galaxies in the bin, the dipole vector direction for that bin and the difference, $\Delta\theta$ between this vector and the CMB dipole vector; (vi)-(ix) give the number of clusters, dipole direction and CMB offset angle for the cluster data for comparison.

Figure Captions

Figure 1. The space density of QDOT galaxies in equal volume shells.

Figure 2. The QDOT dipole (filled circles) with its estimated errors given by equation (5), together with the raw dipole (dashed line) and the dipole simulated by reshuffling the galaxy positions (open circles).

Figure 3. The effect on D/M of varying the luminosity function parameters by 1σ . We plot the ratio of the D/M obtained with different luminosity function parameters to that obtained with the “standard” choice. The upper curve is that obtained if α , σ and L_* all lie at the bottom end of their allowed 1σ uncertainties and the lower curve shows what happens if these parameters take values at the top end of their uncertainty ranges.

Figure 4. The QDOT dipole (cumulative) direction at each step of the integration. The CMB dipole direction is marked with an asterisk.

Figure 5. The Signal-to-Noise ratio, S/N , for each equal volume shell as a function of distance (see text). The only significant contributions to the integrated dipole come from the nearby shell ($S/N \simeq 4$) and the shell between 140 - 160 h^{-1} Mpc ($S/N \simeq 1.5$).

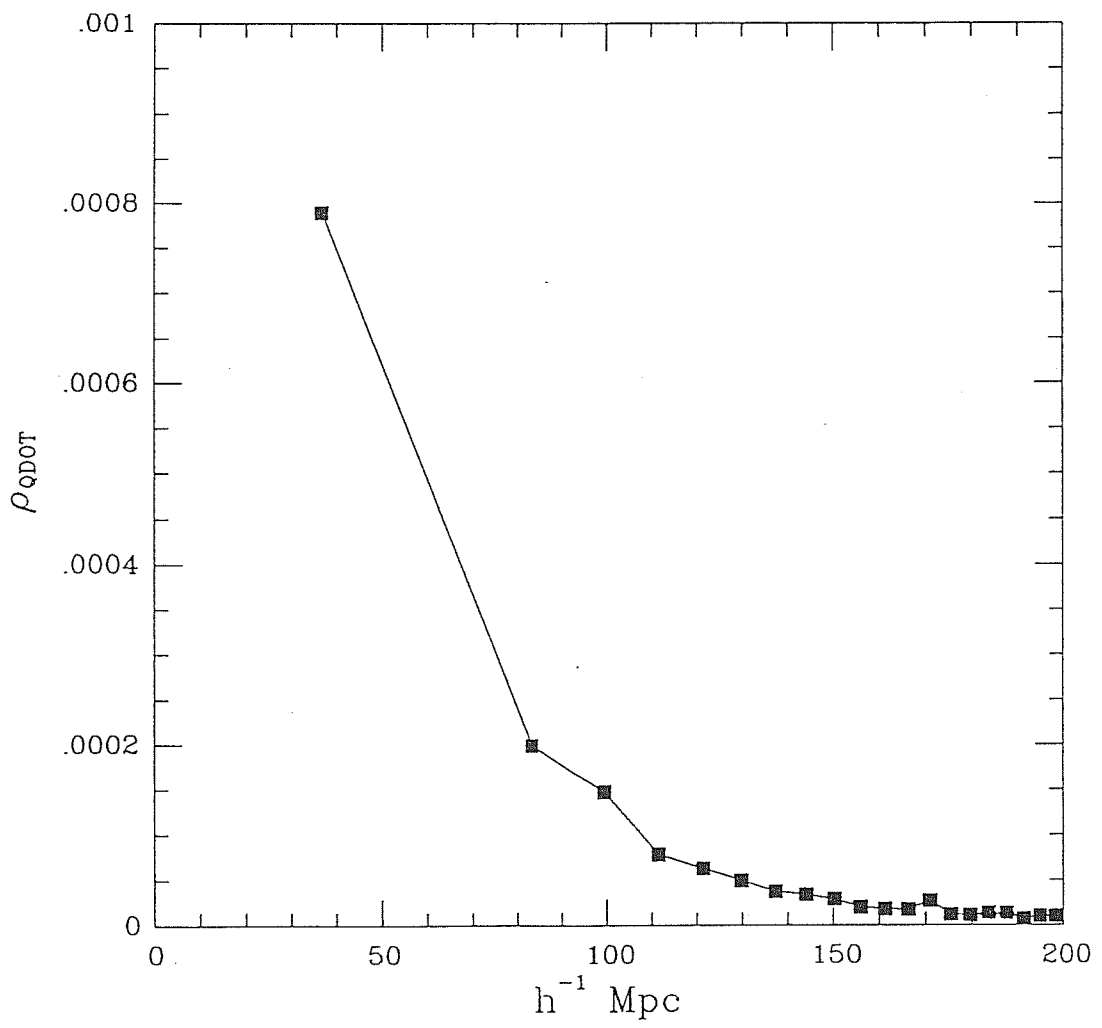


fig. 1

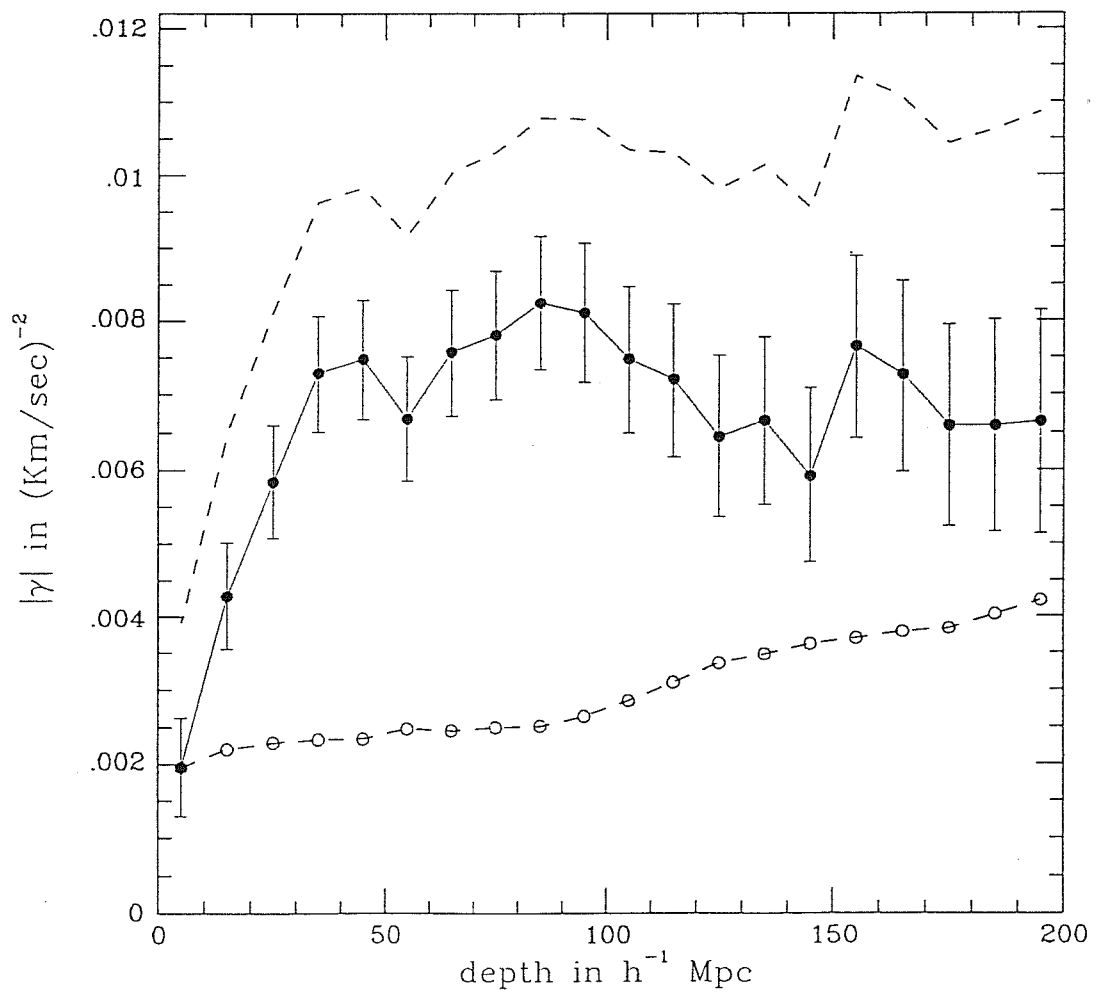


fig. 2

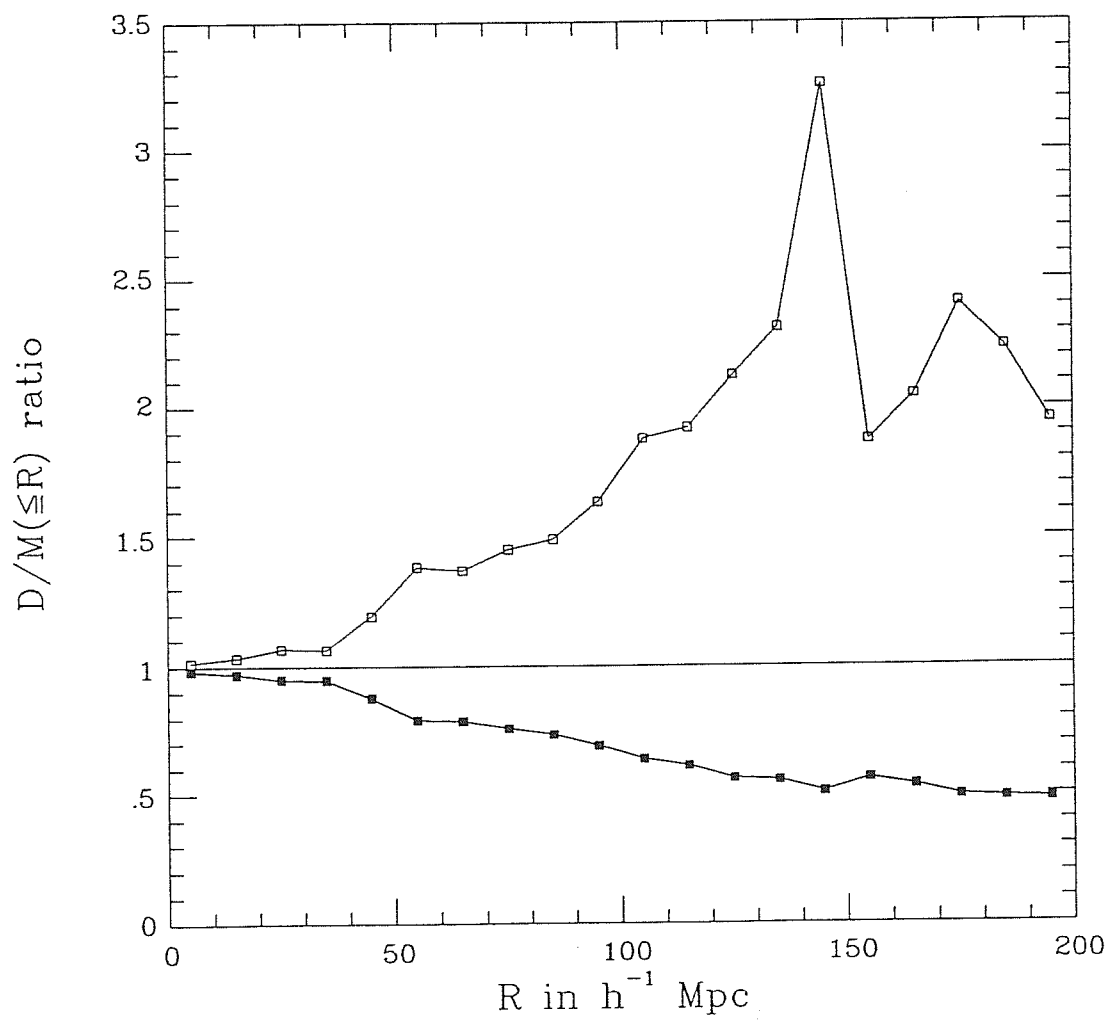


Fig. 3

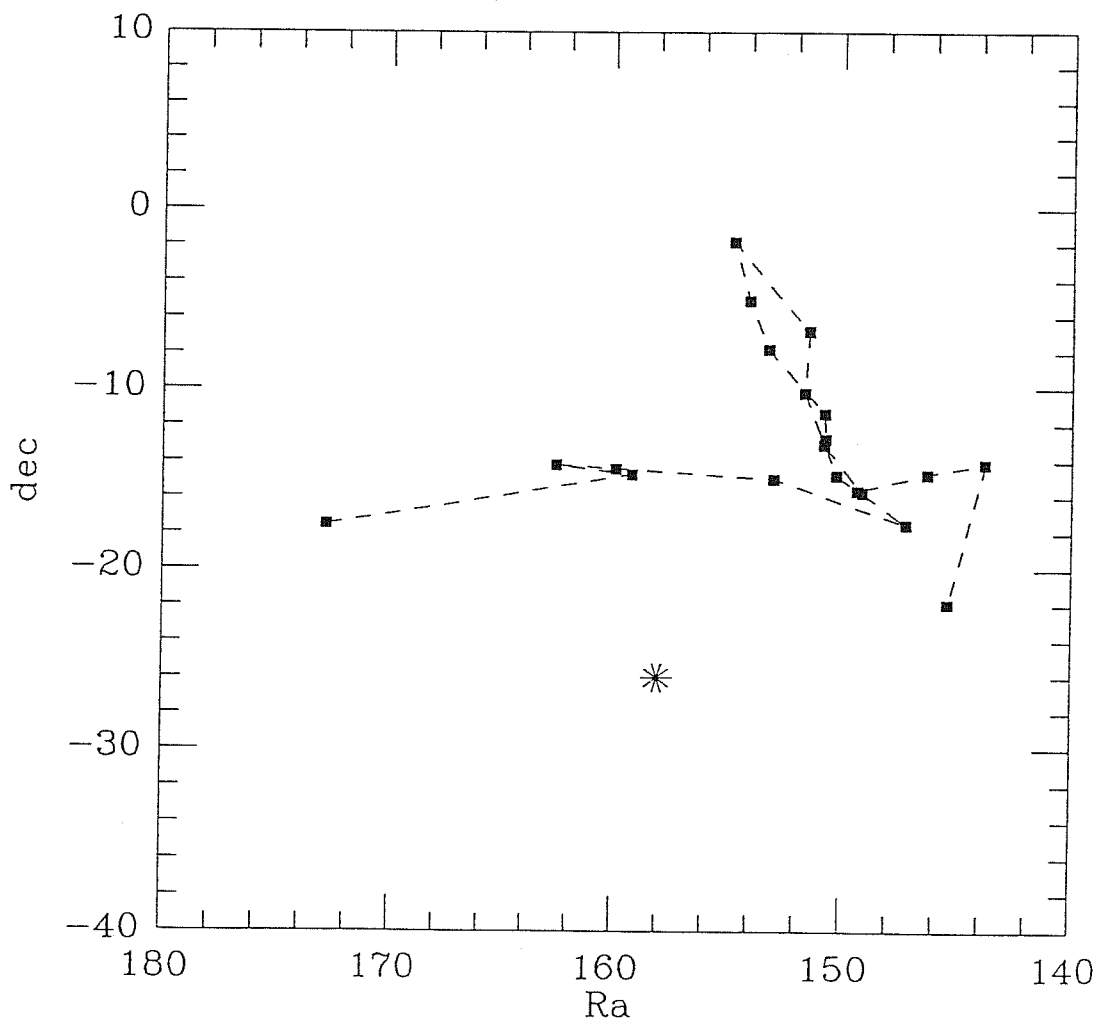


fig. 4

EQUAL VOLUME SHELLS

$$S/N = (D/M)_{\text{shell}} \times \cos(\delta\theta_{\text{cmb}}) / (\text{shot noise})_{\text{shell}}$$

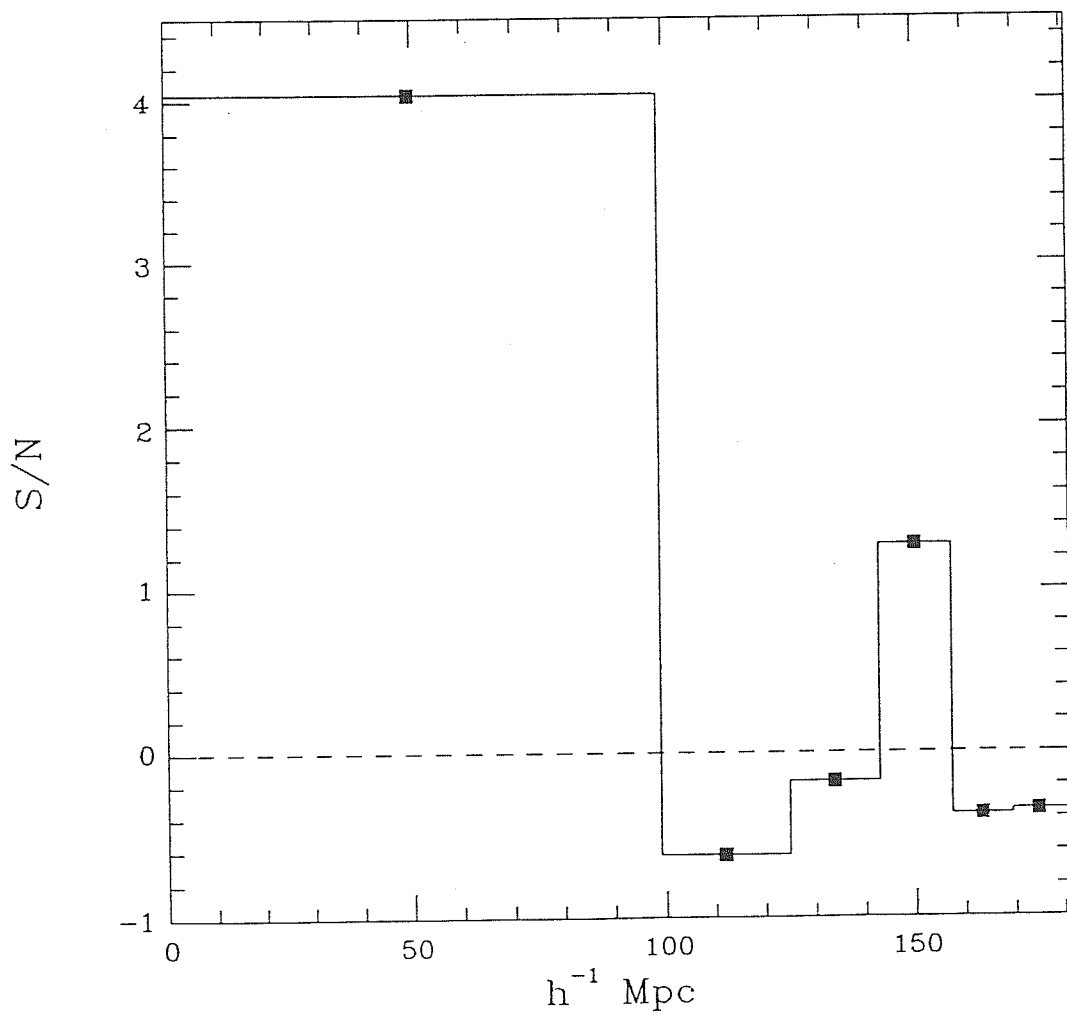


fig. 5

References

- Aaronson M., 1983, *ApJ*, **266**, L11.
- Aaronson M. & Olszewski E.W., 1988, in *Large Scale Structure of the Universe*, IAU Symposium 130, eds. Audouze J., Pelletan M.-C. & Szalay A. (Dordrecht: Kluwer).
- Abbott L.F. & Wise M.B., 1984, *ApJ*, **282**, L47.
- Abbott L.F. & Wise M.B., 1984, *Nuc. Phys.*, **B244**, 541.
- Adler R.J., 1981, *The Geometry of Random Fields*, Chichester: Wiley.
- Allen T.J., Grinstein B. & Wise M., *Phys. Lett.*, **B197**, 66.
- Albrecht A. & Stebbins A., 1992, *Phys. Rev. Lett.*, **68**, 2121.
- Bahcall N., 1988, in *Large Scale Structures of the Universe*, eds. Audouze J. *et al.*, IAU Symposium.
- Bahcall N. & Burgett W.S., 1986, *ApJ*, **300**, L35.
- Bahcall N. & Soneira R., 1983, *ApJ*, **276**, 20.
- Bahcall N. & Soneira R., 1984, *ApJ*, **277**, 27.
- Bean A.J., Efstathiou G., Ellis R.S., Peterson B.A. & Shanks T., 1983, *MNRaS*, **205**, 605.
- Bardeen J.R., 1980, *Phys. Rev.*, **D22**, 1882.
- Bardeen J.R., 1986, in *Inner Space/Outer Space*, eds. Kolb E.W. *et al.*, University of Chicago Press.
- Bardeen J.R., Bond J.R., Kaiser N. & Szalay A.S., 1986, *ApJ*, **304**, 15 (BBKS).
- Bardeen J.R., Steinhardt P.J. & Turner M.S., 1983, *Phys. Rev.*, **D28**, 679.
- Barrow J.D. & Coles P., 1990, *MNRaS*, **244**, 188.
- Barrow J.D. & Turner M.S., 1981, *Nature*, **292**, 37.

- Batuski D.J., Bahcall N.A., Olowin R.P., & Burns J.O., 1989, ApJ, **341**, 599.
- Baumgart D.J. & Fry J.N., 1991, ApJ, **375**, 25.
- Bernardeau F., 1992a, ApJ, in press.
- Bernardeau F., 1992b, ApJ, **390**, L61.
- Bertschinger E., 1988, ApJ, **323**, L103.
- Bertschinger E., 1992, in *New Insights into the Universe*, Proc. UIMP Summer School, eds. Martinez V.J., Portilla M. & Saez D., in press.
- Blumenthal G.R., Faber S.M., Primack J.R. & Rees M.J., 1984, Nature, **311**, 517.
- Bond J.R. & Efstathiou G., 1984, ApJ, **285**, L45.
- Bond J.R. & Efstathiou G., 1991, Phys. Lett., **B265**, 245.
- Bond J.R., Efstathiou G. & Silk J., 1980, Phys. Rev. Lett., **45**, 1980.
- Bond J.R., Kolb E.W. & Silk J., 1982, ApJ, **274**, 443.
- Bond J.R. & Szalay, 1984, ApJ, **274**, 443.
- Bonometto S.A. & Lucchin F., 1978, Astron. Astrophys., **67**, L7
- Borgani S., Jing Y.P. & Plionis M., 1992, ApJ, in press.
- Bosma A., 1981, Astron. J., **86**, 1825.
- Bouchet F.R. & Hernquist L., 1991, preprint.
- Bouchet F.R., Juszkiewicz R., Colombi S. & Pellat R., 1992, ApJ, **394**, L5.
- Bouchet F.R., Strauss M. & Davis M., 1991, Proc. of the 2nd DAEC Workshop, eds. Mamon G. & Gerbal D., Meudon Observatory, Paris.
- Bower R.G., Coles P., Frenk C.S. & White S.D.M., 1992, ApJ, in press.
- Brandenberger R., 1985, Rev. Mod. Phys., **57**, 1.
- Brandenberger R., 1990, in: *Physics of the Early Universe*, eds. Peacock J., Heavens A. & Davies A. (Thirty-Sixth Scottish Universities Summer School in Physics 1989, Edinburgh).
- Buchert T., 1989, Astron. Astrophys., **223**, 9.
- Buchert T., 1992, MNRaS, **254**, 729.
- Burstein D., 1990, Rep. Prog. in Phys., **53**, 421.

- Carignan C. & Freeman K.C., 1985, *ApJ*, **294**, 494.
- Carr B.J., 1978, *Comments on Astrophys.*, **7**, 161.
- Cartwright D.E. & Longuet-Higgins M.S., 1956, *Proc. Roy. Soc.*, **A237**, 212.
- Catelan P., Lucchin F. & Matarrese S., 1988a, *Phys. Rev. Lett.*, **61**, 267.
- Catelan P., Lucchin F. & Matarrese S., 1988b, *Phys. Rev. Lett.*, **61**, 2627.
- Catelan P., Lucchin F., Matarrese S. & Moscardini L., 1992, in progress.
- Cen R.Y., Ostriker J.P., Spergel D.N. & Turok N., 1991, *ApJ*, **383**, 1.
- Centrella J. & Melott A., 1983, *Nature*, **305**, 196.
- Chambers K.C., Miley G.K. & van Breugel W., 1990, *ApJ*, **363**, 21.
- Chandrasekhar S., 1943, *Rev. Mod. Phys.*, **15**, 1.
- Cline J.M., Politzer H.D., Rey S.-J. & Wise M.B., 1987, *Commun. Math. Phys.*, **112**, 217.
- Coles P., 1986, *MNRaS*, **222**, 9P.
- Coles P., 1988, *Phys. Rev. Lett.*, **61**, 2626.
- Coles P., 1989, *MNRaS*, **238**, 319.
- Coles P., 1990, *MNRaS*, **243**, 171.
- Coles P. & Barrow J.D., 1987, *MNRaS*, **228**, 407.
- Coles P. & Frenk C.S., 1991, *MNRaS*, **253**, 727.
- Coles P. & Jones B., 1991, *MNRaS*, **248**, 1.
- Couchman H.M.P., 1987a, *MNRaS*, **225**, 777.
- Couchman H.M.P., 1987b, *MNRaS*, **225**, 795.
- Daly R.A., 1987, *ApJ*, **322**, 20.
- Daly R.A., 1988, *MNRaS*, **232**, 853.
- Dalton G.B., Efstathiou G., Maddox S.J. & Sutherland W.J., 1992, *ApJ Lett.*, **390**, L1.
- Davis M., Efstathiou G., Frenk C.S. & White S.D.M., 1985, *ApJ*, **292**, 371.
- Davis M., Efstathiou G., Frenk C.S. & White S.D.M., 1992, *Nature*, **356**, 489.
- Davis M. & Peebles P.J.E., 1983, *Ann. Rev. Astron. Astrophys.*, **21**, 109.

- Davis M. & Peebles P.J.E., 1983, ApJ, **267**, 465.
- De Lapparent V., Geller M. & Huchra J., 1986, ApJ, **302**, L1.
- Dekel A., 1983, ApJ, **264**, 373.
- Dekel A. & Aarseth S.J., 1984, ApJ, **283**, 1.
- Dekel A., Blumenthal G.R., Primack J.R. & Olivier S., 1989, **338**, L5.
- Dekel A. & Rees M., 1986, Nature, **326**, 455.
- Dekel A. & Silk J., 1986, ApJ, **303**, 39.
- Dicke R.H., Peebles P.J.E., Roll P.G. & Wilkinson D.T., 1965, ApJ, **142**, 414.
- Doroshkevich A.G., 1970, Astrophysica, **6**, 320.
- Dmitriev N.A. & Zel'dovich Ya.B., 1964, Sov. Phys. JETP, **18**, 793.
- Dressler A., 1991, Nature, **350**, 391.
- Dressler A. *et al.*, ApJ, **313**, 42.
- Efstathiou G., 1985, MNRaS, **213**, 29.
- Efstathiou G. *et al.*, 1985, ApJ Supp., **57**, 241.
- Efstathiou G., 1990, in: Physics of the Early Universe, eds. Peacock J., Heavens A. & Davies A. (Thirty-Sixth Scottish Universities Summer School in Physics 1989, Edinburgh).
- Efstathiou G., Dalton G.B., Sutherland W.J. & Maddox S.J., 1992, MNRaS, **257**, 125.
- Efstathiou G., Kaiser N., Saunders W., Lawrence A., Rowan-Robinson M., Ellis R.S. & Frenk C.S., 1990, MNRaS, **247**, 10P.
- Efstathiou G. & Silk J., 1983, Fund. Cos. Phys., **9**, 1.
- Einasto J., Koasik A. & Sear E., 1974, Nature, **250**, 309.
- Einstein A., 1917, S-B Preuss Akad Wiss, 142.
- Ellis G.F.R., 1988, Class. Quantum Grav., **5**, 891.
- Ellis J. *et al.*, 1984, Nucl. Phys., **B238**, 453.
- Ellis J., 1991, Phys. Scripta, **T36**, 145.
- Fabbri R., Guidi I., Melchiorri F. & Natale V., 1980, Phys. Rev. Lett., **44**, 1563.

- Faber S.M., 1984, in *Large-Scale Structure of the Universe, Cosmology and Fundamental Physics*, First ESO-CERN Symposium, eds. Setti G. & Van Hove (Cern: Geneva).
- Faber S.M. & Gallagher J.S., 1979, *Ann. Rev. Astron. Astrophys.*, **17**, 135.
- Faber S.M. & Lin D.N.C., 1983, *ApJ*, **266**, L17.
- Fall S.M., 1979, *Rev. Mod. Phys.*, **51**, 21.
- Fall S.D. & Tremaine S., 1977, *ApJ*, **216**, 682.
- Feller W., 1971, *An Introduction to Probability Theory and Its Applications*, voll. I, II, (New York: Wiley).
- Feynman R.P. & Hibbs A.R., 1965, *Quantum Mechanics and Path Integrals*, Mc Graw-Hill, N.Y.
- Flores R., Blumenthal G.R., Dekel A. & Primack J.R., 1986, *Nature*, **323**, 781.
- Freese K., Price R. & Schramm D.N., 1983, *ApJ*, **275**, 405.
- Frenk C.S., 1986, *Phil. Trans. R. Soc. London*, **A330**, 517.
- Frenk C.S., White S.D.M. & Davis M., 1983, *ApJ*, **271**, 417.
- Frenk C.S., White S.D.M., Davis M. & Efstathiou G., 1988, *ApJ*, **327**, 507.
- Fry J.N., 1984, *ApJ*, **279**, 499.
- Fry J.N., 1985a, *ApJ*, **289**, 10.
- Fry J.N., 1985b, *Phys. Lett.*, **158B**, 211.
- Fry J.N., 1986, *ApJ*, **308**, L71.
- Fry J.N. & Peebles P.J.E., 1978, *ApJ*, **221**, 19.
- Fry J.N. & Seldner M., 1982, *ApJ*, **259**, 474.
- Gamow G., 1946, *Phys. Rev.*, **70**, 527.
- Geller M., 1987, in: *Observational Cosmology*, IAU Symposium, No. 124.
- Gelmini G., Schramm D.N., & Valle J.W.F., 1984, *Phys. Lett.*, **146B**, 311.
- Gerhard O.E. & Spergel D.N., 1992, *ApJ*, **389**, L9.
- Gershtein S.S. & Zel'dovich Ya.B., 1966, *JETP Lett.*, **4**, 120.
- Giovanelli R. & Haynes M.P., 1985, *ApJ*, **292**, 404.
- Giovanelli R. & Haynes M.P. & Chincarini G.L., 1986, *ApJ*, **300**, 77.

- Goldberg H., 1983, Phys. Rev. Lett., **50**, 1419.
- Gooding A.K., Park C., Spergel D.N., Turok N. & Gott III J.R., 1991, Princeton Observatory Preprint, POP-416.
- Goroff M.H., Grinstein B., Rey S.-J. & Wise M.B., 1986, ApJ, **311**, 6.
- Gott III J.R., Gao B. & Park C., 1991, ApJ, **383**, 90.
- Grinstein B. *et al.*, 1987, ApJ, **314**, 431.
- Grinstein B. & Wise M., 1987, ApJ, **314**, 448.
- Groth E.J. & Peebles P.J.E., 1975, Astr. Ap., **41**, 143.
- Groth E.J. & Peebles P.J.E., 1977, ApJ, **217**, 385.
- Gurbatov S.N., Saichev A.I. & Shandarin S.F., 1989, MNRaS, **236**, 385.
- Gush H.P., Halpern M. & Wishnow E.H., 1990, Phys. Rev. Letter, **65**, 537.
- Guth A.H., 1981, Phys. Rev., **D23**, 347.
- Guth A.H. & Pi S.-Y., 1982, Phys. Rev. Lett., **49**, 1110.
- Guth A.H., 1984, Ann. N.Y. Acad. Sci., **422**, 1.
- Guzzo L., Iovino A., Chincarini G., Giovanelli R. & Haynes M., 1991, ApJ Lett., **382**, L5.
- Hamilton A.J.S., Kumar P., Lu E. & Matthews A., ApJ, 1991, **374**, L1.
- Harrison E.R., 1970, Phys.Rev., **D1**, 2726.
- Hauser M. & Peebles P.J.E., 1973, ApJ, **185**, 757.
- Haynes M.P., Giovanelli R., Starosta B. & Magni C., 1988, AJ, **95**, 607.
- Hawking S.W., 1982, Phys. Lett., **B115**, 95.
- Hill C.T., Schramm D.N. & Fry J.N., 1989, Comm. Nucl. Part. Phys., **19**, 25.
- Hime A. & Jelley N.A., 1991, Phys. Lett., **B257**, 441.
- Hoffman G.L., Salpeter E.E. & Wasserman I., ApJ, **263**, 485.
- Huang K., 1963, *Statistical Mechanics*, Cambridge.
- Hubble E., 1934, ApJ, **79**, 8.
- Hubble E., 1936, *The realm of the Nebulae*, Yale Observatory Press, Yale.
- Hucra J.P., 1992, Science, **256**, 321.

- Hucra J.P., Davis M., Latham D.W. & Tonry J., 1983, *ApJ Suppl. Ser.*, **53**, 89.
- Hunter L., 1964, *ApJ*, **139**, 570.
- Ichimaru S., 1973, *Basic Principles of Plasma Physics*, Reading, Mass., Benjamin.
- Ipser J. & Sikivie P., 1983, *Phys. Rev. Lett.*, **50**, 925.
- Irvine W.M., 1965, *Ann. Phys. N.Y.*, **32**, 322.
- Jacoby G.H., Ciardullo R. & Ford H.C., 1990, *ApJ*, **356**, 332.
- Jeans J., 1928, *Astronomy and Cosmogony*, Cambridge University Press, Cambridge.
- Jensen L.G. & Szalay A.S., 1986, *ApJ*, **305**, L5.
- Jing Y.P. & Valdarnini R., 1991, *Astron. Astrophys.*, **250**, 1.
- Jing Y.P. & Zhang J.L., 1989, *ApJ*, **342**, 639.
- Juszkiewicz R., 1981, *MNRaS*, **197**, 931.
- Juszkiewicz R., Bouchet F.R. & Colombi S., 1991, *ApJ*, submitted.
- Juszkiewicz R. & Bouchet F.R., 1991, *Proc. of the 2nd DAEC Workshop*, eds. Mamon G. & Gerbal D., Meudon Observatory, Paris.
- Juszkiewicz R., Sonoda D.H. & Barrow J.D., 1984, *MNRaS*, **209**, 139.
- Kac M. & Logan J., 1979, in: *Fluctuation Phenomena*, eds. Montroll E.W. & Lebowitz J.L., New York: North Holland.
- Kaiser N., 1983, *ApJ*, **273**, L17.
- Kaiser N., 1984, *ApJ*, **284**, L9.
- Kaiser N., 1986, in *Inner Space/Outer Space*, eds. Kolb E.W. *et al.*, University of Chicago Press.
- Kaiser N., 1987, *MNRaS*, **227**, 1.
- Kaiser N., 1990a, *Contemporary Physics*, **31**, 113.
- Kaiser N., 1990b, *MNRaS*, **219**, 785.
- Kaiser N., 1991, in: *After the First Three Minutes*, eds. Holt S. *et al.*, pag. 248.

- Kendall M. & Stuart A., 1977, *The Advanced Theory of Statistics*, vol. 1, Griffin, London.
- Klypin A.A. & Kopilov A.I., 1983, *Soviet Astr. Lett.*, **9**, 41.
- Kodama H. & Sasaki M., 1986, *Int. J. Mod. Phys.*, **A1**, 265.
- Kolb E.W. & Turner M.S., 1990, *The Early Universe*, Addison-Wesley.
- Kofman L.A. & Linde A.D., 1987, *Nuc. Phys.*, **B282**, 555.
- Kofman L.A., Pogosyan D. & Shandarin S., 1990, *MNRaS*, **242**, 200.
- Kofman L.A. & Shandarin S.F., 1988, *Nature*, **334**, 132.
- Landau L.D. & Lifshitz E.M., 1979, *Classical Theory of Fields*, 4th ed. London, Pergamon.
- Layzer D., 1963, *ApJ*, **138**, 174.
- Layzer D., 1964, *Ann. Rev. Astron. Astrophys.*, **2**, 341.
- Lee B.W. & Weinberg S., 1977, *Phys. Rev. Lett.*, **39**, 165.
- Lemaitre G., 1933a, *CR*, **196**, 903; 1085.
- Lemaitre G., 1933b, *Ann. Soc. Sci. Bruxelles*, **A53**, 51.
- Lemaitre G., 1934, *Proc NAS*, **20**, 12.
- Lifshitz E.M., 1946a, *ZhETF*, **16**, 587.
- Lifshitz E.M., 1946b, *J Phys.*, **10**, 116.
- Lightman A. & Schechter P., 1990, *ApJ*.
- Lilje P.D. & Efstathiou G., 1988, *MNRaS*, **231**, 635.
- Lilly S.J., 1988, *ApJ*, **333**, 161.
- Limber D.N., 1953, *ApJ*, **117**, 134.
- Lin D.N.C. & Faber S.M., 1983, **266**, L21.
- Ling E.N., Frenk C.S. & Barrow J.D., 1986, *MNRaS*, **223**, 21P.
- Lucchin F., Matarrese S. & Bonometto S., 1986, *ApJ*, **310**, L21.
- Lucchin F., Matarrese S. & Vittorio N., 1988, *ApJ*, **330**, L21.
- Lucey J., 1983, *MNRaS*, **204**, 33.
- Ma, S.-K., 1985, *Statistical Mechanics*, (Philadelphia: World Scientific).

- Mac Gibbon J.H., 1987, *Nature*, **329**, 308.
- Maddox S.J., Sutherland W.J., Efstathiou G. & Loveday J., 1990, *MNRaS*, **243**, 692.
- Madsen M.S. & Ellis G.F.R., 1988, *MNRaS*, **234**, 67.
- Madsen M.S., Mimoso J.P., Butcher J.A. & Ellis G.F.R., 1992, *Phys. Rev.*, **D46**, 1399.
- Makino N., Sasaki M. & Suto Y., 1992, *Phys. Rev.*, **D46**, 585.
- Martel H. & Freudling W., 1991, *ApJ*, **37**, 11.
- Matarrese S., Lucchin F. & Bonometto S., 1986, *ApJ*, **310**, L21.
- Matarrese S., Lucchin F., Messina A. & Moscardini L., 1991, *MNRaS*, **253**, 35.
- Matarrese S., Lucchin F., Moscardini L. & Saez D., 1992, *MNRaS*, *in press*.
- Matarrese S., Ortolan A., & Lucchin F., 1989, *Phys. Rev.*, **D40**, 290.
- Matarrese S., Pantano O. & Saez D., 1992, *ApJ*, *submitted*.
- Mather J.C. *et al.*, 1990, *ApJ*, **354**, L37.
- Mc Gill C., 1990, *MNRaS*, **242**, 428.
- Mc Gill C. & Couchman H., 1989, *MNRaS*, **236**, 51P.
- Melott A.L. & Fry J.N., 1986, *ApJ*, **305**, 1.
- Messina A., Lucchin F., Matarrese S. & Moscardini L., 1992, *Astroparticle Phys.*, *submitted*.
- Messina A., Moscardini L., Lucchin F. & Matarrese S., 1990, *MNRaS*, **245**, 244.
- Meszaros P., 1974, *Astr. Ap.*, **37**, 225.
- Mollerach S., Matarrese S., Ortolan A. & Lucchin F., *Phys. Rev.*, **D44**, 1670.
- Monin A.S. & Yaglom A.M., 1971, *Statistical Fluid Mechanics*, vols. 1 & 2 (Cambridge: MIT Press).
- Moscardini L., Matarrese S., Lucchin F. & Messina A., 1991, *MNRaS*, **248**, 424.
- Moutarde F., Alimi J.-M., Bouchet F.R., Pellat R. & Ramani A., 1991, *ApJ*, **382**, 377.

- Mukhanov V.F., Feldman H.A. & Brandenberger R., 1992, *Phys. Rep.*, **215**, Nos. 5 & 6, 203.
- Negele J.W. & Orland H., 1988, *Quantum Many-Particle Systems*, (Redwood City: Addison-Wesley).
- Novikov I.D., 1964a, *ZhETF*, **46**, 686.
- Novikov I.D., 1964b, *Soviet Phys. JETP*, **19**, 467.
- Oemler A., 1987, in : *Nearly Normal Galaxies*, ed. Faber S., Springer-Verlag.
- Olive K., Seckel D. & Vishniac E., 1985, *ApJ*, **292**, 1.
- Olivier S., Blumenthal G.R., Dekel A., Primack J.R. & Stanhill D., 1990, *ApJ*, **356**, 1.
- Otto S., Politzer H.D. & Wise M.B., 1986a, *Phys. Rev. Lett.*, **56**, 1878.
- Otto S., Politzer H.D. & Wise M.B., 1986b, *Phys. Rev. Lett.*, **56**, 2772.
- Park C., 1991, *ApJ*, **382**, L59.
- Peacock J.A., 1991, *MNRaS*, **253**, 1P.
- Peacock J.A. & Heavens A.F., 1985, *MNRaS*, **217**, 805.
- Peacock J.A. & Nicholson D., 1991, *MNRaS*, **253**, 307.
- Peebles P.J.E., 1980, *The Large Scale Structure of the Universe*, Princeton University Press, Princeton.
- Peebles P.J.E., 1982a, *ApJ*, **258**, 415.
- Peebles P.J.E., 1982b, *ApJ*, **263**, L1.
- Peebles P.J.E., 1983, *ApJ*, **274**, 1.
- Peebles P.J.E., 1986, *Nature*, **321**, 27.
- Peebles P.J.E., 1987, *ApJ*, **317**, 576.
- Peebles P.J.E. & Yu J.T., 1970, *ApJ*, **162**, 815.
- Penzias A.A. & Wilson R.W., 1965, *ApJ*, **142**, 419.
- Persic M. & Salucci P., 1991, *ApJ*, **368**, 60.
- Plionis M. & Borgani S., 1991, *MNRaS*.
- Plionis M, Coles P. & Catelan P., 1992, *MNRaS*, *submitted*.
- Politzer H.D. & Wise M.B., 1984, *ApJ*, **285**, L1.

- Postman M., Huchra J.P. & Geller M.J., 1992, ApJ, **384**, 404.
- Primack J. & Blumenthal G.R., 1983, in *Formation and Evolution of Galaxies and Large Scale Structures in the Universe*, eds. Audouze J. & Tran Thanh Van J., (Reidel, Dordrecht).
- Primack J., 1984, Proc. of International School of Physics *Enrico Fermi*, Varenna, SLAC-PUB 3387.
- Ramond P., 1989, *Field Theory: A Modern Primer*, (Redwood City: Addison-Wesley).
- Reed M. & Simon B., 1980, *Methods of Modern Mathematical Physics I: Functional Analysis*, (New York: Academic Press).
- Rees M., 1985, MNRaS, **213**, 75P.
- Rice S.O., 1954, in: *Selected Papers on Noise and Stochastic Processes*, ed. Wax N., (New York: Dover).
- Rice S.O. & Gray P., 1965, *The Statistical Mechanics of Simple Liquids*, (New York: Wiley Interscience).
- Rowan-Robinson M. *et al.*, 1990, MNRaS, **247**, 1.
- Salopek D.S., 1992, Phys., Rev., in press.
- Salopek D.S. & Bond J.R., 1991, Phys. Rev., **D43**, 1005.
- Salopek D.S., Bond J.R. & Bardeen J.M., 1989, Phys. Rev., **D43**, 1753.
- Saunders W. *et al.*, 1991, Nature, **349**, 32.
- Scaramella R. *et al.*, 1989, Nature, **338**, 562.
- Scaramella R., Vettolani G. & Zamorani G., 1991, ApJ Lett., **376**, L1.
- Schaeffer R. & Silk J., 1985, ApJ, **292**, 319.
- Schectman S., 1985, ApJ, **57**, 77.
- Scherrer R.J., 1992, ApJ, in press
- Scherrer R.J. & Bertschinger E., 1991, ApJ, **381**, 349.
- Scherrer R.J., Melott A.L. & Bertschinger E., 1989, Phys. Rev. Lett., **62**, 379.
- Schramm D.N. & Steigman G., 1981, ApJ, **241**, 1.
- Sciama D.W., 1990a, Phys. Rev. Lett., **65**, 2839.
- Sciama D.W., 1990b, ApJ, **364**, 549.

- Shandarin S.F. & Zel'dovich Ya.B., 1989, *Rev. Mod. Phys.*, **61**, 185.
- Shanks T., Bean A.J., Efstathiou G., Ellis R.S., Fong R. & Peterson B.A., 1983, *ApJ*, **274**, 529.
- Sharp N.A., Bonometto S.A. & Lucchin F., 1984, *Astron. Astrophys.*, **130**, 79.
- Silk J., 1968, *ApJ*, **151**, 459.
- Silk J. & Juszkiewicz R., 1991, *Nature*, **353**, 386.
- Sikivie P., 1983, *Phys. Rev. Lett.*, **51**, 1415.
- Simpson J.J., 1985, *Phys. Rev. Lett.*, **54**, 1891.
- Smith P.F., 1988, *Contemp. Phys.*, **29**, 159.
- Smoot G.F. *et al.*, 1991, *ApJ*, **371**, L1.
- Smoot G.F. *et al.*, 1992, COBE preprint.
- Splinter R.J. & Melott A.L., 1992, *ApJ*, in press.
- Starobinsky A.A., 1982, *Phys. Lett.*, **b117**, 175.
- Staveley-Smith L. & Davies R.D., 1987, *MNRaS*, **224**, 953.
- Staveley-Smith L. & Davies R.D., 1988, *MNRaS*, **231**, 833.
- Stecker F.W. & Shafi Q., 1983, *Phys. Rev. Lett.*, **50**, 928.
- Strauss M.A. *et al.*, 1992, PaperV, *preprint*.
- Struble M.F. & Rood H.J., 1987, *ApJ Supp.*, **63**, 543.
- Suginohara T., Suto Y., Bouchet F.R. & Hernquist L., 1991, *ApJ Supp.*, **75**, 631.
- Sutherland W.J., 1988, *MNRaS*, **234**, 159.
- Sutherland W.J. & Efstathiou G., 1991, *MNRaS*, **248**, 159.
- Suto Y. & Sasaki M., 1991, *Phys. Rev. Lett.*, **66**, 264.
- Suto Y., Sato K. & Kodama H., 1985, *Prog. Theor. Phys.*, **73**, 1151.
- Szalay A., 1988, *ApJ*, **333**, 21.
- Tomita K., 1967, *Prog. Theor. Phys.*, **37**, 831.
- Tomita K., 1971, *Prog. Theor. Phys.*, **45**, 1747.
- Tomita K., 1972, *Prog. Theor. Phys.*, **47**, 416.

- Tonry J.L., 1991, ApJ, **373**, L1.
- Toth G., Hollosi J. & Szalay A., 1989, ApJ, **344**, 75.
- Totsuji M. & Kihara T., 1969, Publ. Astron. Soc. Japan, **21**, 221.
- Tremaine S.D. & Gunn J.E., 1979, Phys. Rev. Lett. **42**, 407.
- Turner M.S., 1985, Phys. Rev., **D31**, 1212.
- Turner M.S., Steigman G. & Krauss L.M., 1984, Phys. Rev. Lett., **52**, 2090.
- Turok N., 1984, Nucl. Phys., **B242**, 520.
- Turok N., 1989, Phys. Rev. Lett., **63**, 2625.
- Turok N., 1991, Phys. Scripta, **T36**, 135.
- Turok N. & Spergel D., 1990, Phys. Rev. Lett., **64**, 2736.
- Turok N. & Spergel D., 1991, Phys. Rev. Lett., **66**, 3093.
- Uson J.M., Bagri D.S. & Cornwell T.J., 1991, Phys. Rev. Lett., **67**, 3328.
- Uson J.M. & Wilkinson D.T., 1984, ApJ, **277**, L1.
- Valdarnini R. & Bonometto S., 1985, Astron. Astrophys., **146**, 235.
- Vanmarcke E., 1983, *Random Fields: Analysis and Synthesis*, MIT Press.
- Vilenkin A., 1981, Phys. Rev. **D24**, 2082.
- Villumsen J.V., Scherrer R.J. & Bertschinger E., 1991, ApJ, **367**, 37.
- Villumsen J.V. & Brainerd T., 1992, private communication.
- Vishniac E., 1983, MNRaS, **203**, 345.
- Vittorio N. & Silk J., 1984, ApJ, **285**, L39.
- Wagoner R.V., 1973, ApJ, **179**, 343.
- Walker T.P., Steigman G., Schramm D.N., Olive K.A. & Kang H-S., 1991, **376**, 51.
- Warren S.J., Hewett P.C., Osmer P.S. & Irwin M.J., 1987, Nature, **330**, 453.
- Weinberg S., 1972, *Gravitation and Cosmology*, (New York: Wiley)
- Weinberg S., 1978, Phys. Rev. Lett., **40**, 223.
- Weinberg D.H. & Cole S., 1992, *preprint*.

- White S.D.M., 1986, in *Inner Space/Outer Space*, eds. Kolb E.W. *et al.*, University of Chicago Press.
- White S.D.M. *et al.*, 1987a, *Nature*, **330**, 451.
- White S.D.M., Frenk C.S. & Davis M., 1983, *ApJ*, **274**, L1.
- White S.D.M., Frenk C.S., Davis M. & Efstathiou G., 1987b, *ApJ*, **313**, 505.
- Wilczek F., 1978, *Phys. Rev. Lett.*, **40**, 279.
- Yahil A., Tamman G. & Sandage A., 1977, *ApJ*, **217**, 903.
- Yang J., Turner M.S., Steigman G., Schramm D.N. & Olive K.A., 1984, *ApJ*, **281**, 493.
- Zaidi M.H., 1983, *Fort. Phys.*, **7**, 409.
- Zel'dovich Ya.B., 1970, *Astron. Astrophys.*, **5**, 160.
- Zel'dovich Ya.B., 1972, *MNRaS*, **160**, 1P.
- Zel'dovich Ya.B., 1980, *MNRaS*, **192**, 663.
- Zwicky F., 1933, *Helv. Phys. Acta*, **6**, 110.
- Zwicky F., 1937, *ApJ*, **86**, 217.

